Department of Mechanical
and Industrial Engineering

ME TR JPL 952593

July 1970

AN APPROXIMATE THEORY OF IMPERFECT MODELING WITH APPLICATION TO THE THERMAL MODELING OF SPACECRAFTS

by

B. T. Chao and M. N. Huang

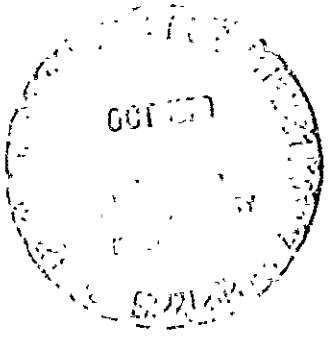

FINAL REPORT

to

JET PROPULSION LABORATORY

California Institute of Technology

Contract No. 952593

University of Illinois at Urbana-Champaign

Urbana, Illinois 61801

N70-20517-20548

SPACE PROCESSING AND MANUFACTURING

George C. Marshall Space Flight Center
Marshall Space Flight Center, Alabama

5 February 1970

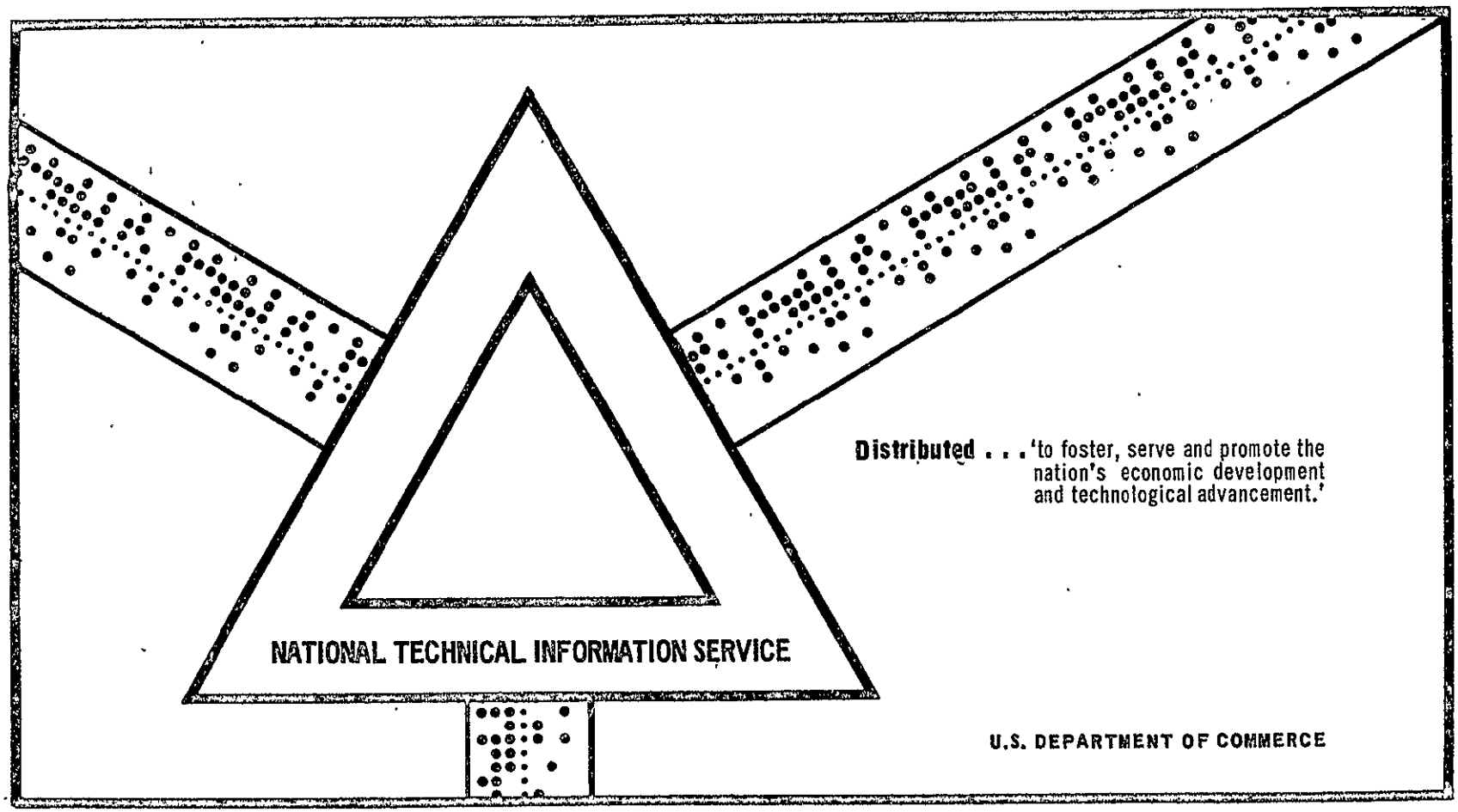

NASA TECHNICAL MEMORANDUM

NASA TM X-53993

NASA TM X-53993

SPACE PROCESSING AND MANUFACTURING

Manufacturing Engineering Laboratory

February 5, 1970

NASA

George C. Marshall Space Flight Center
Marshall Space Flight Center, Alabama

MSFC - Form 3190 (September 1968)

TECHNICAL REPORT STANDARD TITLE PAGE

1. REPORT NO.	2. GOVERNMENT ACCESSION NO.	3. RECIPIENT'S CATALOG NO.
TM X-53993		
4. TITLE AND SUBTITLE: SPACE PROCESSING AND MANUFACTURING		5. REPORT DATE: February 5, 1970
		6. PERFORMING ORGANIZATION CODE
7. AUTHOR(S)		8. PERFORMING ORGANIZATION REPORT #
9. PERFORMING ORGANIZATION NAME AND ADDRESS: Manufacturing Engineering Laboratory, George C. Marshall Space Flight Center, Marshall Space Flight Center, Alabama 35812		10. WORK UNIT NO.
		11. CONTRACT OR GRANT NO.
12. SPONSORING AGENCY NAME AND ADDRESS		13. TYPE OF REPORT & PERIOD COVERED: Technical Memorandum
		14. SPONSORING AGENCY CODE

15. SUPPLEMENTARY NOTES

16. ABSTRACT

This publication contains the presentations from the Space Processing and Manufacturing meeting held at MSFC, Huntsville, Alabama, October 21 and 22, 1969.

Contents consist of the opening keynote address by Dr. von Braun, Director, Marshall Space Flight Center; thirty-one presentations; and the closing remarks by Dr. M. P. Seibel, Manufacturing Engineering Laboratory, MSFC. In addition, there is a complete listing of the speakers showing their affiliation, mailing addresses, phone numbers, biographical sketches, and a list of attendees.

17. KEY WORDS	18. DISTRIBUTION STATEMENT		
19. SECURITY CLASSIF. (of this report)	20. SECURITY CLASSIF. (of this page)	21. NO. OF PAGES	22. PRICE

MSFC - Form 3292 (May 1969)

Department of Mechanical
and Industrial Engineering

ME TR JPL 952593

July 1970

AN APPROXIMATE THEORY OF IMPERFECT MODELING WITH APPLICATION TO THE THERMAL MODELING OF SPACECRAFTS

by

B. T. Chao and M. N. Huang

FINAL REPORT

to

JET PROPULSION LABORATORY

Contract No. 952593

This work was performed for the Jet Propulsion Laboratory, California Institute of Technology, as sponsored by the National Aeronautics and Space Administration under Contract NAS7-100.

University of Illinois at Urbana-Champaign

Urbana, Illinois 61801

TECHNICAL CONTENT STATEMENT

This report contains information prepared by the Department of Mechanical and Industrial Engineering, University of Illinois at Urbana-Champaign under JPL subcontract. Its content is not necessarily endorsed by the Jet Propulsion Laboratory, California Institute of Technology, or the National Aeronautics and Space Administration.

NEW TECHNOLOGY

No reportable items of new technology are identified.

ACKNOWLEDGMENTS

During the course of the investigation, Mr. W. A. Hagemeyer, JPL Technical Representative, provided property data and assistance in many ways without which this work would not have been possible. Professor J. S. de Paiva Netto of Instituto Tecnologico de Aeronautica, Brazil, and, formerly, of the Heat Transfer Laboratory of the Department, conducted preliminary studies of the theory. To both, we offer our sincere thanks.

The assistance of Miss Dianne Merridith in typing and Mr. Don Anderson in preparing the figures and of Mr. George Morris and Mrs. June Kempka in supervising the overall preparation of this report is greatly appreciated.

ABSTRACT

A theory has been proposed for conducting model experimentation which permits the use of imperfect models or test conditions that do not conform strictly to similitude requirements. It is based on a new concept of representing the error states in a multi-dimensional Euclidean space when errors in the modeling parameters are small. A consideration of the error path in the hyperspace leads to expressions from which the global effect of these errors may be evaluated approximately. Conditions under which these expressions would yield satisfactory results are given.

To test the usefulness of the theory, a computer experiment has been carried out for the prediction of the transient and steady state thermal behavior of a hypothetical spacecraft using perfect, as well as imperfect, models. The hypothetical spacecraft has major radiative and conductive heat flow paths that crudely simulate those of the '64 Mariner family of space vehicles. Errors in the conductance and capacitance parameters of up to 25 percent and in surface emittances of up to 20 percent existed in the imperfect models. Extensive temperature data were obtained for the various components of the spacecraft when it was subjected to a sudden heating, due to its exposure to the sun's radiation and the power dissipation within the bus, followed by its attaining the steady state and the subsequent cooling as a result of removing the sun's heat. Data were also acquired under the condition of a cyclically varying thermal environment.

Generally speaking, errors of up to 10, 20, and 30°R, originally present in the data of the imperfect models, were reduced to less than 3°R after correction according to the proposed theory.

NOMENCLATURE

A = area, ft^2

a_{ij} = coefficient matrix defined in (3.2.15)

B = diffuse radiosity, $Btu/hr\text{-}ft^2$

b_{ij} = inverse of a_{ij}, defined in (3.2.17)

C = volumetric heat capacity, $Btu/ft^3\text{-}^oR$

$C_{i,j}$ = weighting factor for δ, defined in (2.1.5)

d = thickness, ft

E = exchange factor

F = shape factor

H = irradiation, $Btu/hr\text{-}ft^2$

k = thermal conductivity, $Btu/hr\text{-}ft\text{-}^oR$

Q = heat flow rate, Btu/hr

q = heat flux, $Btu/hr\text{-}ft^2$

S = solar constant, $Btu/hr\text{-}ft^2$

s = arc length along error path

T = absolute temperature; T_o = absolute reference temperature

t = time, hr

α = surface absorptance

α_j = error ratio defined in (2.1.9)

β_j = error ratio defined in (2.1.14)

δ = error in modeling parameter

δ_{ij} = Kronecker delta function

ε = surface emittance

ρ = surface reflectance; ρ_d = diffuse component of surface reflectance, ρ_s = specular component of surface reflectance

σ = Stefan-Boltzmann radiation constant = 0.1713×10^{-8} Btu/hr-ft^2-$^\circ$R^4

$\mathcal{G}$ = diffuse-specular overall radiant exchange factor

Subscripts

e = refers to empty space

i, j = refers to surfaces A_i, A_j

m = refers to model

p = refers to prototype

Superscripts

$*$ = refers to solar spectrum: B^*, E^*, H^*, Q^*, q^*; α^*, ρ_d^*, and ρ_s^*; also refers to modification experiments: $P^{*(+)}$, $P^{*(-)}$, $s^{*(+)}$, and $s^{*(-)}$

$(+)$ = refers to subspace $S^{(+)}$

$(-)$ = refers to subspace $S^{(-)}$

(Others not found in the list are defined in the text.)

TABLE OF CONTENTS

Chapter 1

MOTIVATION OF A NEW APPROACH TO THERMAL SCALE MODELING

Theoretical requirements for the thermal scale modeling of unmanned spacecrafts are understood quite well at the present time. Difficulties arise in practice when the system to be modeled consists of components fabricated from a number of materials and they all participate in influencing the system's thermal performance. This is particularly true when information on both the steady state and transient behavior is sought. One possible means of satisfying modeling requirements is to modify artificially the thermal conductance of thin struts, plates, shells, etc., by electroplating with a high conductivity metal, such as copper. The main objective of a previous research contract between the University of Illinois and the Jet Propulsion Laboratory, JPL No. 951660, was to develop such a possibility. Test results obtained with prototypes and models of simple configurations have demonstrated the technical feasibility of the concept, either with or without solar simulation. With the availability of adhesive metal foil tapes† in recent years, it is conceivable that they can be applied more conveniently than electroplating. In this connection, one also sees the possibility of modifying the materials' heat capacity by using plastic (teflon) tapes. However, the range

---

†One type of copper and several aluminum foil tapes with pressure sensitive silicone adhesive, manufactured by Mystik Tape, Inc., of Northfield, Illinois, may be suitable for the present purpose.

of thickness of commercially available tapes is limited. Consequently, the desired thermal conductance and capacitance of the various structural members of the system may not be manufactured precisely in this manner. They can only be approximated. Furthermore, the application of a metal foil tape to a surface would also introduce a minor disturbance to its heat capacity. Likewise, the use of a plastic tape would produce a minor influence on its conductance. It is also possible that the desired surface radiation properties may not be duplicated accurately. These considerations prompted us to explore and examine another concept of model testing in which models that do not satisfy the similarity criteria completely are used. The theory, which is presented in the following chapter, contains some heuristic, but plausible, arguments and, in this sense, it is not mathematically rigorous. It was described first, in its rudimentary form, in a preliminary proposal, "Thermal Scale Modeling with Imperfect Models," prepared by the senior author and submitted to JPL for technical evaluation in January 1969. The material contained in Chapter 2 is a generalization of the theory presented in that document. It includes additional information relating to its practical implementation.

To test the validity of the theory, it has been applied to a hypothetical spacecraft having a geometric configuration that crudely simulates the global radiative and conductive paths of the Mariner spacecraft. The results of the present study firmly established the usefulness of the proposed new concept and one sees the welcomed flexibility in the use of model testing--a flexibility heretofore impossible to attain.

Chapter 2

AN APPROXIMATE THEORY OF MODELING WITH IMPERFECT MODELS

To begin with, it should be noted that, while our concern here is the thermal modeling of unmanned spacecrafts, the concept to be expounded herein has general applicability to the immense field of the technology of model testing. As such, the analysis and discussion that follow are presented with this viewpoint.

2.1 BASIC IDEAS

Consider a physical phenomenon y which depends on a number of independent variables $x_1, x_2, \cdots, x_p$. Symbolically, we may write

$$y = y(x_1, x_2, \cdots, x_p) \tag{2.1.1}$$

If the functional relationship has general validity, it must be independent of the units of measurement. Thus, a consideration of the requirement of dimensional homogeneity leads to a dimensionless form of the relation,

$$\phi = \phi(\Pi_1, \Pi_2, \cdots, \Pi_n) \tag{2.1.2}$$

Methods of dimensional analysis, whether based on the governing differential equations of the problem or on the strict algebraic formalism or on physical intuition, have been well documented and need no further deliberation here. Suffice it to state that, for perfect modeling, the Π's in the model system are made indentical to the corresponding Π's in the prototype system.

In the modeling of the thermal performance of spacecrafts, the dependent variables of interest are usually the temperatures of their various components. Thus, the number of ϕ's with which the experimenter has to deal could be quite large. Moreover, as has been noted previously, the precise satisfaction of all modeling requirements may not be possible in practice. In fact, even if it were possible, it might not be desirable from the point of view of economy. This is, then, the fundamental reason for using imperfect models and some deviation in the Π's of the model system from those of the prototype will be tolerated. To facilitate further discussion, we rewrite (2.1.2) as

$$\phi_i^{(0)} = \phi_i (\Pi_1, \Pi_2, \cdots, \Pi_n; \Omega) \tag{2.1.3}$$

where $i = 1, 2, \cdots, N$, N being the number of different components of the spacecraft to which a characteristic temperature is assignable. The subset of all relevant variables or parameters for which the model system is free from error is denoted by Ω. Clearly, for the problem under consideration all elements of Ω are passive and can be ignored. In the transient thermal modeling of unmanned spacecrafts, n is usually several times the value of N, as will become clear later.

If we designate the errors in Π by $\Pi\delta$ and define

$$\tilde{\phi}_i = \phi_i [\Pi_1(1 + \delta_1), \Pi_2(1 + \delta_2), \cdots, \Pi_n(1 + \delta_n); \Omega] \tag{2.1.4}$$

then $\tilde{\phi}_i$ may represent the *measured* entity using the imperfect model;

e.g., the temperature of the component surface A_i of the model spacecraft which does not satisfy the modeling requirements completely. The quantity sought is, of course, $\phi_i^{(0)}$. When the δ's are sufficiently small, the right-hand side of (2.1.4) can be linearized to become

$$\tilde{\phi}_i \doteq \phi_i^{(0)} + \sum_{j=1}^{n} C_{i,j}\,\delta_j \tag{2.1.5}$$

in which the coefficients $C_{i,j}$ are not known. It may be noted that, if Taylor's series is used, then

$$C_{i,j} = \Pi_j \frac{\partial \phi_{(i)}^{(0)}}{\partial \Pi_j} \tag{2.1.6}$$

However, (2.1.6) does not necessarily give the best estimate of the coefficient $C_{i,j}$. In fact, the validity of (2.1.5) does not require the usual restriction that needs to be imposed on the function for the existence of the Taylor expansion.

To evaluate $\phi_i^{(0)}$ from the measured $\tilde{\phi}_i$, one would require theoretically the knowledge of the n unknown coefficients $C_{i,j}$. This means that n experiments will have to be conducted with n different sets of δ's. The work may become formidable even when n is only moderately large; say, 20 or so. Furthermore, the accuracy required of the experimental measurements under such circumstance could be so high that they become impractical. We, therefore, seek alternative solutions with some loss of accuracy.

We begin by noting that the δ's associated with the imperfect model may be either positive or negative. For reasons to be seen later, they are grouped separately. We designate that $\delta_1, \delta_2, \cdots, \delta_r$ are positive and that $\delta_{r+1}, \delta_{r+2}, \cdots, \delta_n$ are negative. Furthermore, we define

$$\Delta_i^{(+)} = \sum_{j=1}^{r} C_{i,j}\,\delta_j \tag{2.1.7a}$$

$$\Delta_i^{(-)} = \sum_{j=r+1}^{n} C_{i,j}\,\delta_j \tag{2.1.7b}$$

Clearly, $\Delta_i^{(+)}$ and $\Delta_i^{(-)}$ may be either positive or negative. With the foregoing, (2.1.5) may be rewritten as

$$\tilde{\phi}_i = \phi_i^{(0)} + \Delta_i^{(+)} + \Delta_i^{(-)} \tag{2.1.8}$$

If the imperfect model is modified or if the model test condition is altered (in either case, the extent of modification must be restricted so as not to violate seriously the linear approximation used in the theory), then $\Delta_i^{(+)}$ and $\Delta_i^{(-)}$ will change also. A possible practical means of effecting model modification is through the use of adhesive metal and plastic tapes for altering the thermal conductance and heat capacity as indicated in [1]†. Thus, originally positive errors will become more positive, while originally negative errors will become less negative or positive. In what follows, the errors following

†Numbers in brackets refer to entries in REFERENCES.

modification will be designated with an asterisk.

Let us consider that the modifications are carried out in two steps. In the first, only the positive errors are altered, leaving the negative errors intact or essentially unchanged. We denote the error ratio by α. Thus,

$$\delta_j^*/\delta_j = \alpha_j , \quad j = 1, 2, \cdots, r \tag{2.1.9}$$

If $\tilde{\phi}_i^{*(+)}$ represents the experimental data so obtained, then

$$\tilde{\phi}_i^{*(+)} \doteq \phi_i^{(0)} + \sum_{j=1}^{r} C_{i,j}\, \alpha_j\, \delta_j + \sum_{j=r+1}^{n} C_{i,j}\, \delta_j \tag{2.1.10}$$

Eliminating $\phi_i^{(0)}$ from (2.1.5) and (2.1.10) yields

$$\tilde{\phi}_i^{*(+)} - \tilde{\phi}_i \doteq \sum_{j=1}^{r} C_{i,j}\, \delta_j\, (\alpha_j - 1) \tag{2.1.11}$$

If a weighted average of the error ratio is defined according to

$$\bar{\alpha} = \frac{\sum_{j=1}^{r} C_{i,j}\, \delta_j\, \alpha_j}{\sum_{j=1}^{r} C_{i,j}\, \delta_j} \tag{2.1.12}$$

then (2.1.11) can be rewritten as

$$\tilde{\phi}_i^{*(+)} - \tilde{\phi}_i = (\bar{\alpha} - 1) \sum_{j=1}^{r} C_{i,j}\, \delta_j$$

and, consequently, there is obtained from (2.1.7a)

$$\Delta_i^{(+)} = \frac{\tilde{\phi}_i^{*(+)} - \tilde{\phi}_i}{\bar{\alpha} - 1} \tag{2.1.13}$$

Obviously, $\bar{\alpha}$ cannot be evaluated without the prior knowledge of $C_{i,j}$. However, in the event that all α_j's are identical, say, α, then $\bar{\alpha} = \alpha$ and no knowledge of $C_{i,j}$ is needed. While such special condition is usually not met in practice, the foregoing observation does suggest that, in testing with imperfect models, the experimenter should seek small deviations in α_j's.

In the second step of modification, only the negative errors are altered. For clarity and for convenience of later discussion, the error ratio is to be denoted by β. Thus,

$$\delta_j^*/\delta_j = \beta_j, \quad j = r+1, r+2, \cdots, n \tag{2.1.14}$$

In this instance, the measured data, $\tilde{\phi}_i^{*(-)}$, can be written as

$$\tilde{\phi}_i^{*(-)} \doteq \phi_i^{(0)} + \sum_{j=1}^{r} C_{i,j}\,\delta_j + \sum_{j=r+1}^{n} C_{i,j}\,\beta_j\,\delta_j \tag{2.1.15}$$

It follows, then,

$$\tilde{\phi}_i^{*(-)} - \tilde{\phi}_i \doteq \sum_{j=r+1}^{n} C_{i,j}\,\delta_j\,(\beta_j - 1) \tag{2.1.16}$$

As in the first case, if a weighted average of the error ratio is

defined, namely,

$$\bar{\beta} = \frac{\sum_{j=r+1}^{n} C_{i,j}\,\delta_j\,\beta_j}{\sum_{j=r+1}^{n} C_{i,j}\,\delta_j} \tag{2.1.17}$$

then

$$\Delta_i^{(-)} = \frac{\tilde{\phi}_i^{*(-)} - \tilde{\phi}_i}{\bar{\beta} - 1} \tag{2.1.18}$$

The observation previously noted for $\bar{\alpha}$ can likewise be made for $\bar{\beta}$. Thus, without the knowledge of $C_{i,j}$'s, the precise evaluation of both $\bar{\alpha}$ and $\bar{\beta}$ is not possible. However, they can be approximated. It is this desire of finding the appropriate mean values of the error ratios that led to the creation of a new concept of model testing with imperfect models.

2.2 GEOMETRIC REPRESENTATION OF ERROR STATES

The central idea to be explored herein is the representation of error states in a multidimensional Euclidean space whose elements are δ_j. This will be referred to as the *simple* error space in contrast to the *weighted* error space to be discussed later. Such representation is compatible with the linear theory considered in the present study.

For j ranging from 1 to n, there exist the following three points in the n-dimensional error space:

$$P(\delta_1, \delta_2, \cdots, \delta_r, \delta_{r+1}, \cdots, \delta_n)$$

$$P^{*(+)}(\delta_1^*, \delta_2^*, \cdots, \delta_r^*, \delta_{r+1}, \cdots, \delta_n)$$

$$P^{*(-)}(\delta_1, \delta_2, \cdots, \delta_r, \delta_{r+1}^*, \cdots, \delta_n^*)$$

There are also two subspaces $S^{(+)}$ and $S^{(-)}$ with their respective origin at $O^{(+)}$ and $O^{(-)}$. The elements of subspace $S^{(+)}$ are $\delta_1, \delta_2, \cdots, \delta_r$ and those of $S^{(-)}$ are $\delta_{r+1}, \delta_{r+2}, \cdots, \delta_n$. If the error ratio α is a constant, the three points $O^{(+)}$, P, and $P^{*(+)}$ are colinear in $S^{(+)}$. The straight line which originates at $O^{(+)}$ and passes through the said points will be labeled $\xi^{(+)}$. Similarly, if β is a constant, $O^{(-)}$, P, and $P^{*(-)}$ are colinear in $S^{(-)}$ and the straight line joining them will be labeled $\xi^{(-)}$. When $n = 3$, the foregoing can be represented pictorially as is illustrated in Fig. 2.1. No such pictorial representation is possible when $n > 3$.

In $S^{(+)}$, the lengths of the line segments $\overline{O^{(+)}P}$ and $\overline{O^{(+)}P^{*(+)}}$ are

$$\overline{O^{(+)}P} = \left[\sum_{j=1}^{r} \delta_j^2\right]^{1/2}$$

and

$$\overline{O^{(+)}P^{*(+)}} = \left[\sum_{j=1}^{r} (\delta_j^*)^2\right]^{1/2} = \alpha \left[\sum_{j=1}^{r} \delta_j^2\right]^{1/2} = \alpha\, \overline{O^{(+)}P}$$

If we regard $\xi^{(+)}$ as the abscissa of a plane plot with ϕ_i as its ordinate,

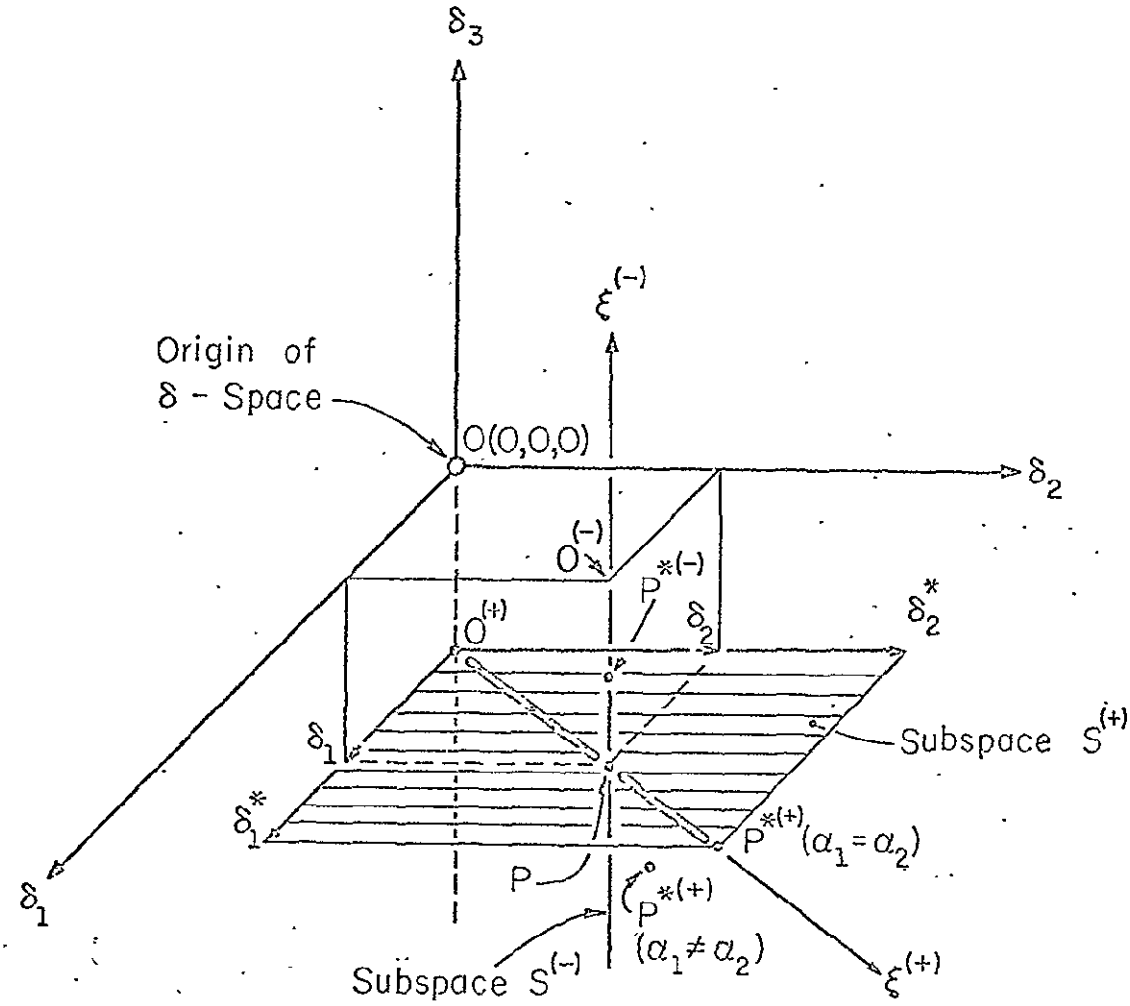

Figure 2.1 Illustration of subspace $S^{(+)}$ and $S^{(-)}$ in a 3-dimensional simple error space. (δ_1, δ_2 are +, δ_3 is -; $S^{(+)}$ is a plane while $S^{(-)}$ is a line).

then a point $\tilde{\phi}_i$ corresponding to P and another point $\tilde{\phi}_i^{*(+)}$ corresponding to $P^{*(+)}$ may be located as shown in Fig. 2.2(a). A conjecture introduced in [1] is that ϕ_i depends uniquely on $\xi^{(+)}$ and varies linearly with it. It follows then

$$\Delta_i^{(+)} = \frac{\tilde{\phi}_i^{*(+)} - \tilde{\phi}_i}{\frac{\overline{O^{(+)}P^{*(+)}}}{\overline{O^{(+)}P}} - 1} = \frac{\tilde{\phi}_i^{*(+)} - \tilde{\phi}_i}{\alpha - 1} \tag{2.2.1}$$

which is identical to (2.1.13) when $\overline{\alpha} = \alpha$, as is the case here.

An analysis based on analogous arguments can be made in subspace $S^{(-)}$. Thus,

$$\overline{O^{(-)}P} = \left[\sum_{j=r+1}^{n} \delta_j^2 \right]^{1/2},$$

$$\overline{O^{(-)}P^{*(-)}} = \left[\sum_{j=r+1}^{n} (\delta_j^*)^2 \right]^{1/2} = \beta \, \overline{O^{(-)}P}$$

and, from the ϕ_i vs $\xi^{(-)}$ plot as illustrated in Fig. 2.2(b), it can be shown readily that

$$\Delta_i^{(-)} = \frac{\tilde{\phi}_i^{*(-)} - \tilde{\phi}_i}{\frac{\overline{O^{(-)}P^{*(-)}}}{\overline{O^{(-)}P}} - 1} = \frac{\tilde{\phi}_i^{*(-)} - \tilde{\phi}_i}{\beta - 1} \tag{2.2.2}$$

which is precisely (2.1.18) when $\overline{\beta} = \beta$.

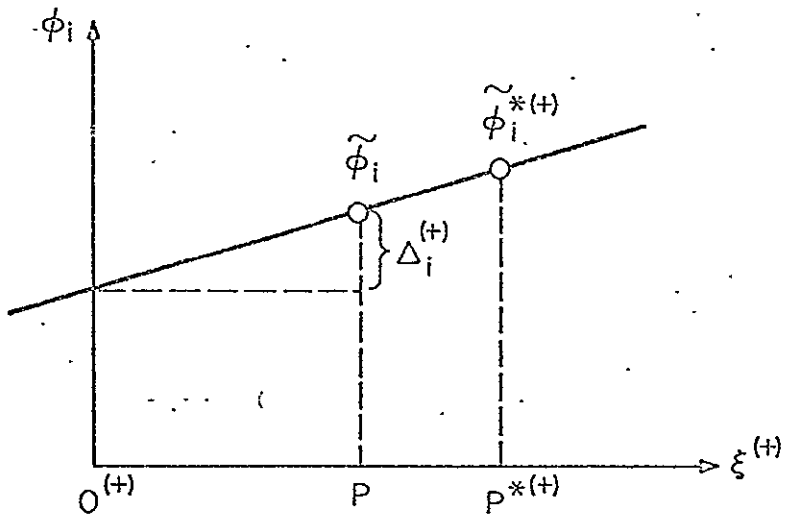

(a)

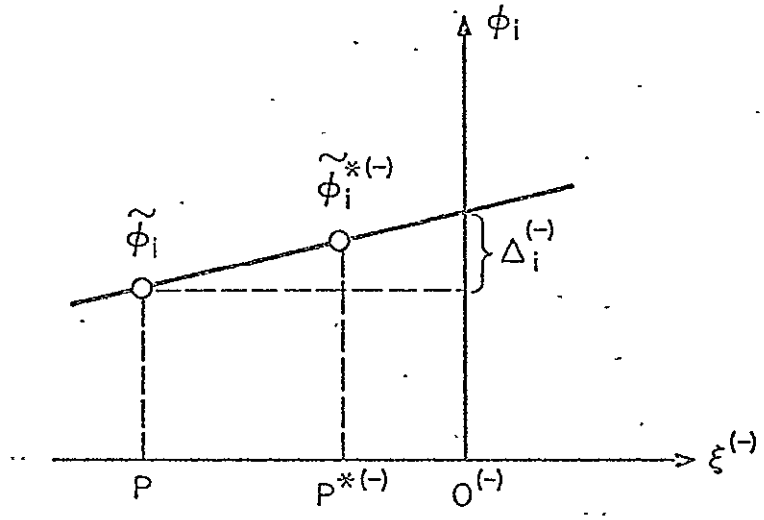

(b)

Figure 2.2 Linear dependence of ϕ_i with θ in $S^{(+)}$ and $S^{(-)}$

The foregoing analysis, plausible as it may seem, is subject to immediate criticism. Referring to (2.1.5), one recognizes that the deviation of $\tilde{\phi}_i$ from $\phi_i^{(0)}$ depends on the products $C_{i,j}\,\delta_j$ instead of δ_j alone. The coefficients $C_{i,j}$ are, in essence, weighting factors which prescribe the relative importance of the various errors in influencing the dependent variable. Thus, a *weighted* error space --whose elements are $|C_{i,j}|\delta_j$ should be used instead of the simple error space and it is more logical to assume that the distance ascertained in such error space from its origin is an appropriate measure of the resultant error in ϕ_i.

A question which naturally arises is: Why is it, then, that for constant α and β, the analysis made in the *simple* error space leads to correct results? The reason for this may be seen easily. In $S^{(+)}$ of the weighted error space, the lengths of the line segments $\overline{O^{(+)}P}$ and $\overline{O^{(+)}P^{*(+)}}$ are

$$\overline{O^{(+)}P} = \left[\sum_{j=1}^{r} (C_{i,j}\,\delta_j)^2\right]^{1/2}$$

and

$$\overline{O^{(+)}P^{*(+)}} = \left[\sum_{j=1}^{r} (C_{i,j}\,\delta_j^*)^2\right]^{1/2}$$

Hence, when α is a constant, $\overline{O^{(+)}P^{*(+)}} = \alpha\,\overline{O^{(+)}P}$ and the three points $O^{(+)}$, P, and $P^{*(+)}$ are colinear. Since only the *ratio of distances*

is involved in the expression for $\Delta_i^{(+)}$, it is seen that (2.2.1) remains unaltered. For the same reason, (2.2.2) also holds. It is significant that the linear correction formulae (2.2.1) and (2.2.2), valid for constant α and β and originally deduced from a conjecture in the simple error space, are formally identical to those based on a consideration in the weighted error space. It goes without saying that the experimenter has normally no knowledge of $C_{i,j}$ and, hence, the error state points like P, $P^{*(+)}$, and $P^{*(-)}$ cannot actually be plotted in the weighted error space.

2.3 GLOBAL EFFECT OF POSITIVE AND NEGATIVE δ'S ON ϕ_i --PARABOLIC ERROR PATH. WORKING FORMULAE.

We now proceed to examine the more realistic case for which the error ratios α_j and β_j are not constants. We restrict ourselves to the consideration that the range of variation among the α_j's and among the β_j's is limited. The analysis which follows closely parallels that described in [1] for the evaluation of the global effect of the errors based on a consideration made in the simple error space.

Referring to Fig. 2.3(a.1), the line joining $O^{(+)}$ and $P^{*(+)}$ is designated as the $\xi^{(+)}$-axis. Since α_j is not a constant, but varies with j, P does not lie in this line. Hence, the point P and the $\xi^{(+)}$-axis together determine a plane in $S^{(+)}$ of the weighted error space. In this plane, a line $O^{(+)}\eta^{(+)}$ is erected normal to the $\xi^{(+)}$-axis as shown. For convenience, the $\eta^{(+)}$-axis is so oriented that P lies on the positive side. It is pertinent that $\xi^{(+)}$ and $\eta^{(+)}$ imply $\xi_i^{(+)}$

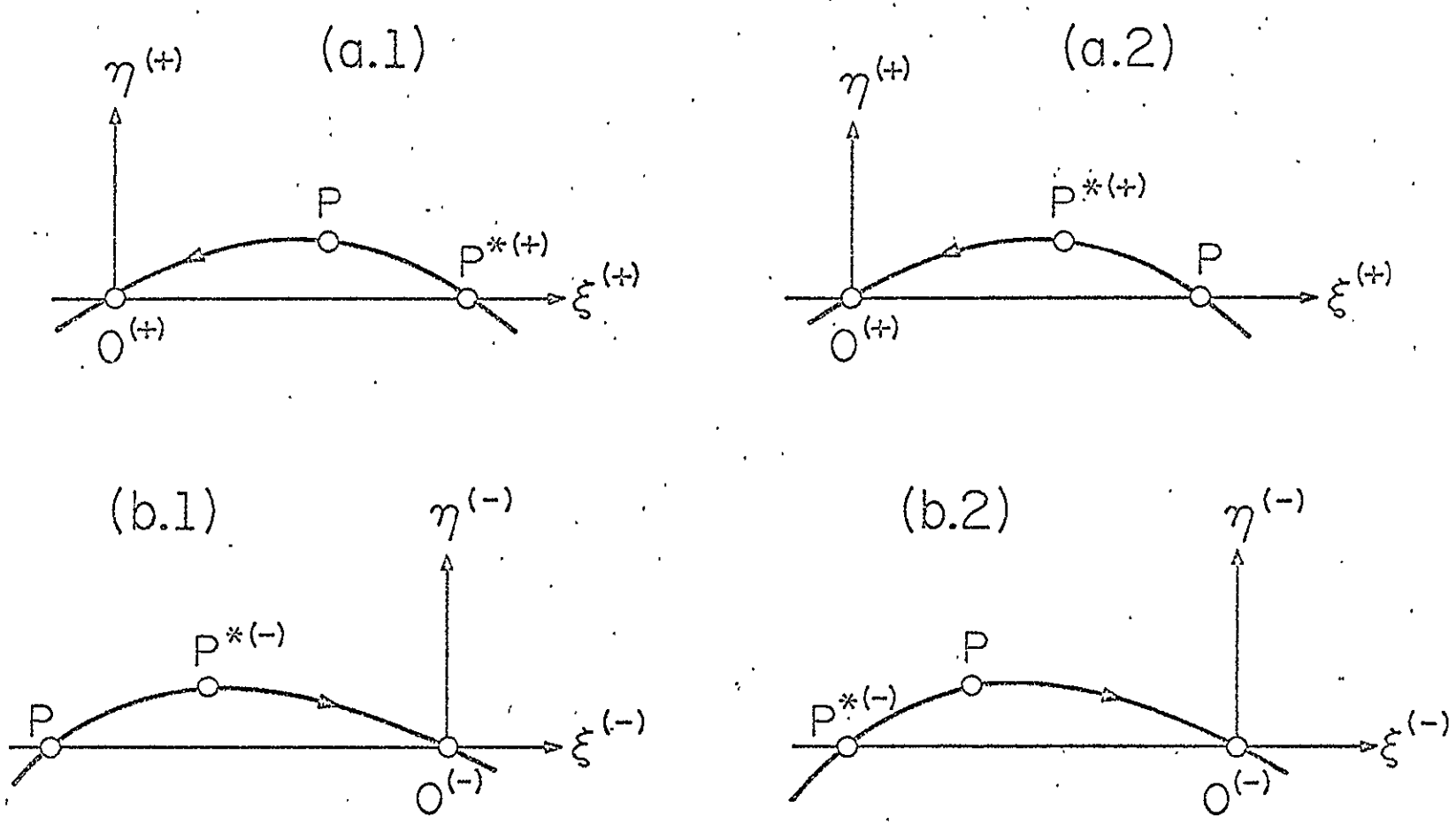

Figure 2.3 Parabolic error paths in $S^{(+)}$ and $S^{(-)}$

and $\eta_i^{(+)}$ since the scale of the coordinates in the weighted error space depends on i. For simplicity, the subscript i is omitted.

Passing through the three points $0^{(+)}$, P, and $P^{*(+)}$, a parabola can be constructed. Tracing the points along the parabola and toward the origin $0^{(+)}$ may be interpreted as conducting a series of experiments with controlled errors of successively diminishing magnitude. As the origin is approached, all positive errors become vanishingly small. Thus, *the arc length along the curve measured from* $0^{(+)}$ *is an appropriate measure of the global effect of all positive errors in* ϕ_i. The choice of a parabola as the error path is, to some extent, arbitrary, but it is certainly reasonable. Further argument in support of the choice will be given later.

The equation of the parabola in the $\xi^{(+)}$-$\eta^{(+)}$ plane is

$$\eta^{(+)} = a\xi^{(+)} + b(\xi^{(+)})^2 \tag{2.3.1}$$

where $a > 0$ and $b < 0$. The coordinates of $P^{*(+)}$ are

$$\xi_{P^*}^{(+)} = \left[\sum_{j=1}^{r} (C_j \delta_j^*)^2\right]^{1/2} \tag{2.3.2a}$$

$$\eta_{P^*}^{(+)} = 0 \tag{2.3.2b}$$

In (2.3.2a), C_j implies $C_{i,j}$. The coordinates of P are

$$\xi_P^{(+)} = \frac{\overrightarrow{0^{(+)}P} \cdot \overrightarrow{0^{(+)}P^{*(+)}}}{\left|\overrightarrow{0^{(+)}P^{*(+)}}\right|} = \frac{\sum_{j=1}^{r} C_j^2 \delta_j \delta_j^*}{\left[\sum_{j=1}^{r} (C_j \delta_j^*)^2\right]^{1/2}} \tag{2.3.3a}$$

$$\eta_P^{(+)} = [|\overrightarrow{O^{(+)}P}|^2 - (\xi_P^{(+)})^2]^{1/2} = \left[\sum_{j=1}^{r} (c_j \delta_j)^2 - (\xi_P^{(+)})^2\right]^{1/2} \qquad (2.3.3b)$$

in which the overscore arrow denotes vectors. It can be shown that

$$a = \frac{\eta_P^{(+)}}{\xi_P^{(+)}} \frac{1}{1 - \frac{\xi_P^{(+)}}{\xi_{P*}^{(+)}}}, \quad b = -\frac{a}{\xi_{P*}^{(+)}} \qquad (2.3.4a,b)$$

The arc length $\overset{\frown}{O^{(+)}P^{*(+)}}$ is

$$s^{*(+)} = \int_0^{\xi_{P*}^{(+)}} \left[1 + \left(\frac{d\eta^{(+)}}{d\xi^{(+)}}\right)^2\right]^{1/2} d\xi^{(+)}$$

$$= -\frac{1}{2b} \{a(1 + a^2)^{1/2} + \ell n [(1 + a^2)^{1/2} + a]\} \qquad (2.3.5a)$$

and the arc length $\overset{\frown}{O^{(+)}P}$ is

$$s^{(+)} = \int_0^{\xi_P^{(+)}} \left[1 + \left(\frac{d\eta^{(+)}}{d\xi^{(+)}}\right)^2\right]^{1/2} d\xi^{(+)}$$

$$= -\frac{1}{4b} \{a(1 + a^2)^{1/2} + \ell n [(1 + a^2)^{1/2} + a]$$

$$- a\lambda(1 + a^2\lambda^2)^{1/2} - \ell n [(1 + a^2\lambda^2)^{1/2} + a\lambda]\} \qquad (2.3.5b)$$

where

$$\lambda = 1 + \frac{2b}{a} \xi_P^{(+)} = 1 - 2 \frac{\xi_P^{(+)}}{\xi_{P*}^{(+)}} \qquad (-1 < \lambda < 1) \qquad (2.3.5c)$$

The ratio of the two arc lengths is

$$\frac{s^{*(+)}}{s^{(+)}} = \frac{2}{1 - f(a,\lambda)} \tag{2.3.6a}$$

where

$$f(a,\lambda) = \frac{a\lambda(1 + a^2\lambda^2)^{1/2} + \ell n\,[(1 + a^2\lambda^2)^{1/2} + a\lambda]}{a(1 + a^2)^{1/2} + \ell n\,[(1 + a^2)^{1/2} + a]} \tag{2.3.6b}$$

and a is given by (2.3.4a) and λ by (2.3.5c). In the latter two equations, we further note that

$$\frac{\eta_P^{(+)}}{\xi_P^{(+)}} = \left[\frac{\sum (C_j\,\delta_j)^2}{(\xi_P^{(+)})^2} - 1\right]^{1/2} = \left[\frac{\left(\sum C_j^2\delta_j^2\right)\cdot\sum C_j^2(\delta_j^*)^2}{\left(\sum C_j^2\,\delta_j\,\delta_j^*\right)^2} - 1\right]^{1/2} \tag{2.3.7a}$$

$$\frac{\xi_P^{(+)}}{\xi_{P*}^{(+)}} = \frac{\sum C_j^2\,\delta_j\,\delta_j^*}{\sum C_j^2\,(\delta_j^*)^2} \tag{2.3.7b}$$

In the foregoing, the summand $\sum$ implies $\sum_{j=1}^{R}$. Consequently, within the context of the present theory, the correction required for all positive errors is

$$\Delta_i^{(+)} = \frac{\tilde{\phi}_i^{*(+)} - \tilde{\phi}_i}{\frac{s^{*(+)}}{s^{(+)}} - 1} \tag{2.3.8}$$

and the appropriate mean $\bar{\alpha}$ is seen to be given by the ratio $s^{*(+)}/s^{(+)}$

For the practical application of these results, the following observations are made.

(A) When the range of α_j is restricted, (2.3.7a) and (2.3.7b) are weak functions of C_j. They may be replaced by the following approximate expressions.

$$\frac{\eta_p^{(+)}}{\xi_p^{(+)}} = \left[\frac{\left(\sum \delta_j^2 \right) \cdot \sum (\delta_j^*)^2}{\left(\sum \delta_j \, \delta_j^* \right)^2} - 1 \right]^{1/2} \tag{2.3.9a}$$

$$\frac{\xi_p^{(+)}}{\xi_{p*}^{(+)}} = \frac{\sum \delta_j \, \delta_j^*}{\sum (\delta_j^*)^2} \tag{2.3.9b}$$

Alternatively, if the physical nature of the problem is such that the dominant C_j's are of similar magnitude, our experience indicates that these approximations are also valid.

Following a detailed error analysis based on the same arguments, but made for the *simple* error space, it was found that (2.3.6a,b), (2.3.4a), and (2.3.5c) remained unaltered provided that, in the latter two expressions, the ratios $\eta_p^{(+)}/\xi_p^{(+)}$ and $\xi_p^{(+)}/\xi_{p*}^{(+)}$ were calculated according to (2.3.9a) and (2.3.9b).

(B) If the experimental conditions are so chosen that, in the weighted error space, $2(\xi_p^{(+)}/\xi_{p*}^{(+)}) = 1$, then $\lambda = f(a,\lambda) = 0$ and

$s^{*(+)}/s^{(+)} = 2$ which is independent of the C_j's. This condition is, of course, not generally met in practice. However, if 'a' is small, say, less than 0.5, then $f(a,\lambda)$ becomes somewhat insensitive to variations in 'a'. Furthermore, if we require that $|\lambda|$ be kept small, say, within 0.1 or 0.2, then $f(a,\lambda)$ is small compared to 1. Under these conditions, the error in the calculated ratio of the arc lengths resulting from inaccuracies in 'a' and λ will likewise be small. Thus, the use of the parabolic error path provides guidance to the proper selection of the experimental conditions for reducing errors due to the lack of knowledge of the weighting factors C_j.

The foregoing observations (A) and (B), taken together, suggest that, in the application of the linear correction formula (2.3.8), the ratio of the arc lengths (or its equivalent $\bar{\alpha}$) can be evaluated from a consideration of the *simple* error-space when the range of α_j is restricted and/or when the experimental conditions are chosen as explained.

If, in the modified experiments, the positive errors are made *less* positive, the relative location of P and $P^{*(+)}$ with respect to the origin of $S^{(+)}$ would be as shown in Fig. 2.3(a.2). The $\xi^{(+)}$-axis is now chosen to pass through P. Following a similar analysis, it was found that

$$\Delta_i^{(+)} = \frac{\tilde{\phi}_i - \tilde{\phi}_i^{*(+)}}{1 - \frac{s^{*(+)}}{s^{(+)}}} \qquad (2.3.10a)$$

in which

$$\frac{s^{*(+)}}{s^{(+)}} = \frac{1 - f(a,\lambda)}{2} \tag{2.3.10b}$$

and $f(a,\lambda)$ is given by (2.3.6b) with 'a' and λ redefined as follows

$$a = \frac{\eta_{P*}^{(+)}}{\xi_{P*}^{(+)}} \frac{1}{1 - \frac{\xi_{P*}^{(+)}}{\xi_{P}^{(+)}}} \tag{2.3.10c}$$

$$\lambda = 1 - 2 \frac{\xi_{P*}^{(+)}}{\xi_{P}^{(+)}} \tag{2.3.10d}$$

wherein

$$\frac{\eta_{P*}^{(+)}}{\xi_{P*}^{(+)}} = \left[\frac{\left(\sum C_j^2 \delta_j^2 \right) \cdot \sum C_j^2 (\delta_j^*)^2}{\left(\sum C_j^2 \delta_j \delta_j^* \right)^2} - 1 \right]^{1/2} \tag{2.3.10e}$$

and

$$\frac{\xi_{P*}^{(+)}}{\xi_{P}^{(+)}} = \frac{\sum C_j^2 \delta_j \delta_j^*}{\sum C_j^2 \delta_j^2} \tag{2.3.10f}$$

Again, if the range of α_j is restricted and/or if the experimental condition is such that $|\lambda|$ is small as compared to unity, the ratios $\eta_{P*}^{(+)}/\xi_{P*}^{(+)}$ and $\xi_{P*}^{(+)}/\xi_{P}^{(+)}$ can be calculated from a consideration of

the *simple* error space, namely,

$$\frac{\eta_{P*}^{(+)}}{\xi_{P*}^{(+)}} = \left[\frac{\left(\sum \delta_j^2 \right) \cdot \sum (\delta_j^*)^2}{\left(\sum \delta_j \, \delta_j^* \right)^2} - 1 \right]^{1/2} \qquad (2.3.11a)$$

and

$$\frac{\xi_{P*}^{(+)}}{\xi_{P}^{(+)}} = \frac{\sum \delta_j \, \delta_j^*}{\sum \delta_j^2} \qquad (2.3.11b)$$

Clearly, in (2.3.10e,f) and (2.3.11a,b), the summand $\sum$ implies $\sum_{j=1}^{r}$.

The analysis of the global effect of the negative δ's on ϕ_i can likewise be treated. If the negative errors are *less* negative in the modified experiments, the error path in $S^{(-)}$ would be as shown in Fig. 2.3(b.1). We shall refrain from presenting the details of the calculation and, instead, shall summarize the results as follows.

$$\Delta_i^{(-)} = \frac{\tilde{\phi}_i - \tilde{\phi}_i^{*(-)}}{1 - \frac{s^{*(-)}}{s^{(-)}}} \qquad (2.3.12a)$$

where the ratio of the arc lengths along the error path is

$$\frac{s^{*(-)}}{s^{(-)}} = \frac{1 - f(a,\lambda)}{2} \qquad (2.3.12b)$$

and $f(a,\lambda)$ is again given by (2.3.6b) with 'a' and λ, respectively, denoting

$$a = \frac{\eta_{p*}^{(-)}}{\xi_{p*}^{(-)}} \frac{1}{1 - \frac{\xi_{p*}^{(-)}}{\xi_{p}^{(-)}}} \tag{2.3.12c}$$

$$\lambda = 1 - 2\frac{\xi_{p*}^{(-)}}{\xi_{p}^{(-)}} \tag{2.3.12d}$$

wherein

$$\frac{\eta_{p*}^{(-)}}{\xi_{p*}^{(-)}} = \left[\frac{\left(\sum C_j^2 \delta_j^2 \right) \cdot \sum C_j^2 (\delta_j^*)^2}{\left(\sum C_j^2 \delta_j \delta_j^* \right)^2} - 1 \right]^{1/2} \tag{2.3.12e}$$

and

$$\frac{\xi_{p*}^{(-)}}{\xi_{p}^{(-)}} = \frac{\sum C_j^2 \delta_j \delta_j^*}{\sum C_j^2 \delta_j^2} \tag{2.3.12f}$$

In the above, $\sum$ implies $\sum_{j=r+1}^{n}$. The ratio $s^{*(-)}/s^{(-)}$ clearly denotes the mean $\bar{\beta}$.

The error path would be as that depicted in Fig. 2.3(b.2) if the negative errors become *more* negative after modification. In this case,

$$\Delta_i^{(-)} = \frac{\tilde{\phi}_i^{*(-)} - \tilde{\phi}_i}{\frac{s^{*(-)}}{s^{(-)}} - 1} \qquad (2.3.13a)$$

where

$$\frac{s^{*(-)}}{s^{(-)}} = \frac{2}{1 - f(a,\lambda)} \qquad (2.3.13b)$$

and $f(a,\lambda)$ is as defined earlier, with 'a' and λ, respectively, given by (2.3.4a) and (2.3.5c) when the superscript (+) is replaced by (-). The ratios $\eta_p^{(-)}/\xi_p^{(-)}$ and $\xi_p^{(-)}/\xi_{p*}^{(-)}$ are given by (2.3.7a) and (2.3.7b) with the summand $\sum$ reinterpreted to mean $\sum_{j=r+1}^{n}$. The discussion on the validity of using approximations deducible from the *simple* error space also holds.

Finally, the quantity sought is

$$\phi_i^{(0)} = \tilde{\phi}_i - \Delta_i^{(+)} - \Delta_i^{(-)} \qquad (2.3.14)$$

Chapter 3

APPLICATION OF THE THEORY TO THE THERMAL MODELING OF A HYPOTHETICAL SPACECRAFT-PRELIMINARIES

3.1 THE HYPOTHETICAL SPACECRAFT

To ascertain the usefulness of the approximate correction theory for imperfect modeling as expounded in the previous chapter, we consider a hypothetical spacecraft shown in Fig. 3.1. The geometric configuration chosen is intended to simulate the global radiative and conductive paths of the Mariner '64 spacecraft but with all secondary and minor details omitted. The solar panels A_1-A_2 and A_3-A_4 are fabricated of an aggregate of aluminum sheets, silicon crystals for energy conversion and glass plate covers, all mounted in an aluminum alloy celled structure. While the local thermal properties are of a highly anisotropic and inhomogeneous character, it is quite feasible to describe its *overall* behavior by equivalent values of thermal conductivity and heat capacity. Based on the information transmitted to us from JPL†, it appears that a reasonable value of kd for the solar panel is 0.058 Btu/hr-F. Also, the mean specific heat of the aggregate is reported to be 0.20 Btu/lb-F and a typical Mariner solar panel of 3 ft X 7 ft weighs about 30 lbs. From these, it is estimated that the Cd of the solar panel is approximately 0.29 Btu/ft^2-F.

†Through Mr. William A. Hagemeyer.

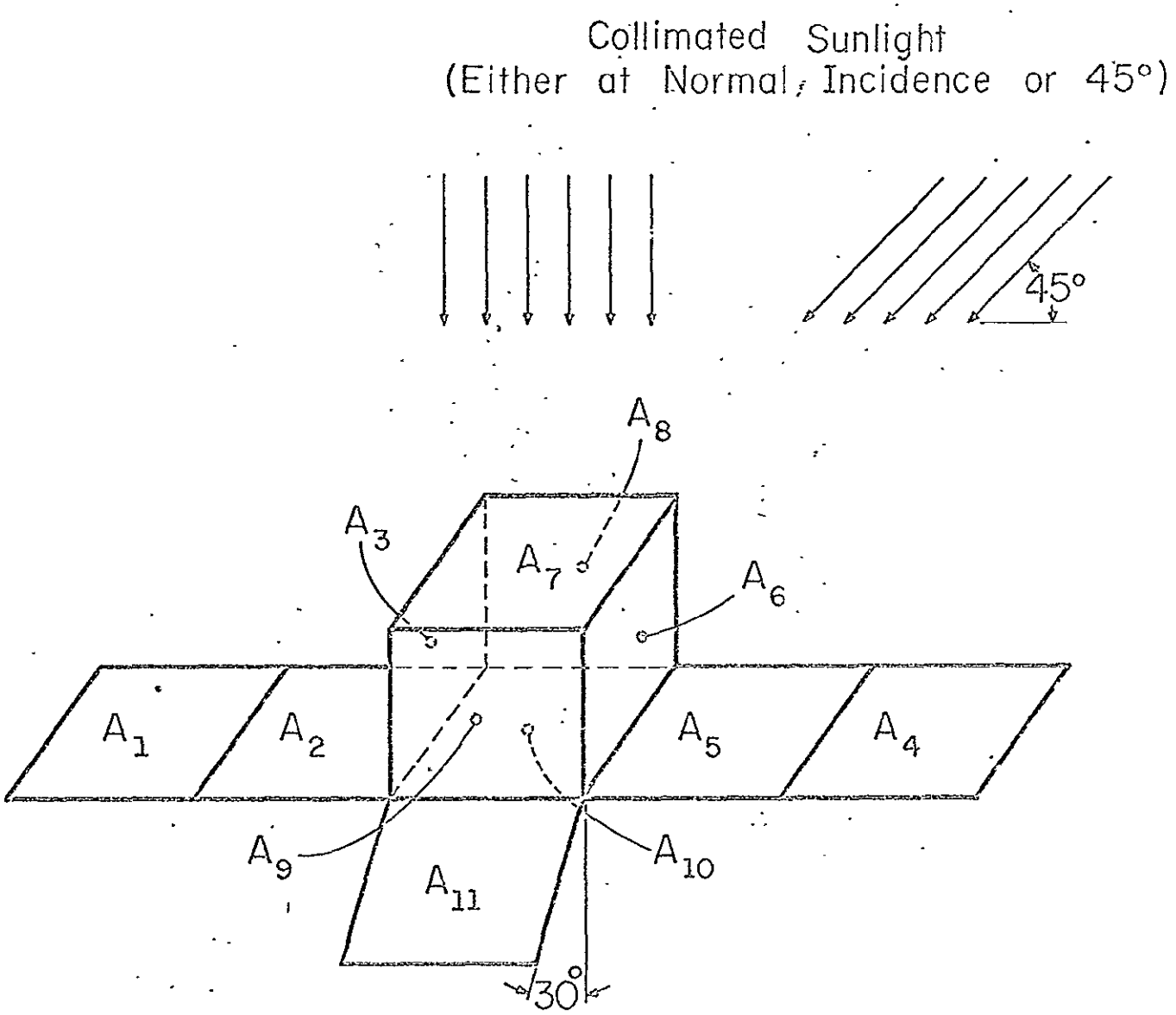

Solar Panel: A_1, A_2, A_4, A_5

Bus: $A_3, A_6, A_7, A_8, A_9, A_{10}$

(A_7 and A_{10} are covered with superinsulation)

Antenna: A_{11}

All areas are identical and equal to 4 ft.^{2}

Figure 3.1 Hypothetical spacecraft

To keep the radiation geometry associated with the diffuse-specular surfaces as simple as possible, the bus of the spacecraft is taken to be a cubical box instead of the usual polygonal configuration. The top and bottom faces of the bus are covered with multilayer superinsulation. The collimated sun's rays are assumed to be either perpendicular to the solar panels or slanted at 45° to them, but remain parallel to the front and back faces of the bus. TABLE 3.1 lists the materials selected for the six component faces of the spacecraft bus. The thicknesses indicated are *equivalent* values; they take into account the electronic packaging subassemblies bolted to them. Included is the relevant information for the main directional antenna. As will be shown in Section 3.4, perfect modeling requires that the corresponding surfaces of the model and the prototype have identical radiation properties. Furthermore, when the temperature fields are two-dimensional, the kd and Cd of all component surfaces of the model must bear a fixed relationship to those of the corresponding surfaces of the prototype. TABLE 3.2 summarizes al pertinent surface properties and the equivalent (kd)'s and (Cd)'s for the hypothetical spacecraft.

3.2 RADIATION HEAT TRANSFER ANALYSIS AND THE DETERMINATION OF THE OVERALL EXCHANGE FACTOR $\mathcal{G}$

When the surfaces of a spacecraft are under the irradiation of the sun, the absorbed and reflected radiation are in a wavelength region totally different from that of the emitted radiation. While it is possible to perform a general formulation of the problem, there is neither the need nor the justification of doing such analysis at the present time. It is well known that approximately 98 percent of sun's radiation

TABLE 3.1

MATERIAL LIST FOR THE HYPOTHETICAL SPACECRAFT

(a) Solar Panel

Aggregate of silicon, glass, aluminum and its alloy

(b) Bus

Panel	Material	k Btu/hr-ft-F	C Btu/ft^3-F	Equivalent Thickness d, in.
A_3	Magnesium Alloy AN-M-29	47.0	25.9	0.125
A_6	Aluminum Alloy 5086	80.2	37.1	0.1875
A_7	Titanium Alloy A-110-AT	4.60	35.0	0.10
A_8	Magnesium Alloy A781A(T4)	29.1	28.0	0.1875
A_9	Magnesium Alloy ZK51-A	63.0	27.6	0.125
A_{10}	Titanium Alloy 150-A(2)	8.38	38.5	0.025

(c) Antenna

Aluminum alloy 2011 (k = 82.3 Btu/hr-ft-F and C = 39.3 Btu/ft^3-F),

Thickness - 0.0625 in.

TABLE 3.2

SURFACE PROPERTIES AND OTHER DATA FOR THE HYPOTHETICAL SPACECRAFT

			Solar			Infra-red			kd (equivalent)	Cd (equivalent)
			ρ_d^*	ρ_s^*	α^*	ρ_d	ρ_s	$\alpha(=\varepsilon)$		
Solar Panel	Sunlit Surfaces: A_1, A_2, A_4, A_5		0	0.20	0.80	0.20	0	0.80	0.058	0.29
	Surface Away from Sun: $A_{1'}$,$A_{2'}$,$A_{4'}$,$A_{5'}$ (painted with PV-100 white paint)		0.80	0	0.20	0.17	0	0.83		
Bus	A_3	exterior (PV-100 paint)	0.80	0	0.20	0.17	0	0.83	0.489	0.269
		interior (partially painted)	--	--	--	0.80	0	0.20		
	A_6	exterior (PV-100 paint)	0.80	0	0.20	0.17	0	0.83	1.25	0.580
		interior (partially painted)	--	--	--	0.80	0	0.20		
	A_7	exterior (superinsulation)	0	0.85	0.15	0.50	0	0.50	0.0383	0.292
		interior (black paint)	--	--	--	0.15	0	0.85		
	A_8	exterior (PV-100 paint)	0.80	0	0.20	0.17	0	0.83	0.455	0.437
		interior (black paint)	--	--	--	0.15	0	0.85		
	A_9	exterior (polished aluminum)	0	0.80	0.20	0	0.95	0.05	0.655	0.287
		interior (black paint)	--	--	--	0.15	0	0.85		
	A_{10}	exterior (superinsulation)	0	0.85	0.15	0.50	0	0.50	0.0175	0.080
		interior (black paint)	--	--	--	0.15	0	0.85		
Antenna	A_{11}	sunlit face (green paint)	0.25	0.05	0.70	0.18	0	0.82	0.428	0.204
		face away from sun	--	--	--	0.95	0	0.05		

All (kd)'s are in Btu/hr-F, (Cd)'s in Btu/ft^2-F.

is contained within the 0-3 μm range. On the other hand, less than 0.01 percent of the radiant energy emitted by a black surface at 530 R (room temperature) is in that wavelength range. Even at 750 R†, less than 0.4 percent of the emitted radiation is of wavelengths below 3 μm. The semigray or two-band analysis suggested by Bobco [2] is based on the foregoing facts. The use of such a two-band model to account for the spectral dependence of the surface properties of spacecrafts has been examined by Plamondon and Landram [3] and found to yield very good results.

A simple and often realistic description of the directional properties of the surfaces is a subdivision of the hemispherical reflectance into diffuse and specular components; i.e., $\rho = \rho_d + \rho_s$. In the analysis that follows, we shall adopt such an idealization which, together with the semigray approximation and the assumption of diffuse emission, makes possible an analytical treatment of the problem in a reasonably straightforward manner. The essence of such approach was used in a recent paper by Hering [4].

3.2.1 Radiant Flux in the Solar Spectrum

We first present a general formulation for an enclosure of N surfaces, each of which has a uniform temperature and is uniformly irradiated. The results will then be applied to the relatively simple configuration selected for the hypothetical spacecraft. All properties and radiant energies associated with the solar spectrum will be designated with an asterisk.

According to the two-band model, the emitted radiation in the

†This far exceeds the ordinary operating temperature range of present day spacecrafts.

solar spectrum from any surface of the system is completely negligible. Hence, the radiosity of a surface A_i is given by

$$B_i^* = \rho_{d,i}^* (SE_i^* + H_i^*) \tag{3.2.1}$$

in which E_i^* is a type of exchange factor, denoting the fraction of the solar flux incident on A_i directly and by all possible specular reflections. The irradiation H_i^* is given by

$$H_i^* = \sum_{j=1}^{N} E_{i-j}^* B_j^* \tag{3.2.2}$$

where the exchange factor E_{i-j}^* denotes the fraction of the diffuse radiation in the solar spectrum leaving A_i which arrives at A_j both directly and by all possible intervening specular reflections. We note that, in writing (3.2.2), the reciprocity relation $A_j E_{j-i}^* = A_i E_{i-j}^*$ has been used. Eliminating H_i^* from (3.2.1) and (3.2.2) yields

$$B_i^* = \rho_{d,i}^* SE_i^* + \rho_{d,i}^* \sum_{j=1}^{N} E_{i-j}^* B_j^* \tag{3.2.3}$$

which forms a system of N simultaneous, linear, algebraic equations for the N unknown radiosities. Once the B_i^*'s are known, the rate of solar energy absorbed by A_i can be calculated from

$$Q_i^* = A_i \alpha_i^* (SE_i^* + H_i^*)$$

$$= A_i \frac{\alpha_i^*}{\rho_{d,i}^*} B_i^* \qquad (3.2.4)$$

Obviously, B_i^* and, consequently, Q_i^* are independent of the system temperatures. The decoupling of the solar fluxes from those of the infrared radiation results in significant simplification of the analysis.

If a surface A_k reflects purely specularly, then $\rho_{d,k}^* = 0$ and, accordingly, B_k^* vanishes. In this case,

$$Q_k^* = A_k \alpha_k^* (SE_k^* + H_k^*) \qquad (3.2.5)$$

We now proceed to apply the foregoing results to the hypothetical spacecraft when the sun's rays are parallel to the front and rear faces of the bus and are either inclined at 45° or normal to the solar panels. Figure 3.2 shows the relevant geometries involved. To evaluate Q_1^*, Q_2^* and Q_3^*, we need only to consider an enclosure consisting of A_1, A_2, A_3 and an imaginary black surface $A_{e,L}$ at absolute zero. The latter comprises a rectangle with its long sides shown as the dotted line in Fig. 3.2 and two identical right triangles, both adjoining the rectangle. Clearly, $B_{e,L}^* = 0$. It is easy to see that

$$\left.\begin{aligned} E_1^* &= \cos 45^\circ,\ E_{1-1}^* = E_{1-2}^* = 0,\ E_{1-3}^* = F_{1-3} \\ E_2^* &= E_3^* = E_{2-2}^* = E_{3-3}^* = 0,\ E_{2-3}^* = F_{2-3} \end{aligned}\right\} \qquad (3.2.6a)$$

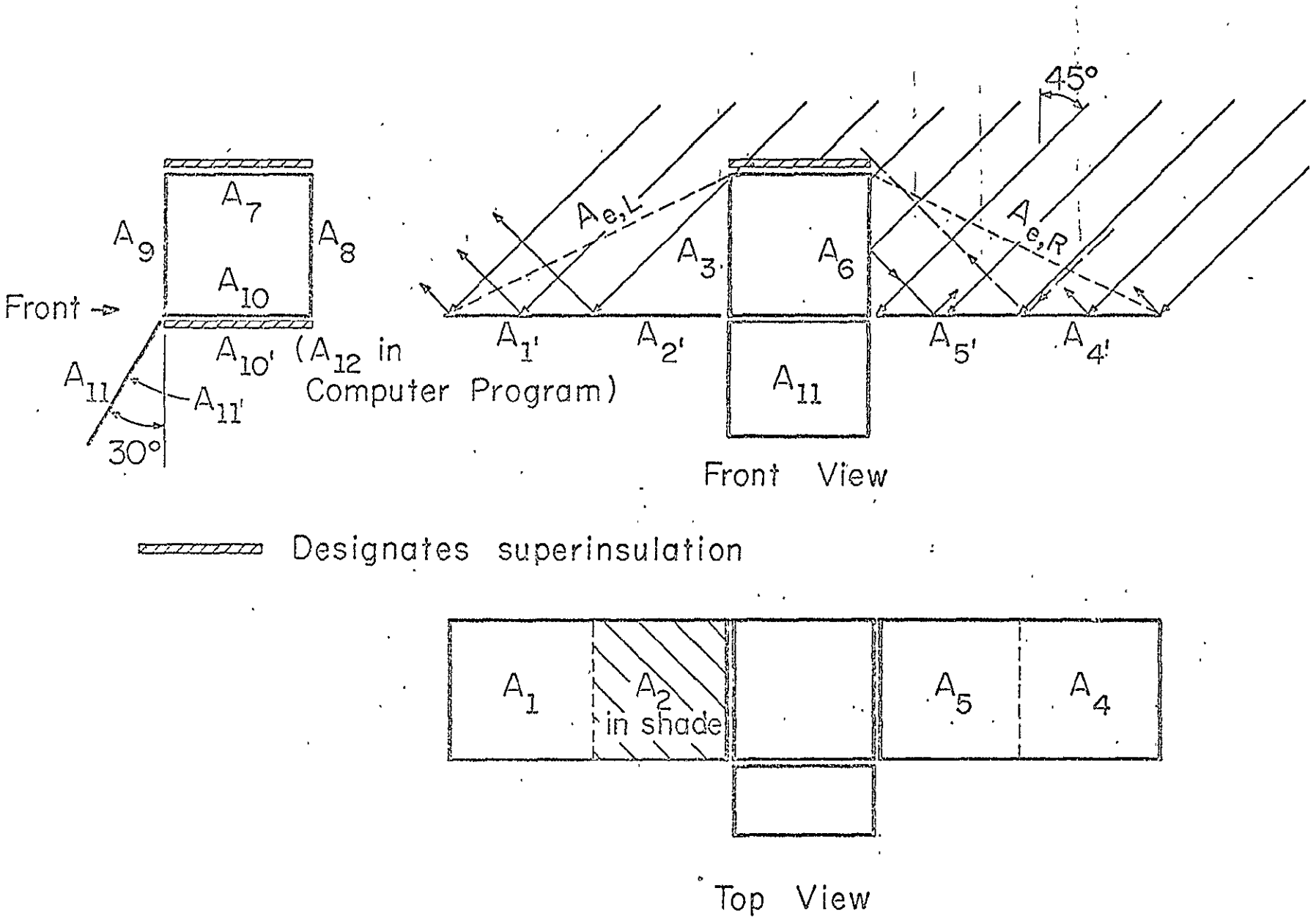

Figure 3.2 Radiation geometry associated with hypothetical spacecraft

Consequently, (3.2.3) becomes

$$\left.\begin{aligned} B_1^* - \rho_{d,1}^* F_{1-3} B_3^* &= \rho_{d,1}^* S \cos 45^\circ \\ B_2^* - \rho_{d,2}^* F_{2-3} B_3^* &= 0 \\ \rho_{d,3}^* (F_{3-1} B_1^* + F_{3-2} B_2^*) - B_3^* &= 0 \end{aligned}\right\} \qquad (3.2.7a)$$

When the radiosities are evaluated, Q_1^*, Q_2^* and Q_3^* can be determined from (3.2.4) or (3.2.5).

When the sun's rays are normal to the solar panel,

$$\left.\begin{aligned} E_1^* &= 1, \; E_{1-1}^* = E_{1-2}^* = 0, \; E_{1-3}^* = F_{1-3} \\ E_2^* &= 1, \; E_{2-2}^* = 0, \; E_{2-3}^* = F_{2-3} \\ E_3^* &= 0, \; E_{3-3}^* = 0 \end{aligned}\right\} \qquad (3.2.6b)$$

Consequently,

$$\left.\begin{aligned} B_1^* - \rho_{d,1}^* F_{1-3} B_3^* &= \rho_{d,1}^* S \\ B_2^* - \rho_{d,2}^* F_{2-3} B_3^* &= \rho_{d,2}^* S \\ \rho_{d,3}^* (F_{3-1} B_1^* + F_{3-2} B_2^*) - B_3^* &= 0 \end{aligned}\right\} \qquad (3.2.7b)$$

To evaluate Q_4^*, Q_5^* and Q_6^* we consider a similar enclosure consisting of A_4, A_5, A_6 and the associated imaginary black surface $A_{e,R.}$ at absolute zero. Again, referring to Fig. 3.2, we have

$$\left.\begin{aligned} E_4^* &= \cos 45^\circ, \; E_{4-4}^* = 0, \; E_{4-5}^* = 0, \; E_{4-6}^* = F_{4-6} \\ E_5^* &= (1 + \rho_{s,6}^*) \cos 45^\circ, \; E_{5-5}^* = 0, \; E_{5-6}^* = F_{5-6} \\ E_6^* &= (1 + \rho_{s,5}^*) \cos 45^\circ, \; E_{6-6}^* = 0 \end{aligned}\right\} \qquad (3.2.8)$$

and,

$$\left.\begin{aligned} B_4^* - \rho_{d,4}^* F_{4-6} B_6^* &= \rho_{d,4}^* S \cos 45^\circ \\ B_5^* - \rho_{d,5}^* F_{5-6} B_6^* &= \rho_{d,5}^* (1 + \rho_{s,6}^*) S \cos 45^\circ \\ \rho_{d,6}^* (F_{6-4} B_4^* + F_{6-5} B_5^*) - B_6^* &= -\rho_{d,6}^* (1 + \rho_{s,5}^*) S \cos 45^\circ \end{aligned}\right\} \qquad (3.2.9)$$

As before, when the radiosities are evaluated, Q_4^*, Q_5^* and Q_6^* can be readily calculated.

When the sun's rays are normal to the solar panel, the relevant radiosities can be evaluated from (3.2.7b) provided that the subscripts 1, 2 and 3 are replaced by 4, 5 and 6, respectively.

By following the same procedure, we may evaluate Q_9^* and Q_{11}^*. The results are:

(a) For oblique solar irradiation

$$Q_9^* = A_9 \alpha_9^* \frac{\rho_{d,11}^* F_{9-11}}{1 - \rho_{d,9}^* \rho_{d,11}^* F_{9-11} F_{11-9}} S \cos 45^\circ \sin 30^\circ \qquad (3.2.10a)$$

$$Q_{11}^* = A_{11} \alpha_{11}^* \frac{1}{1 - \rho_{d,9}^* \rho_{d,11}^* F_{9-11} F_{11-9}} S \cos 45^\circ \sin 30^\circ \qquad (3.2.10b)$$

(b) For normal solar irradiation

It is only necessary to replace cos 45° in (3.2.10a,b) by unity.

The top face A_7 of the spacecraft bus is completely shielded from the sun's rays by a multilayer superinsulation. The Appendix of this report gives a detailed analysis of the thermal resistance of the superinsulation and presents an expression from which the leakage flux may be determined. The rear and bottom face A_8 and A_{10} of the

bus do not receive radiation in the solar spectrum, either directly or indirectly. Hence, $Q_8^* = Q_{10}^* = 0$.

3.2.2 Radiation Heat Transfer in the Infrared

Once again for generality, we first consider an enclosure of N surfaces, each having a uniform temperature and being uniformly irradiated. It is assumed that all emitted radiations are diffuse and that the surface reflectances can be adequately described by the ρ_d-ρ_s model. Our objective here is to deduce expressions for the overall radiant exchange factor similar to Hottel's diffuse exchange factor $\mathcal{J}$. All surfaces are taken as gray within the spectral range. Clearly, the results will be directly applicable to the determination of similar exchange factors for internal radiation within the spacecraft bus.

For any surface A_i of the enclosure,

$$B_i = \varepsilon_i \sigma T_i^4 + \rho_{d,i} H_i \tag{3.2.11}$$

and

$$H_i = \sum_{j=1}^{N} E_{i-j} B_j \tag{3.2.12}$$

Thus,

$$B_i = \varepsilon_i \sigma T_i^4 + \rho_{d,i} \sum_{j=1}^{N} E_{i-j} B_j \tag{3.2.13}$$

The system of simultaneous, linear, algebraic equations (3.2.13) can be rewritten as

$$\sum_{j=1}^{N} a_{ij} B_j = \varepsilon_i \sigma T_i^4, \quad i = 1, 2, \cdots, N \tag{3.2.14}$$

where,

$$a_{ij} = \delta_{ij} - \rho_{d,i} E_{i-j} \tag{3.2.15}$$

To evaluate the diffuse-specular overall exchange factor $\mathcal{G}_{i-k}$, we set $\sigma T_i^4 = 1$ and the temperatures of *all remaining surfaces* to zero. The heat flow rate at A_k is

$${}_iQ_k = A_k \alpha_{k\,i} H_k = A_k \alpha_k \sum E_{k-j}\ {}_iB_j \tag{3.2.16}$$

where the presubscript i is a reminder of the original source of the flux. We recognize that ${}_iB_j$ $(j = 1, 2, \cdots, N)$ is the solution set of (3.2.14) with the latter's right-hand side set to zero except for the ith equation, for which it is ε_i. It is most convenient to evaluate ${}_iB_j$ by matrix inversion.

Let $[b_{ij}]$ be the inverse of the coefficient matrix $[a_{ij}]$. That is,

$$\left[a_{ij}\right]^{-1} = \left[b_{ij}\right] = \begin{bmatrix} b_{11} & b_{12} & \cdots & b_{1N} \\ b_{21} & b_{22} & \cdots & b_{2N} \\ \vdots & & & \\ b_{N1} & b_{N2} & \cdots & b_{NN} \end{bmatrix} \tag{3.2.17}$$

It can be readily demonstrated that

$$_{i}B_{j} = \varepsilon_{i} b_{ji} \tag{3.2.18}$$

By definition, $_{i}Q_{k} = A_{i}\,\mathcal{F}_{i-k}$, it follows then

$$\mathcal{F}_{i-k} = \frac{A_k}{A_i}\,\alpha_k \varepsilon_i \sum_{j=1}^{N} E_{k-j} b_{ji} \tag{3.2.19}$$

We now proceed to apply the foregoing general results to evaluate $\mathcal{F}$ for the spacecraft's exterior surfaces. We first consider the enclosure formed by A_1, A_2, A_3 and $A_{e,L}$, the latter being black and at absolute zero.

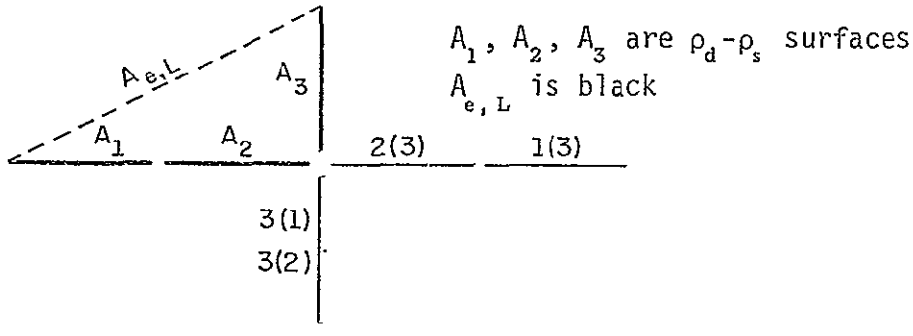

Figure 3.3 Mirror Images of Interacting Surfaces in an Enclosure Consisting of A_1, A_2, A_3 and $A_{e,L}$

In Fig. 3.3, the surfaces under consideration are identified with letters or numerals *immediately adjacent* to them. Thus, A_1 refers to the upper surface of the solar panel and A_3 the exterior surface of the left face of the spacecraft bus. The image surfaces are designated with two numerals; the one in parentheses refers to the mirror in which a surface in question is seen. For instance, 2(3) is the image of A_2 as seen in the mirror A_3. With the aid of Fig. 3.3, the various exchange factors can be readily written. They are:

$$\left.\begin{aligned} &E_{1-1} = E_{1-2} = 0, \quad E_{1-3} = F_{1-3}, \quad E_{1-e} = F_{1-e} + \rho_{s,3} F_{1(3)-e} \\ &E_{2-2} = 0, \quad E_{2-3} = F_{2-3}, \quad E_{2-e} = F_{2-e} + \rho_{s,3} F_{2(3)-e} \\ &E_{3-3} = 0, \quad E_{3-e} = F_{3-e} + \rho_{s,1} F_{3(1)-e} + \rho_{s,2} F_{3(2)-e} \end{aligned}\right\} \qquad (3.2.20a)$$

and the elements of the corresponding coefficient matrix are

$$\left.\begin{aligned} &a_{11} = 1, \quad a_{12} = 0, \quad a_{13} = -\rho_{d,1} E_{1-3}, \quad a_{1e} = -\rho_{d,1} E_{1-e} \\ &a_{21} = 0, \quad a_{22} = 1, \quad a_{23} = -\rho_{d,2} E_{2-3}, \quad a_{2e} = -\rho_{d,2} E_{2-e} \\ &a_{31} = -\rho_{d,3} E_{3-1}, \quad a_{32} = -\rho_{d,3} E_{3-2}, \quad a_{33} = 1, \quad a_{3e} = -\rho_{d,3} E_{3-e} \\ &a_{e1} = 0, \quad a_{e2} = 0, \quad a_{e3} = 0, \quad a_{ee} = 1 \end{aligned}\right\} \qquad (3.2.20b)$$

In (3.2.20a,b), the subscript e refers to $A_{e,L}$. Using the foregoing information, the diffuse-specular overall radiant exchange factors $\mathcal{F}_{1-2}$, $\mathcal{F}_{1-3}$, $\mathcal{F}_{1-e}$, $\mathcal{F}_{2-3}$, $\mathcal{F}_{2-e}$ and $\mathcal{F}_{3-e}$ can be evaluated immediately from (3.2.19). Exchange factors associated with A_4, A_5, A_6 and $A_{e,R}$ can likewise be determined. Surface A_8 sees *only* the empty space, thus the relevant $\mathcal{F}$ factor becomes its surface emittance.

Next, we consider the enclosure formed by A_9, A_{11} (upper surface of antenna) and the associated black surrounding $A_{e,F}$. Figure 3.4 shows the two relevant mirror images 9(11) and 11(9) associated with the system.

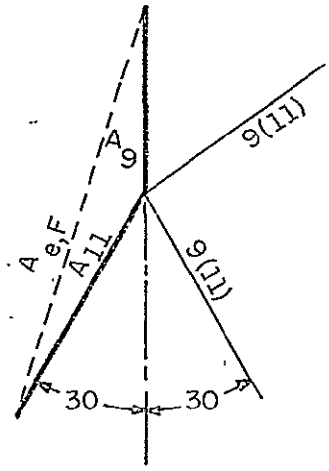

Figure 3.4 Mirror Images of Interacting Surfaces in an Enclosure Consisting of A_9, A_{11} and $A_{e,F}$

It is easy to see from Fig. 3.4 that the exchange factors are (with subscript e referring to $A_{e,F}$)

$$\left.\begin{aligned} E_{9-9} &= 0, \quad E_{9-11} = F_{9-11}, \quad E_{9-e} = F_{9-e} + \rho_{s,11} F_{9(11)-e} \\ E_{11-11} &= 0, \quad E_{11-e} = F_{11-e} + \rho_{s,9} F_{11(9)-e} \end{aligned}\right\} \qquad (3.2.21a)$$

and the corresponding a_{ij}'s are

$$\left.\begin{aligned} a_{9-9} &= 1, \quad a_{9-11} = -\rho_{d,9} E_{9-11}, \quad a_{9-e} = -\rho_{d,9} E_{9-e} \\ a_{11-9} &= -\rho_{d,11} E_{11-9}, \quad a_{11-11} = 1, \quad a_{11-e} = -\rho_{d,11} E_{11-e} \end{aligned}\right\} \qquad (3.2.21b)$$

The remaining system of the spacecraft's exterior surfaces for which the $\mathcal{J}$ factors are needed consists of the dark side of the solar

panels (A_1, A_2, A_4 and A_5), the outermost plastic film A_{10} of the superinsulation covering A_{10}, the shaded side of the antenna A_{11} and the associated empty space. Since none of the surfaces involved has a specular component of reflectances in the infrared region, the evaluation of a_{ij} and, subsequently, $\mathcal{G}_{i-j}$ requires information on shape factors, but not on exchange factors. The formulation presented in this section and the expressions (3.2.11) to (3.2.19) remain valid. All one needs to do is to replace $\rho_{d,i}$ by ρ_i and E_{i-j} by F_{i-j}. It goes without saying that the $\mathcal{G}$ factors for interior surfaces of the bus can be likewise evaluated.

3.3 NODAL HEAT BALANCE EQUATIONS

To formulate the nodal heat balance equations, we need to evaluate, in addition to the overall radiant exchange factors $\mathcal{F}$, the conductances of the various heat flow paths. We shall assume that there is no conductive link between the solar panels and the spacecraft bus, nor between the bus and the antenna. Further, the eleven sections (22 surfaces) which make up the spacecraft are taken to be identical squares† as illustrated in Fig. 3.2. Each section may have a different thickness, however. Under the foregoing conditions, the conductance between two adjacent areas, A_i and A_j, having a common edge is

$$K_{i-j} = 2\,\frac{(kd)_i\,(kd)_j}{(kd)_i + (kd)_j} \tag{3.3.1}$$

Clearly, $K_{i-j} = K_{j-i}$. If A_i and A_j are fabricated from the same material and are of identical thickness, like A_1 and A_2 (or A_4 and A_5) of the solar panel, then (3.3.1) reduces to

$$K_{i-j} = (kd)_i = (kd)_j \tag{3.3.1a}$$

It is pertinent to note that the crude subdivision used in the analysis should in no way jeopardize our present objective since the model is to be subdivided in *precisely* the same manner. In this regard, we may further add that, solely from the viewpoint of ascertaining the usefulness of the proposed theory, it makes no difference

†A significant simplification of the arithmetic results from this choice. It is <u>not</u> a restriction necessarily imposed on the analysis.

whether a continuum model or a discrete model is used in the analysis.

The top and bottom faces of the spacecraft bus are covered with superinsulation. The exposed layer of the superinsulation for the bottom face interacts radiatively with $A_{11'}$ and, thenceforth, with $A_{1'}$, $A_{2'}$, $A_{4'}$ and $A_{5'}$. An exact analysis of the thermal transients associated with its many layers is too involved and is not warranted for the problem under consideration. If we ignore its heat capacity, then a reasonably simple analysis can be made. It is demonstrated in APPENDIX A that the outward leakage flux (from the base plate A_{10} toward the outer surface of the insulation) is

$$\frac{Q}{A} = \frac{\sigma(T_{10}^4 - T_{10'}^4)}{\sum R} \tag{3.3.2}$$

where $\sum R = (n - 1)R + R'$. All quantities have been defined in APPENDIX A.

We now proceed to present the heat balance equations. The dimensional form will first be given: Set (3.3.3)

$$\begin{aligned} A_1: \quad (Cd)_1 \frac{dT_1}{dt} = q_1^* &- (\mathcal{F}_{1-2} + \mathcal{F}_{1'-2'})\sigma(T_1^4 - T_2^4) - \mathcal{F}_{1-3}\sigma(T_1^4 - T_3^4) \\ &- (\mathcal{F}_{1-e} + \mathcal{F}_{1'-e'})\sigma T_1^4 - \mathcal{F}_{1'-4'}\sigma(T_1^4 - T_4^4) \\ &- \mathcal{F}_{1'-5'}\sigma(T_1^4 - T_5^4) - \mathcal{F}_{1'-10'}\sigma(T_1^4 - T_{10'}^4) \\ &- \mathcal{F}_{1'-11'}\sigma(T_1^4 - T_{11}^4) - \frac{K_{1-2}}{A}(T_1 - T_2) \end{aligned}$$

$$A_2: \quad (Cd)_2 \frac{dT_2}{dt} = q_2^* - (\mathcal{F}_{2-1} + \mathcal{F}_{2'-1'})\sigma(T_2^4 - T_1^4) - \mathcal{F}_{2-3}\sigma(T_2^4 - T_3^4)$$
$$- (\mathcal{F}_{2'-e'} + \mathcal{F}_{2-e})\sigma T_2^4 - \mathcal{F}_{2'-4'}\sigma(T_2^4 - T_4^4)$$
$$- \mathcal{F}_{2'-5'}\sigma(T_2^4 - T_5^4) - \mathcal{F}_{2'-10'}\sigma(T_2^4 - T_{10'}^4)$$
$$- \mathcal{F}_{2'-11'}\sigma(T_2^4 - T_{11}^4) - \frac{K_{2-1}}{A}(T_2 - T_1)$$

$$A_3: \quad (Cd)_3 \frac{dT_3}{dt} = q_3^* + q_3 - \mathcal{F}_{3-1}\sigma(T_3^4 - T_1^4) - \mathcal{F}_{3-2}\sigma(T_3^4 - T_2^4)$$
$$- \mathcal{F}_{3-e}\sigma T_3^4 - \mathcal{F}_{3-6}\sigma(T_3^4 - T_6^4) - \mathcal{F}_{3-7}\sigma(T_3^4 - T_7^4)$$
$$- \mathcal{F}_{3-8}\sigma(T_3^4 - T_8^4) - \mathcal{F}_{3-9}\sigma(T_3^4 - T_9^4)$$
$$- \mathcal{F}_{3-10}\sigma(T_3^4 - T_{10}^4) - \frac{K_{3-7}}{A}(T_3 - T_7)$$
$$- \frac{K_{3-8}}{A}(T_3 - T_8) - \frac{K_{3-9}}{A}(T_3 - T_9)$$
$$- \frac{K_{3-10}}{A}(T_3 - T_{10})$$

$$A_4: \quad (Cd)_4 \frac{dT_4}{dt} = q_4^* - (\mathcal{F}_{4-5} + \mathcal{F}_{4'-5'})\sigma(T_4^4 - T_5^4) - \mathcal{F}_{4-6}\sigma(T_4^4 - T_6^4)$$
$$- (\mathcal{F}_{4-e} + \mathcal{F}_{4'-e'})\sigma T_4^4 - \mathcal{F}_{4'-1'}\sigma(T_4^4 - T_1^4)$$
$$- \mathcal{F}_{4'-2'}\sigma(T_4^4 - T_2^4) - \mathcal{F}_{4'-10'}\sigma(T_4^4 - T_{10'}^4)$$
$$- \mathcal{F}_{4'-11'}\sigma(T_4^4 - T_{11}^4) - \frac{K_{4-5}}{A}(T_4 - T_5)$$

$$A_5: \quad (Cd)_5 \frac{dT_5}{dt} = q_5^* - (\mathcal{F}_{5-4} + \mathcal{F}_{5'-4'})\sigma(T_5^4 - T_4^4) - \mathcal{F}_{5-6}\sigma(T_5^4 - T_6^4)$$
$$- (\mathcal{F}_{5-e} + \mathcal{F}_{5'-e'})\sigma T_5^4 - \mathcal{F}_{5'-1'}\sigma(T_5^4 - T_1^4)$$
$$- \mathcal{F}_{5'-2'}\sigma(T_5^4 - T_2^4) - \mathcal{F}_{5'-10'}\sigma(T_5^4 - T_{10'}^4)$$
$$- \mathcal{F}_{5'-11'}\sigma(T_5^4 - T_{11}^4) - \frac{K_{5-4}}{A}(T_5 - T_4)$$

$$A_6: \quad (Cd)_6 \frac{dT_6}{dt} = q_6^* + q_6 - \mathcal{F}_{6-4}\sigma(T_6^4 - T_4^4) - \mathcal{F}_{6-5}\sigma(T_6^4 - T_5^4)$$
$$- \mathcal{F}_{6-e}\sigma T_6^4 - \mathcal{F}_{6-3}\sigma(T_6^4 - T_3^4) - \mathcal{F}_{6-7}\sigma(T_6^4 - T_7^4)$$
$$- \mathcal{F}_{6-8}\sigma(T_6^4 - T_8^4) - \mathcal{F}_{6-9}\sigma(T_6^4 - T_9^4)$$
$$- \mathcal{F}_{6-10}\sigma(T_6^4 - T_{10}^4) - \frac{K_{6-7}}{A}(T_6 - T_7)$$
$$- \frac{K_{6-8}}{A}(T_6 - T_8) - \frac{K_{6-9}}{A}(T_6 - T_9) - \frac{K_{6-10}}{A}(T_6 - T_{10})$$

$$A_7: \quad (Cd)_7 \frac{dT_7}{dt} = \frac{1}{\sum R}\left(\frac{\alpha_p^*}{\varepsilon_p} S \cos\theta_s - \sigma T_7^4\right) - \mathcal{F}_{7-3}\sigma(T_7^4 - T_3^4)$$
$$- \mathcal{F}_{7-6}\sigma(T_7^4 - T_6^4) - \mathcal{F}_{7-8}\sigma(T_7^4 - T_8^4)$$
$$- \mathcal{F}_{7-9}\sigma(T_7^4 - T_9^4) - \mathcal{F}_{7-10}\sigma(T_7^4 - T_{10}^4)$$
$$- \frac{K_{7-3}}{A}(T_7 - T_3) - \frac{K_{7-6}}{A}(T_7 - T_6) - \frac{K_{7-8}}{A}(T_7 - T_8)$$
$$- \frac{K_{7-9}}{A}(T_7 - T_9)$$

$$A_8: \quad (Cd)_8 \frac{dT_8}{dt} = q_8 - \varepsilon_8 \sigma T_8^4 - \mathcal{F}_{8-3}\sigma(T_8^4 - T_3^4) - \mathcal{F}_{8-6}\sigma(T_8^4 - T_6^4)$$
$$- \mathcal{F}_{8-7}\sigma(T_8^4 - T_7^4) - \mathcal{F}_{8-9}\sigma(T_8^4 - T_9^4)$$
$$- \mathcal{F}_{8-10}\sigma(T_8^4 - T_{10}^4) - \frac{K_{8-3}}{A}(T_8 - T_3)$$
$$- \frac{K_{8-6}}{A}(T_8 - T_6) - \frac{K_{8-7}}{A}(T_8 - T_7)$$
$$- \frac{K_{8-10}}{A}(T_8 - T_{10})$$

$$A_9: \quad (Cd)_9 \frac{dT_9}{dt} = q_9^* + q_9 - \mathcal{F}_{9-11}\sigma(T_9^4 - T_{11}^4) - \mathcal{F}_{9-e}\sigma T_9^4$$
$$- \mathcal{F}_{9-3}\sigma(T_9^4 - T_3^4) - \mathcal{F}_{9-6}\sigma(T_9^4 - T_6^4)$$
$$- \mathcal{F}_{9-7}\sigma(T_9^4 - T_7^4) - \mathcal{F}_{9-8}\sigma(T_9^4 - T_8^4)$$
$$- \mathcal{F}_{9-10}\sigma(T_9^4 - T_{10}^4) - \frac{K_{9-3}}{A}(T_9 - T_3)$$
$$- \frac{K_{9-6}}{A}(T_9 - T_6) - \frac{K_{9-7}}{A}(T_9 - T_7) - \frac{K_{9-10}}{A}(T_9 - T_{10})$$

$$A_{10}: (Cd)_{10} \frac{dT_{10}}{dt} = - \frac{1}{\sum R}\sigma(T_{10}^4 - T_{10}^4) - \mathcal{F}_{10-3}\sigma(T_{10}^4 - T_3^4)$$
$$- \mathcal{F}_{10-6}\sigma(T_{10}^4 - T_6^4) - \mathcal{F}_{10-7}\sigma(T_{10}^4 - T_7^4)$$
$$- \mathcal{F}_{10-8}\sigma(T_{10}^4 - T_8^4) - \mathcal{F}_{10-9}\sigma(T_{10}^4 - T_9^4)$$
$$- \frac{K_{10-3}}{A}(T_{10} - T_3) - \frac{K_{10-6}}{A}(T_{10} - T_6)$$
$$- \frac{K_{10-8}}{A}(T_{10} - T_8) - \frac{K_{10-9}}{A}(T_{10} - T_9)$$

$$A_{10'}: \quad 0 = \frac{1}{\sum R}\,\sigma(T_{10}^4 - T_{10'}^4) - \mathcal{F}_{10'-1'}\,\sigma(T_{10'}^4 - T_1^4)$$

$$- \mathcal{F}_{10'-2'}\,\sigma(T_{10'}^4 - T_2^4) - \mathcal{F}_{10'-4'}\,\sigma(T_{10}^4 - T_4^4)$$
$$- \mathcal{F}_{10'-5'}\,\sigma(T_{10'}^4 - T_5^4) - \mathcal{F}_{10'-11'}\,\sigma(T_{10'}^4 - T_{11}^4)$$
$$- \mathcal{F}_{10'-e'}\,\sigma T_{10'}^4$$

$$A_{11}: \quad (Cd)_{11}\frac{dT_{11}}{dt} = q_{11}^* - \mathcal{F}_{11-9}\sigma(T_{11}^4 - T_9^4) - \mathcal{F}_{11-e}\sigma T_{11}^4$$
$$- \mathcal{F}_{11'-1'}\,\sigma(T_{11}^4 - T_1^4) - \mathcal{F}_{11'-2'}\,\sigma(T_{11}^4 - T_2^4)$$
$$- \mathcal{F}_{11'-4'}\,\sigma(T_{11}^4 - T_4^4) - \mathcal{F}_{11'-5'}\,\sigma(T_{11}^4 - T_5^4)$$
$$- \mathcal{F}_{11'-10'}\,\sigma(T_{11}^4 - T_{10'}^4) - \mathcal{F}_{11'-e'}\,\sigma T_{11}^4$$

Nodal Heat Balance Equations in Dimensionless Form

To reduce the system of heat balance equations to appropriate dimensionless forms, we introduce the following nondimensional variables:

$$\phi_i = \frac{T_i}{T_o} \tag{3.3.4a}$$

$$\tau_i = \frac{k_i}{C_i}\frac{t}{A} \tag{3.3.4b}$$

$$\beta_i = \frac{\sigma T_o^3 A}{(kd)_i} \tag{3.3.4c}$$

where i = 1, 2, 3, etc., and T_o is a suitable reference temperature for the problem. Its choice is, to some extent, arbitrary. For instance, T_o may be taken as the initial uniform temperature of the

spacecraft or some representative average of its steady state temperatures prior to the initiation of thermal transients. Since the physical time t must necessarily be the same for all i's, the dimensionless time τ_i for the various component parts A_i must be so related that:

$$\tau_1 : \tau_2 : \tau_3 \cdots = \frac{k_1}{C_1} : \frac{k_2}{C_2} : \frac{k_3}{C_3} \cdots \tag{3.3.5}$$

By using (3.3.4a,b,c), we obtain the following non-dimensional form of the nodal heat balance equations: set (3.3.6)

$$A_1 : \frac{d\phi_1}{d\tau_1} = \frac{q_1^* A}{(kd)_1 T_o} - \beta_1 \Big[(\mathcal{F}_{1-2} + \mathcal{F}_{1-3} + \mathcal{F}_{1-e} + \mathcal{F}_{1'-2'} + \mathcal{F}_{1'-4'} + \mathcal{F}_{1'-5'} + \mathcal{F}_{1'-10'} + \mathcal{F}_{1'-11'} + \mathcal{F}_{1'-e'})\phi_1^4 - (\mathcal{F}_{1-2} + \mathcal{F}_{1'-2'})\phi_2^4 - \mathcal{F}_{1-3}\phi_3^4 - \mathcal{F}_{1'-4'}\phi_4^4 - \mathcal{F}_{1'-5'}\phi_5^4 - \mathcal{F}_{1'-10'}\phi_{10'}^4 - \mathcal{F}_{1'-11'}\phi_{11}^4 \Big] - \frac{K_{1-2}}{(kd)_1}(\phi_1 - \phi_2)$$

$$A_2 : \frac{d\phi_2}{d\tau_2} = \frac{q_2^* A}{(kd)_2 T_o} - \beta_2 \Big[\mathcal{F}_{2-1} + \mathcal{F}_{2-3} + \mathcal{F}_{2-e} + \mathcal{F}_{2'-1'} + \mathcal{F}_{2'-4'} + \mathcal{F}_{2'-5'} + \mathcal{F}_{2'-10'} + \mathcal{F}_{2'-11'} + \mathcal{F}_{2'-e'})\phi_2^4 - (\mathcal{F}_{2-1} + \mathcal{F}_{2'-1'})\phi_1^4 - \mathcal{F}_{2-3}\phi_3^4 - \mathcal{F}_{2'-4'}\phi_4^4 - \mathcal{F}_{2'-5'}\phi_5^4 - \mathcal{F}_{2'-10'}\phi_{10'}^4 - \mathcal{F}_{2'-11'}\phi_{11}^4 \Big] - \frac{K_{2-1}}{(kd)_2}(\phi_2 - \phi_1)$$

$$A_3: \quad \frac{d\phi_3}{d\tau_3} = \frac{(q_3^{*} + q_3)A}{(kd)_3 T_o} - \beta_3 \left[(\mathcal{F}_{3-1} + \mathcal{F}_{3-2} + \mathcal{F}_{3-e} + \mathcal{F}_{3-6} + \mathcal{F}_{3-7} + \mathcal{F}_{3-8} + \mathcal{F}_{3-9} + \mathcal{F}_{3-10})\phi_3^4 - \mathcal{F}_{3-1}\phi_1^4 - \mathcal{F}_{3-2}\phi_2^4 - \mathcal{F}_{3-6}\phi_6^4 - \mathcal{F}_{3-7}\phi_7^4 - \mathcal{F}_{3-8}\phi_8^4 - \mathcal{F}_{3-9}\phi_9^4 - \mathcal{F}_{3-10}\phi_{10}^4 \right] - \frac{1}{(kd)_3}(K_{3-7} + K_{3-8} + K_{3-9} + K_{3-10})\phi_3 + \frac{K_{3-7}}{(kd)_3}\phi_7 + \frac{K_{3-8}}{(kd)_3}\phi_8 + \frac{K_{3-9}}{(kd)_3}\phi_9 + \frac{K_{3-10}}{(kd)_3}\phi_{10}$$

$$A_4: \quad \frac{d\phi_4}{d\tau_4} = \frac{q_4^{*}A}{(kd)_4 T_o} - \beta_4 \left[(\mathcal{F}_{4-5} + \mathcal{F}_{4-6} + \mathcal{F}_{4-e} + \mathcal{F}_{4'-1'} + \mathcal{F}_{4'-2'} + \mathcal{F}_{4'-5'} + \mathcal{F}_{4'-10'} + \mathcal{F}_{4'-11'} + \mathcal{F}_{4'-e'})\phi_4^4 - (\mathcal{F}_{4-5} + \mathcal{F}_{4'-5'})\phi_5^4 - \mathcal{F}_{4-6}\phi_6^4 - \mathcal{F}_{4'-1'}\phi_1^4 - \mathcal{F}_{4'-2'}\phi_2^4 - \mathcal{F}_{4'-10'}\phi_{10'}^4 - \mathcal{F}_{4'-11'}\phi_{11}^4 \right] - \frac{K_{4-5}}{(kd)_4}(\phi_4 - \phi_5)$$

$$A_5: \quad \frac{d\phi_5}{d\tau_5} = \frac{q_5^{*}A}{(kd)_5 T_o} - \beta_5 \left[(\mathcal{F}_{5-4} + \mathcal{F}_{5-6} + \mathcal{F}_{5-e} + \mathcal{F}_{5'-4'} + \mathcal{F}_{5'-1'} + \mathcal{F}_{5'-2'} + \mathcal{F}_{5'-10'} + \mathcal{F}_{5'-11'} + \mathcal{F}_{5'-e'})\phi_5^4 - (\mathcal{F}_{5-4} + \mathcal{F}_{5'-4'})\phi_4^4 - \mathcal{F}_{5-6}\phi_6^4 - \mathcal{F}_{5'-1'}\phi_1^4 - \mathcal{F}_{5'-2'}\phi_2^4 - \mathcal{F}_{5'-10'}\phi_{10'}^4 - \mathcal{F}_{5'-11'}\phi_{11}^4 \right] - \frac{K_{5-4}}{(kd)_5}(\phi_5 - \phi_4)$$

$$A_6: \quad \frac{d\phi_6}{d\tau_6} = \frac{(q_6^* + q_6)A}{(kd)_6 T_o} - \beta_6 \Big[(\mathcal{F}_{6-4} + \mathcal{F}_{6-5} + \mathcal{F}_{6-e} + \mathcal{F}_{6-3} + \mathcal{F}_{6-7} + \mathcal{F}_{6-8} + \mathcal{F}_{6-9} + \mathcal{F}_{6-10})\phi_6^4 - \mathcal{F}_{6-4}\phi_4^4 - \mathcal{F}_{6-5}\phi_5^4 - \mathcal{F}_{6-3}\phi_3^4 - \mathcal{F}_{6-7}\phi_7^4 - \mathcal{F}_{6-8}\phi_8^4 - \mathcal{F}_{6-9}\phi_9^4 - \mathcal{F}_{6-10}\phi_{10}^4 \Big] - \frac{1}{(kd)_6}(K_{6-7} + K_{6-8} + K_{6-9} + K_{6-10})\phi_6 + \frac{K_{6-7}}{(kd)_6}\phi_7 + \frac{K_{6-8}}{(kd)_6}\phi_8 + \frac{K_{6-9}}{(kd)_6}\phi_9 + \frac{K_{6-10}}{(kd)_6}\phi_{10}$$

$$A_7: \quad \frac{d\phi_7}{d\tau_7} = \frac{1}{\sum R}\frac{\alpha_p^*}{\varepsilon_p}\frac{SA\cos\theta_s}{(kd)_7 T_o} - \beta_7 \Big[\Big(\frac{1}{\sum R} + \mathcal{F}_{7-3} + \mathcal{F}_{7-6} + \mathcal{F}_{7-8} + \mathcal{F}_{7-9} + \mathcal{F}_{7-10} \Big) \phi_7^4 - \mathcal{F}_{7-3}\phi_3^4 - \mathcal{F}_{7-6}\phi_6^4 - \mathcal{F}_{7-8}\phi_8^4 - \mathcal{F}_{7-9}\phi_9^4 - \mathcal{F}_{7-10}\phi_{10}^4 \Big] - \frac{1}{(kd)_7}(K_{7-3} + K_{7-6} + K_{7-8} + K_{7-9})\phi_7 + \frac{K_{7-3}}{(kd)_7}\phi_3 + \frac{K_{7-6}}{(kd)_7}\phi_6 + \frac{K_{7-8}}{(kd)_7}\phi_8 + \frac{K_{7-9}}{(kd)_7}\phi_9$$

$$A_8: \quad \frac{d\phi_8}{d\tau_8} = \frac{q_8 A}{(kd)_8 T_o} - \beta_8 \Big[(\varepsilon_8 + \mathcal{F}_{8-3} + \mathcal{F}_{8-6} + \mathcal{F}_{8-7} + \mathcal{F}_{8-9} + \mathcal{F}_{8-10})\phi_8^4 - \mathcal{F}_{8-3}\phi_3^4 - \mathcal{F}_{8-6}\phi_6^4 - \mathcal{F}_{8-7}\phi_7^4 - \mathcal{F}_{8-9}\phi_9^4 - \mathcal{F}_{8-10}\phi_{10}^4 \Big] - \frac{1}{(kd)_8}(K_{8-3} + K_{8-6} + K_{8-7} + K_{8-10})\phi_8 + \frac{K_{8-3}}{(kd)_8}\phi_3 + \frac{K_{8-6}}{(kd)_8}\phi_6 + \frac{K_{8-7}}{(kd)_8}\phi_7 + \frac{K_{8-10}}{(kd)_8}\phi_{10}$$

$$A_9: \quad \frac{d\phi_9}{d\tau_9} = \frac{(q_9^{\ddagger} + q_9)A}{(kd)_9 T_o} - \beta_9 \left[(\mathcal{F}_{9-11} + \mathcal{F}_{9-e} + \mathcal{F}_{9-3} + \mathcal{F}_{9-6} + \mathcal{F}_{9-7} + \mathcal{F}_{9-8} + \mathcal{F}_{9-10})\phi_9^4 - \mathcal{F}_{9-11}\phi_{11}^4 - \mathcal{F}_{9-3}\phi_3^4 - \mathcal{F}_{9-6}\phi_6^4 - \mathcal{F}_{9-7}\phi_7^4 - \mathcal{F}_{9-8}\phi_8^4 - \mathcal{F}_{9-10}\phi_{10}^4 \right] - \frac{1}{(kd)_9}(K_{9-3} + K_{9-6} + K_{9-7} + K_{9-10})\phi_9 + \frac{K_{9-3}}{(kd)_9}\phi_3 + \frac{K_{9-6}}{(kd)_9}\phi_6 + \frac{K_{9-7}}{(kd)_9}\phi_7 + \frac{K_{9-10}}{(kd)_9}\phi_{10}$$

$$A_{10}: \quad \frac{d\phi_{10}}{d\tau_{10}} = -\beta_{10} \left[\left(\frac{1}{\sum R} + \mathcal{F}_{10-3} + \mathcal{F}_{10-6} + \mathcal{F}_{10-7} + \mathcal{F}_{10-8} + \mathcal{F}_{10-9} \right) \phi_{10}^4 - \frac{1}{\sum R}\phi_{10'}^4 - \mathcal{F}_{10-3}\phi_3^4 - \mathcal{F}_{10-6}\phi_6^4 - \mathcal{F}_{10-7}\phi_7^4 - \mathcal{F}_{10-8}\phi_8^4 - \mathcal{F}_{10-9}\phi_9^4 \right] - \frac{1}{(kd)_{10}}(K_{10-3} + K_{10-6} + K_{10-8} + K_{10-9})\phi_{10} + \frac{K_{10-3}}{(kd)_{10}}\phi_3 + \frac{K_{10-6}}{(kd)_{10}}\phi_6 + \frac{K_{10-8}}{(kd)_{10}}\phi_8 + \frac{K_{10-9}}{(kd)_{10}}\phi_9$$

$$A_{10'}: \quad 0 = \frac{1}{\sum R}\phi_{10}^4 + \mathcal{F}_{10'-1'}\phi_1^4 + \mathcal{F}_{10'-2'}\phi_2^4 + \mathcal{F}_{10'-4'}\phi_4^4 + \mathcal{F}_{10'-5'}\phi_5^4 + \mathcal{F}_{10'-11'}\phi_{11}^4 - \left(\frac{1}{\sum R} + \mathcal{F}_{10'-1'} + \mathcal{F}_{10'-2'} + \mathcal{F}_{10'-4'} + \mathcal{F}_{10'-5'} + \mathcal{F}_{10'-11'} + \mathcal{F}_{10'-e'} \right)\phi_{10'}^4$$

$$A_{11}: \quad \frac{d\phi_{11}}{d\tau_{11}} = \frac{q^{*}_{11} A}{(kd)_{11} T_o} - \beta_{11} \Big[(\mathcal{F}_{11-9} + \mathcal{F}_{11-e} + \mathcal{F}_{11'-1'} + \mathcal{F}_{11'-2'} + \mathcal{F}_{11'-4'} + \mathcal{F}_{11'-5'} + \mathcal{F}_{11'-10'} + \mathcal{F}_{11'-e'}) \phi^4_{11} - \mathcal{F}_{11-9} \phi^4_9 - \mathcal{F}_{11'-1'} \phi^4_1 - \mathcal{F}_{11'-2'} \phi^4_2 - \mathcal{F}_{11'-4'} \phi^4_4 - \mathcal{F}_{11'-5'} \phi^4_5 - \mathcal{F}_{11'-10'} \phi^4_{10'} \Big]$$

In numerical computations, if we arbitrarily select τ_3 as the "standard" dimensionless time, then

$$\frac{d\phi_1}{d\tau_1} = \left(\frac{k_3}{k_1} \frac{C_1}{C_3}\right) \frac{d\phi_1}{d\tau_3}$$

$$\frac{d\phi_2}{d\tau_2} = \left(\frac{k_3}{k_2} \frac{C_2}{C_3}\right) \frac{d\phi_2}{d\tau_3}, \text{ etc.}$$

3.4 MODELING REQUIREMENTS

An inspection of the dimensionless heat balance equations reveals that, for perfect modeling, the following scaling requirements must be met.

1. Model and prototype are geometrically similar in order that all configuration factors among corresponding surfaces are identical. (Thickness distortion would have very minor or little influence on radiation exchange and is thus permitted.)

2. Radiation properties of all corresponding surfaces are identical.

The satisfaction of (1) and (2) ensures that the model and the prototype have the same $\mathcal{F}$ for all corresponding surfaces.

3. The simulated solar radiation used in model testing has a spectral distribution, intensity and direction the same as those of the local sun's rays incident on the spacecraft.

4. The (kd)'s and (Cd)'s of all corresponding surfaces must satisfy the following relationships:

$$\frac{(kd)_m}{(kd)_p} = \frac{A_m}{A_p} = \left(\frac{L_m}{L_p}\right)^2 \quad , \quad \text{a fixed quantity} \tag{3.3.7a}$$

$$\frac{(Cd)_m}{(Cd)_p} = \frac{t_m}{t_p} \quad , \quad \text{a fixed quantity} \tag{3.3.7b}$$

The first is associated with the geometric scale ratio and the second the time scale ratio.

5. The internal power dissipation, when expressed in terms of the equivalent surface flux, is the same for the prototype and the model, i.e.,

$$q_m = q_p \tag{3.3.7c}$$

for all corresponding surfaces of the spacecraft bus.

Finally, we note that, for complete similitude, the initial temperature field of the model and of the prototype must either be uniform or have identical distributions. The foregoing modeling requirements have previously been stated in the literature, e.g., [5], and experimental verifications are available [6a,b,c].

Chapter 4

SOLAR FLUXES, DIFFUSE-SPECULAR OVERALL EXCHANGE FACTORS AND CONDUCTANCES OF HEAT FLOW PATHS ASSOCIATED WITH THE HYPOTHETICAL SPACECRAFT

As a prerequisite for the numerical solution of the nodal heat balance equations, the solar fluxes Q_i^*/A_i, the overall radiant exchange factors $\mathcal{F}_{i-j}$ and the conductance of the heat flow paths K_{i-j} associated with the various surfaces of the hypothetical spacecraft must be evaluated. All relevant configuration factors can be readily determined since all surfaces or their subdivisions are chosen to be identical squares as illustrated in Fig. 3.1. The results are listed in TABLES 4.3 and 4.8 for surfaces facing the sun and in TABLE 4.13 for surfaces away from the sun. The data were taken either directly from an NACA Technical Note by Hamilton and Morgan [7] or indirectly evaluated from the information given therein. The solar exchange factors were calculated from (3.2.6a or b) and (3.2.8) and the solar radiosities from (3.2.7a or b) and (3.2.9). The irradiation H_i^* is then given by (3.2.2) and the required Q_i^* follows from (3.2.4) or (3.2.5). For surfaces A_9 and A_{11}, the solar fluxes can be directly determined from (3.2.10a or b). In these calculations, the solar constant S was arbitrarily assumed to be 442 Btu/hr-ft^2 and the relevant reflectances and absorptances were taken from TABLE 3.2. The solar fluxes so calculated are listed in TABLES 4.1 and 4.2, respectively, for the normal and oblique incidence of sun's rays.

The procedure used in the determination of the diffuse-specular overall exchange factors for the spacecraft's *exterior* surfaces has been explained in detail in Chapter 3. Following the evaluation of the exchange factor E_{i-j}, the elements of the coefficient matrix a_{i-j} were calculated according to (3.2.15) and those of its inverse b_{i-j} were determined by using an available subroutine in our computer laboratory. For the convenience of the reader, these intermediate data are listed in TABLES 4.4 and 4.9 for E_{i-j}, in TABLES 4.5, 4.10, and 4.14 for a_{i-j} and in TABLES 4.6, 4.11, and 4.15 for b_{i-j}. The desired diffuse-specular overall exchange factors $\mathcal{G}_{i-j}$ were calculated from (3.2.19) and the results are listed in TABLES 4.7 and 4.12 for surfaces facing the sun and in TABLE 4.16 for surfaces away from the sun. It is pertinent to note that, for an enclosure of N surfaces, the overall exchange factors satisfy the following simple relation

$$\sum_{j=1}^{N} \mathcal{G}_{i-j} = \varepsilon_i \tag{4.1}$$

which is the consequence of the requirement of energy conservation. Equation (4.1) has been used to check the numerical accuracy of the data list in the three tables last mentioned.

For the *interior* of the spacecraft bus, the radiation was assumed to be devoid of specular component and, hence, only the diffuse overall exchange factor is involved. TABLES 4.17, 4.18, 4.19,

and 4.20 list, respectively, the data for the configuration factors F_{i-j}, the elements of the coefficient matrix a_{i-j}, the elements of the inverted matrix b_{i-j} and the diffuse overall exchange factors $\mathscr{F}_{i-j}$.

Finally, the conductances K_{i-j} are listed in TABLE 4.21. They were evaluated from (3.3.1) using information given in TABLE 3.2. It may be noted that there is no conductive link between the solar panels and the spacecraft bus, nor between the bus and the antenna.

NOTE: EXTERIOR OF SURFACE 10 IS DESIGNATED AS SURFACE 12

*** TABLE 4.1 SOLAR FLUX AT NORMAL INCIDENCE, Q*/A, BTU/HR,SQ.FT ***

1	2	3	4	5	6	7	8	9	10	11	12
353.5999	353.5999	0.0	353.5999	353.5999	0.0	0.0	0.0	0.2376	0.0	154.7000	0.0

*** TABLE 4.2 SOLAR FLUX AT 45 DEG INCIDENCE, Q*/A, BTU/HR,SQ.FT ***

1	2	3	4	5	6	7	8	9	10	11	12
250.0340	0.0	0.0	257.9092	298.0498	75.0102	0.0	0.0	0.1680	0.0	109.3899	0.0

********** EXTERIOR SURFACES **********

*** TABLE 4.3 CONFIGURATION FACTORS FA(I,J) ***

I / J	1	2	3	E
1	0.0	0.0	0.032810	0.967190
2	0.0	0.0	0.200040	0.799960
3	0.032810	0.200040	0.0	0.767150
1(3)	*********	*********	0.032810	0.032810
2(3)	*********	*********	0.200040	0.200040
3(1)	0.032810	*********	*********	0.032810
3(2)	*********	0.200040	*********	0.200040

*** TABLE 4.3 CONTINUED ***

I / J	4	5	6	E
4	0.0	0.0	0.032810	0.967190
5	0.0	0.0	0.200040	0.799960
6	0.032810	0.200040	0.0	0.767150
4(6)	*********	*********	0.032810	0.032810
5(6)	*********	*********	0.200040	0.200040
6(4)	0.032810	*********	*********	0.032810
6(5)	*********	0.200040	*********	0.200040

*** TABLE 4.4 EXCHANGE FACTORS E(I,J) **

I / J	1	2	3	E
1	0.0	0.0	0.032810	0.967190
2	0.0	0.0	0.200040	0.799960
3	0.032810	0.200040	0.0	0.767190

*** TABLE 4.4 CONTINUED ***

I / J	4	5	6	E
4	0.0	0.0	0.032810	0.967190
5	0.0	0.0	0.200040	0.799960
6	0.032810	0.200040	0.0	0.767190

*** TABLE 4.5 COEFFICIENT MATRIX AA(I,J) ***

I / J	1	2	3	E
1	1.000000	0.0	-0.006562	-0.193438
2	0.0	1.000000	-0.040008	-0.159992
3	-0.005578	-0.034007	1.000000	-0.130422
E	0.0	0.0	0.0	1.000000

*** TABLE 4.5 CONTINUED ***

I / J	4	5	6	E
4	1.000000	0.0	-0.006562	-0.193438
5	0.0	1.000000	-0.040008	-0.159992

FOLDOUT FRAME 2

6	-0.005578	-0.034007	1.000000	-0.130422
E	0.0	0.0	0.0	1.000000

*** TABLE 4.6 INVERSE OF COEFFICIENT MATRIX BB[I,J] ***

I / J	1	2	3	E
1	1.000036	0.000223	0.006571	0.194338
2	0.000223	1.001362	0.040064	0.165478
3	0.005585	0.034054	1.001399	0.137133
E	0.0	0.0	0.0	1.000000

*** TABLE 4.6 CONTINUED ***

I / J	4	5	6	E
4	1.000036	0.000223	0.006571	0.194338
5	0.000223	1.001362	0.040064	0.165478
6	0.005585	0.034054	1.001399	0.137133
E	0.0	0.0	0.0	1.000000

*** TABLE 4.7 DIFFUSE-SPECULAR OVER-ALL EXCHANGE FACTORS FF[I,J] ***

I / J	1	2	3	E
1	0.000117	0.000715	0.021816	0.777351
2	0.000715	0.004360	0.133012	0.661913
3	0.021816	0.133012	0.005670	0.669534

*** TABLE 4.7 CONTINUED ***

I / J	4	5	6	E
4	0.000117	0.000715	0.021816	0.777351
5	0.000715	0.004360	0.133012	0.661913
6	0.021816	0.133012	0.005670	0.669534

*** TABLE 4.8 CONFIGURATION FACTORS FA(I,J) ***

I / J	9	11	E
9	0.0	0.021500	0.978500
11	0.021500	0.0	0.978500
9(11)	0.489250	0.489250	0.0
11(9)	*********	0.021500	0.021500

*** TABLE 4.9 EXCHANGE FACTORS E(I,J) **

I / J	9	11	E
9	0.0	0.021500	0.978500
11	0.021500	0.0	0.998925

*** TABLE 4.10 COEFFICIENT MATRIX AA(I,J) ***

I / J	9	11	E
9	1.000000	0.0	0.0
11	-0.003870	1.000000	-0.179806
E	0.0	0.0	1.000000

*** TABLE 4.11 INVERSE OF COEFFICIENT MATRIX BB(I,J) ***

I / J	9	11	E
9	1.000000	0.0	0.0
11	0.003870	1.000000	0.179806
E	0.0	0.0	1.000000

*** TABLE 4.12 DIFFUSE-SPECULAR OVER-ALL EXCHANGE FACTORS FF(I,J) ***

I / J	9	11	E
9	0.000000	0.000881	0.049118
11	0.000881	0.0	0.819118

FOLDOUT FRAME 1

FOLDOUT FRAME 2

*** TABLE 4.13 CONFIGURATION FACTORS FA(I,J) ***

I / J	1'	2'	10'	5'	4'	11'	E
1'	0.0	0.0	0.0	0.0	0.0	0.002700	0.997300
2'	0.0	0.0	0.0	0.0	0.0	0.019500	0.980500
10'	0.0	0.0	0.0	0.0	0.0	0.087000	0.913000
5'	0.0	0.0	0.0	0.0	0.0	0.002700	0.997300
4'	0.0	0.0	0.0	0.0	0.0	0.019500	0.980500
11'	0.002700	0.019500	0.087000	0.002700	0.019500	0.0	0.868600

*** TABLE 4.14 COEFFICIENT MATRIX AA(I,J) ***

I / J	1'	2'	10'	5'	4'	11'	E
1'	1.000000	0.0	0.0	0.0	0.0	-0.000459	-0.169541
2'	0.0	1.000000	0.0	0.0	0.0	-0.003315	-0.166685
10'	0.0	0.0	1.000000	0.0	0.0	-0.043500	-0.456500
5'	0.0	0.0	0.0	1.000000	0.0	-0.000459	-0.169541
4'	0.0	0.0	0.0	0.0	1.000000	-0.003315	-0.166685
11'	-0.002565	-0.018525	-0.082650	-0.002565	-0.018525	1.000000	-0.825170

*** TABLE 4.15 INVERSE OF COEFFICIENT MATRIX BB(I,J) ***

I / J	1'	2'	10'	5'	4'	11'	E
1'	1.000001	0.000009	0.000038	0.000001	0.000009	0.000461	0.169942
2'	0.000009	1.000061	0.000275	0.000009	0.000062	0.003327	0.169580
10'	0.000112	0.000809	1.003608	0.000112	0.000809	0.043662	0.494484
5'	0.000001	0.000009	0.000038	1.000001	0.000009	0.000461	0.169942
4'	0.000009	0.000062	0.000275	0.000009	1.000061	0.003327	0.169580
11'	0.002575	0.018594	0.082959	0.002575	0.018594	1.003734	0.873194

*** TABLE 4.16 DIFFUSE OVER-ALL EXCHANGE FACTORS FB(I,J) ***

I / J	1'	2'	10'	5'	4'	11'	E
1'	0.000005	0.000035	0.000093	0.000005	0.000035	0.000112	0.829715
2'	0.000035	0.000250	0.000671	0.000035	0.000250	0.000812	0.827947
10'	0.000093	0.000671	0.001804	0.000093	0.000671	0.002183	0.494483
5'	0.000005	0.000035	0.000093	0.000005	0.000035	0.000112	0.829715
4'	0.000035	0.000250	0.000671	0.000035	0.000250	0.000812	0.827947
11'	0.000112	0.000812	0.002183	0.000112	0.000812	0.000010	0.045958

FOLDOUT FRAME 1

FOLDOUT FRAME 2

*** TABLE 4.17 CONFIGURATION FACTORS FA(I,J) ***

I / J	3	6	7	10	8	9
3	0.0	0.199820	0.200040	0.200040	0.200040	0.200040
6	0.199820	0.0	0.200040	0.200040	0.200040	0.200040
7	0.200040	0.200040	0.0	0.199820	0.200040	0.200040
10	0.200040	0.200040	0.199820	0.0	0.200040	0.200040
8	0.200040	0.200040	0.200040	0.200040	0.0	0.199820
9	0.200040	0.200040	0.200040	0.200040	0.199820	0.0

*** TABLE 4.18 COEFFICIENT MATRIX AA(I,J) ***

I / J	3	6	7	10	8	9
3	1.000000	-0.159856	-0.160032	-0.160032	-0.160032	-0.160032
6	-0.159856	1.000000	-0.160032	-0.160032	-0.160032	-0.160032
7	-0.030006	-0.030006	1.000000	-0.029973	-0.030006	-0.030006
10	-0.030006	-0.030006	-0.029973	1.000000	-0.030006	-0.030006
8	-0.030006	-0.030006	-0.030006	-0.030006	1.000000	-0.029973
9	-0.030006	-0.030006	-0.030006	-0.030006	-0.029973	1.000000

*** TABLE 4.19 INVERSE OF COEFFICIENT MATRIX BB(I,J) ***

I / J	3	6	7	10	8	9
3	1.057707	0.195533	0.220391	0.220391	0.220391	0.220391
6	0.195533	1.057709	0.220391	0.220391	0.220391	0.220391
7	0.041323	0.041323	1.017411	0.046514	0.046545	0.046545
10	0.041323	0.041323	0.046514	1.017411	0.046545	0.046545
8	0.041323	0.041323	0.046545	0.046545	1.017412	0.046514
9	0.041323	0.041323	0.046545	0.046545	0.046514	1.017412

*** TABLE 4.20 DIFFUSE OVER-ALL EXCHANGE FACTORS FF(I,J) ***

I / J	3	6	7	10	8	9
3	0.002885	0.009777	0.046833	0.046833	0.046833	0.046833
6	0.009777	0.002885	0.046833	0.046833	0.046833	0.046833
7	0.046833	0.046833	0.083875	0.224043	0.224193	0.224193
10	0.046833	0.046833	0.224043	0.083875	0.224193	0.224193
8	0.046833	0.046833	0.224193	0.224193	0.083875	0.224043

FOLDOUT FRAME 1

FOLDOUT FRAME 2

9	0.046833	0.046833	0.224193	0.224193	0.224043	0.083875

*** TABLE 4.21 DIMENSIONAL CONDUCTION LINKS AK(I,J), BTU/HR,DEG ***

I / J	1	2	3	4	5	6
1	0.0	0.058000	0.0	0.0	0.0	0.0
2	0.058000	0.0	0.0	0.0	0.0	0.0
3	0.0	0.0	0.0	0.0	0.0	0.0
4	0.0	0.0	0.0	0.0	0.058000	0.0
5	0.0	0.0	0.0	0.058000	0.0	0.0
6	0.0	0.0	0.0	0.0	0.0	0.0
7	0.0	0.0	0.071100	0.0	0.0	0.074391
8	0.0	0.0	0.471490	0.0	0.0	0.667263
9	0.0	0.0	0.560795	0.0	0.0	0.861395
10	0.0	0.0	0.033714	0.0	0.0	0.034437
11	0.0	0.0	0.0	0.0	0.0	0.0
12	0.0	0.0	0.0	0.0	0.0	0.0

*** TABLE 4.21 CONTINUED ***

I / J	7	8	9	10	11	12
1	0.0	0.0	0.0	0.0	0.0	0.0
2	0.0	0.0	0.0	0.0	0.0	0.0
3	0.071100	0.471490	0.560795	0.033714	0.0	0.0
4	0.0	0.0	0.0	0.0	0.0	0.0
5	0.0	0.0	0.0	0.0	0.0	0.0
6	0.074391	0.667263	0.861395	0.034437	0.0	0.0
7	0.0	0.070706	0.072435	0.0	0.0	0.0
8	0.070706	0.0	0.0	0.033626	0.0	0.0
9	0.072435	0.0	0.0	0.034012	0.0	0.0
10	0.0	0.033626	0.034012	0.0	0.0	0.0
11	0.0	0.0	0.0	0.0	0.0	0.0
12	0.0	0.0	0.0	0.0	0.0	0.0

FOLDOUT FRAME 2

FOLDOUT FRAME 1

CHAPTER 5

NUMERICAL SOLUTION OF NODAL HEAT BALANCE EQUATIONS

5.1 A RECAPITULATION

The dimensionless nodal heat balance equations for the hypothetical spacecraft presented in Chapter 3 and designated by the set (3.3.6) are simultaneous, non-linear, first order ordinary differential equations. They can be compactly described by (5.1.1) which is written for an arbitrary node i.

$$M_i \frac{d\phi_i}{d\tau} = Q_i - \beta_i \left[\left(C_{i-j} + \sum_j \mathcal{G}_{i-j} + \sum_{j'} \mathcal{G}_{i-j'} \right) \phi_i^4 - \left(C_{i-j} \phi_j^4 + \sum_j \mathcal{G}_{i-j} \phi_j^4 + \sum_{j'} \mathcal{G}_{i'-j'} \phi_{j'}^4 \right) \right] - \frac{1}{(kd)_i} \left(\phi_i \sum_{j \neq i} K_{i-j} - \sum_{j \neq i} K_{i-j} \phi_j \right) \qquad (5.1.1)$$

where

$\phi_{j'} \equiv \phi_j$

$M_i = \dfrac{k_o C_i}{k_i C_o}$, subscript o refers to a convenient reference surface for which the dimensionless time τ is related to the physical time t according to $\tau = (k_o/C_o A)t$. One of the surfaces in the system may suitably serve for this purpose.

$$Q_i = \frac{(q_i^* + q_i)A}{(kd)_i T_o}, \quad \text{except } Q_7 \text{ which is}$$

$$\frac{1}{\Sigma R} \frac{\alpha_P^*}{\varepsilon_P} \frac{S\ A \cos\theta_s}{(kd)_7 T_o}. \quad \text{Also, } Q_{10} = Q_{12} = 0$$

C_{i-j} = conductance of multi-layer insulation, $(\Sigma R)^{-1}$. The three nonvanishing conductances are C_{7-e}. C_{10-12} and C_{12-10}.

$\mathcal{F}_{i-j}$ = overall radiant exchange factor between A_i and A_j. The indicated summand refers to all A_j's which have direct and/or indirect radiant exchange with A_i. When approriate, A_j includes the empty space. A similar interpretation should be given to $\sum_{j'} \mathcal{F}_{i-j'}$.

K_{i-j} = conductance between A_i and A_j. Here, the indicated summand refers *only* to those surfaces which have physical contact with A_i.

All other quantities have previously been defined in Chapter 3.

The introduction of the dimensionless parameter M_i is to obtain a uniform time scale for all component surfaces in the system. An alternative is to replace the left hand side of (5.1.1) by

$$\frac{C_i A}{k_i} \frac{d\phi_i}{dt}$$

and the integration is to be carried out in the physical time domain. The latter is indeed adopted in our computer program for which separate

documents were prepared and submitted to JPL.

5.2 NODAL HEAT BALANCE EQUATIONS IN FINITE DIFFERENCE FORM AND THE METHOD OF SOLUTION

Equation (5.1.1) may be integrated from τ to $\tau + \Delta\tau$, $\Delta\tau$ being a small increment, to give

$$M_i [\phi_i (\tau + \Delta\tau) - \phi_i (\tau)] = Q_i \Delta\tau - \beta_i \Big(C_{i-j} + \sum_j \mathcal{G}_{i-j} + \sum_{j'} \mathcal{G}_{i'-j'} \Big) \int \phi_i^4 \, d\tau$$

$$+ \beta_i \Big(C_{i-j} \int \phi_j^4 \, d\tau + \sum_j \mathcal{G}_{i-j} \int \phi_j^4 \, d\tau$$

$$+ \sum_{j'} \mathcal{G}_{i'-j'} \int \phi_{j'}^4 d\tau \Big) - \frac{1}{(kd)_i} \Big(\sum_{j \neq i} K_{i-j} \int \phi_i \, d\tau$$

$$- \sum_{j \neq i} K_{i-j} \int \phi_j \, d\tau \Big) \qquad (5.2.1)$$

In (5.2.1), all integrals $\int$ imply $\int_\tau^{\tau+\Delta\tau}$. They will now be replaced by the the approximate, two point integration formula, namely,

$$\int_\tau^{\tau + \Delta\tau} \phi \, d\tau \doteq \Delta\tau[(1 - \alpha)\phi(\tau) + \alpha\phi(\tau + \Delta\tau)] \qquad (5.2.2a)$$

$$\int_\tau^{\tau + \Delta\tau} \phi^4 \, d\tau \doteq \Delta\tau[(1 - \alpha)\phi^4(\tau) + \alpha\phi^4(\tau + \Delta\tau)] \qquad (5.2.2b)$$

in which α is the so-called integration parameter and is a pure numeral between 0 and 1. This scheme of approximation has been used by Strong

and Emslie [8] in their treatment of relatively simple systems involving combined radiation and conduction heat transport. Upon substituting (5.2.2a,b) into (5.2.1), followed by some rearrangement, one obtains

$$f_{4,i}\,\phi_i^4(\tau+\Delta\tau) + f_{1,i}\,\phi_i(\tau+\Delta\tau) + f_{0,i} = 0 \tag{5.2.3}$$

where

$$f_{4,i} = \alpha\beta_i\left(C_{i-g} + \sum_{j} \mathscr{F}_{i-j} + \sum_{j'} \mathscr{F}_{i'-j'}\right) \tag{5.2.3a}$$

$$f_{1,i} = \frac{\alpha}{(kd)_i} \sum_{j \neq i} K_{i-j} + \frac{M_i}{\Delta\tau} \tag{5.2.3b}$$

$$f_{0,i} = -Q_i - \frac{M_i}{\Delta\tau}\phi_i(\tau) + \frac{1-\alpha}{(kd)_i} \sum_{j \neq i} K_{i-j}\,\phi_i(\tau)$$

$$+ (1-\alpha)\beta_i\left[C_{i-j} + \sum_{j} \mathscr{F}_{i-j} + \sum_{j'} \mathscr{F}_{i'-j'}\right]\phi_i^4(\tau)$$

$$- \frac{1-\alpha}{(kd)_i} \sum_{j \neq i} K_{i-j}\,\phi_j(\tau)$$

$$- (1-\alpha)\beta_i\left[C_{i-j}\,\phi_j^4(\tau) + \sum_{j} \mathscr{F}_{i-j}\,\phi_j^4(\tau)\right.$$

$$\left. + \sum_{j'} \mathscr{F}_{i'-j'}\,\phi_{j'}^4(\tau)\right] - \alpha\beta_i\left[C_{i-j}\phi_j^4(\tau+\Delta\tau)\right.$$

$$+ \sum_{j} \mathcal{A}_{i-j} \phi_j^4(\tau + \Delta\tau) + \sum_{j'} \mathcal{A}_{i'-j'} \phi_{j'}^4 (\tau + \Delta\tau)\Big] \qquad (5.2.3c)$$

Here again, $\phi_{j'}(\tau) \equiv \phi_j(\tau)$ and $\phi_{j'}(\tau + \Delta\tau) \equiv \phi_j(\tau + \Delta\tau)$.

The equation set (5.2.3) was solved by a modified Gauss-Seidel iterative procedure. Current values of $\phi_j(\tau)$ were used as starting approximations for $\phi_j(\tau + \Delta\tau)$ and the Newton-Raphson method was used for finding the physically meaningful roots. If we denote the current root by $\tilde{\phi}_i(\tau + \Delta\tau)$, then the new value of $\phi_i(\tau + \Delta\tau)$ is calculated from

$$\phi_i(\tau + \Delta\tau)_{new} = \phi_i(\tau + \Delta\tau)_{old} + \gamma\Big[\tilde{\phi}_i(\tau + \Delta\tau) - \phi_i(\tau + \Delta\tau)_{old}\Big] \qquad (5.2.4)$$

where γ is the acceleration factor. The next equation in the set, which is for A_{i+1}, is solved in precisely the same manner using improved values of $\phi_j(\tau + \Delta\tau)$ as soon as they are generated. It has been found that, in general, α and γ taken together have a decisive influence on the convergence rate of the iterative process.

The steady state solution was obtained in a similar manner except, of course, that it does not involve α. By setting the left hand side of (5.1.1) to zero and rearranging, we obtain

$$g_{4,i}\phi_i^4 + g_{1,i}\phi_i + g_{0,i} \simeq 0 \qquad (5.2.5)$$

where

$$g_{4,i} = \beta_i\Big(C_{i-j} + \sum_{j} \mathcal{A}_{i-j} + \sum_{j'} \mathcal{A}_{i'-j'}\Big) \qquad (5.2.5a)$$

$$g_{1,i} = \frac{1}{(kd)_i} \sum_{j \neq i} K_{i-j} \tag{5.2.5b}$$

$$g_{0,1} = -Q_i - \frac{1}{(kd)_i} \sum_{j \neq i} K_{i-j}\,\phi_j$$

$$- \beta_i \left(C_{i-j}\,\phi_j^4 + \sum_{j} \mathcal{F}_{i-j}\,\phi_j^4 + \sum_{j'} \mathcal{F}_{i'-j'}\,\phi_{j'}^4 \right) \tag{5.2.5c}$$

The iteration began with a suitable set of guessed values of ϕ_j. For each node, the Newton-Raphson procedure of successive approximations was again used for determining the root $\tilde{\phi}_i$ of (5.2.5). The new value of ϕ_i is calculated according to

$$\phi_{i,new} = \phi_{i,old} + \gamma(\tilde{\phi}_i - \phi_{i,old}) \tag{5.2.6}$$

Thus, for either the transient or steady state computations, there are two distinct iterations involved. One is associated with the Newton-Raphson method of evaluating the roots of (5.2.3) or (5.2.5) and another is associated with the Gauss-Seidel procedure. In the former, when the successive ϕ_i's differ by less than 0.01 percent, the result is considered satisfactory and the calculation will proceed to the next node. The Gauss-Seidel iteration will terminate when the residual of each nodal equation is less than a specified value. This residual is a measure of the deviation from the perfect heat balance required for

each node. Thus, we may write

$$HB_i = g_{0,i} + g_{1,i}\phi_i + g_{4,i}\phi_i^4 \qquad (5.2.7a)$$

for the steady state problem, and

$$HB_i = f_{0,i} + f_{1,i}\phi_i + f_{4,i}\phi_i^4 \qquad (5.2.7b)$$

for the transient case. For the hypothetical spacecraft described in Chapter 3, $g_{0,i}$ or $f_{0,i}$ is of the order 10^2 for all sunlit surfaces and, hence, we have arbitrarily set $HB_i \leq 10^{-3}$ as the condition to stop the iteration. This value was chosen essentially from a consideration of the computer time on one hand and the desired accuracy of computed results on the other hand.

5.3 DETERMINATION OF OPTIMUM γ AND α

To ascertain the optimum values of γ and α for rapid convergence of the iterative process, a series of preliminary computer experiments was conducted. The results for the steady case with normal incidence from the sun and with a distribution of electronic package heating similar to Mariner '64 spacecraft† are shown in TABLE 5.1. A redistribution of the heating source inside the bus or a change in the relative importance of the radiative and conductive mode of heat transfer would alter the number of iterations required to achieve the same heat balance.

†This calls for the following distribution: A_3-29 percent, A_6-24 percent, A_8-36 percent, and A_9-11 percent. (See Figs. 3.1 and 3.2 for identification).

TABLE 5.1

INFLUENCE OF ACCELERATION FACTOR ON THE CONVERGENCE RATE OF THE ITERATIVE PROCEDURE-STEADY STATE

Acceleration factor γ	No. of iterations required to achieve $HB_i \leq 10^{-3}$
0.3	>80
0.5	65
0.7	38
0.9	24
1.1	14
1.3	10
1.5	17
1.7	33
1.9	>80

Note: Normal incidence from the sun; distribution of heat generation inside the bus similar to Mariner '64 spacecraft.

i.e., $HB_i \leq 10^{-3}$. However, these changes, if kept within reasonable limits, have only a minor effect on the optimum value of γ which is around 1.3. This finding is at variance with the suggestion made by Strong and Emslie [8].

The transient results are presented in TABLE 5.2. They were obtained for the assumed condition that the spacecraft had initially a uniform temperature of 400°R and, at an arbitrarily chosen instant $t = 0$, the internal heating over bus surfaces A_3, A_6, A_8, and A_9 was suddenly raised to their full power and, simultaneously, the spacecraft's exterior surfaces were exposed to sun's irradiation. To a large extent, the table is self-explanatory. It is seen that the acceleration factor has a dominant influence on the convergence rate while the integration parameter plays only a minor role. The optimum value of the acceleration factor has been found to be 1.1 under the stated conditions.

The computed temperature data for the 12 nodal surfaces of the hypothetical spacecraft at 10, 100 and 300 minutes after the thermal disturbance are listed in TABLE 5.3. Included are the data for the steady state temperatures. As one might expect, the solar panels, antenna and the exterior surface of the multi-layer insulation (A_{12}) respond very rapidly to the changing environmental condition.

TABLE 5.2

INFLUENCE OF INTEGRATION PARAMETER AND ACCELERATION FACTOR ON THE CONVERGENCE RATE OF THE ITERATIVE PROCEDURE--TRANSIENT CASE

Integration parameter α	Acceleration factor γ	No. of iterations required to achieve $HB_i \leq 10^{-3}$		
		Prototype time interval, min.		
		0-10	90-100	290-300
0.2	0.9	5	5	4
0.4	0.9	5	5	5
0.6	0.9	6	6	5
0.8	0.9	6	6	5
1.0	0.9	6	7	6
0.2	1.1	5	4	3
0.4	1.1	5	4	3
0.6	1.1	5	4	3
0.8	1.1	5	4	3
1.0	1.1	5	4	3
0.2	1.3	9	7	6
0.4	1.3	9	8	6
0.6	1.3	9	8	6
0.8	1.3	9	7	6
1.0	1.3	9	7	6
0.2	1.5	16	13	10
0.4	1.5	16	12	10
0.6	1.5	16	11	9
0.8	1.5	16	11	9
1.0	1.5	16	11	9
0.2	1.7	31	24	18
0.4	1.7	31	21	17
0.6	1.7	31	26	19
0.8	1.7	31	24	18
1.0	1.7	31	23	18

Note: 1. Prototype Δt = 10 min.

2. Normal incidence from the sun; distribution of heat generation inside the bus similar to Mariner '64 spacecraft.

TABLE 5.3

THERMAL RESPONSE BEHAVIOR OF THE HYPOTHETICAL SPACECRAFT

Uniform Initial Temperature = 400°R

	Temperature, °R			
	t = 10 min.	t = 100 min.	t = 300 min.	Steady State
A_1	518.1	597.8	597.9	598.0
A_2	520.5	603.8	604.7	604.8
A_3	429.4	519.1	533.9	534.4
A_4	518.1	597.6	597.9	597.9
A_5	520.2	602.8	604.2	604.3
A_6	412.2	498.8	524.4	525.5
A_7	401.5	479.6	527.7	529.5
A_8	420.7	499.5	524.0	525.0
A_9	415.9	511.6	546.2	547.5
A_{10}	403.0	490.8	527.7	529.0
A_{11}	476.3	568.0	568.1	568.1
A_{12} (= $A_{10'}$)	152.8	181.1	184.8	185.0

Note: 1. Normal incidence from the sun, solar constant taken to be 442 Btu/hr-ft^2.

2. Cubical bus consists of six 4 ft^2 surfaces; total electronic package dissipation 1100 Btu/hr distributed over surfaces A_3 (29 percent), A_6 (24 percent), A_8 (36 percent), and A_9 (11 percent).

Chapter 6

RESULTS, DISCUSSIONS AND CONCLUSIONS

The similitude requirements for the thermal modeling of the hypothetical spacecraft have been given in Section 3.4. In the present study, it was assumed that the models entail errors in the desired values of kd, Cd, ε, and ε' (the prime refers to the interior of the surfaces). There was no error arising from the requirement of geometric similarity, nor was there error in the heat fluxes q and q*. As has been noted previously, this choice of error distribution is based primarily on a consideration of practical model fabrication with the present-day technology. It has no bearing on the theory itself.

The general theory of imperfect modeling presented in Chapter 2 is described logically in terms of dimensionless quantities. However, in the present instance, it is possible to speak of errors in the dimensional quantities like (kd) and (Cd) since not only are they the only quantities which may be varied in their respective dimensionless groups, but also they are physically apprehended more readily by the designer.

6.1 SPACECRAFT SUBJECTED TO SIMPLE HEATING AND COOLING

To ascertain the usefulness and limitations of the proposed theory, several sets of errors in the modeling parameters have been assigned. TABLE 6.1 lists the values for the first of such sets. In the table

TABLE 6.1 Errors in modeling parameters

Surface	Percentage Error in Modeling Parameters											
	Model MI				Model MII				Model MIII			
	δ_{kd} X 100	δ_{Cd} X 100	δ_{ε} X 100	$\delta_{\varepsilon'}$ X 100	δ_{kd} X 100	δ_{Cd} X 100	δ_{ε} X 100	$\delta_{\varepsilon'}$ X 100	δ_{kd} X 100	δ_{Cd} X 100	δ_{ε} X 100	$\delta_{\varepsilon'}$ X 100
A_1	0	0	0	0	0	0	0	0	0	0	0	0
A_2	0	0	0	0	0	0	0	0	0	0	0	0
A_3	25.0	25.0	-18.0	10.0	55.0	52.5	-18.0	20.0	25.0	25.0	-28.8	10.0
A_4	0	0	0	0	0	0	0	0	0	0	0	0
A_5	0	0	0	0	0	0	0	0	0	0	0	0
A_6	25.0	20.0	-20.0	10.0	45.0	50.0	-20.0	20.0	25.0	20.0	-32.0	10.0
A_7	20.0	25.0	15.0	-8.0	40.0	55.0	27.0	-8.0	20.0	25.0	15.0	-14.7
A_8	25.0	25.0	-18.0	-8.0	57.5	57.5	-18.0	-8.0	25.0	25.0	-25.9	-11.5
A_9	25.0	25.0	25.0	-8.0	45.0	45.0	45.0	-8.0	25.0	25.0	25.0	-16.0
A_{10}	20.0	25.0	15.0	-8.0	44.0	60.0	33.0	-8.0	20.0	25.0	15.0	-12.8
A_{11}	0	0	0	0	0	0	0	0	0	0	0	0
$A_{12}(=A_{10'})$	0	0	15.0	0	0	0	33.0	0	0	0	15.0	0

δ_{ε} refers to the exterior of the surface in question and $\delta_{\varepsilon'}$ refers to its interior

and others which follow, model MI refers to the 'original' imperfect model. MII refers to that for which the positive errors are modified (in this case, they become *more* positive) while the negative errors remain unaltered and MIII denotes that for which the negative errors are modified (in this case, they become *more* negative) while the positive errors are unchanged. Thus, the error state of model MI would be represented by the point P in the multidimensional hyperspace referred to in Chapter 2. Likewise, the error states of model MII and MIII are represented respectively by $P^{*(+)}$ and $P^{*(-)}$.

Initially, the spacecraft is assumed to have a uniform temperature of 400°R. At some arbitrarily selected instant, t = 0, internal heating within the spacecraft's bus and of a distribution as prescribed in TABLE 5.3 is assumed to begin instantaneously and, at the same instant, its exterior surfaces are exposed to sun's irradiation. Subsequent to the establishment of a steady thermal condition, the spacecraft is conceived to move into the shade of a planet, thus cutting off the sun's irradiation. In this manner, a cooling transient is created.

Using the equation set (3.3.3) and the computational procedure explained in Chapter 5, temperature data for the heating transient, the steady state, and the cooling transient are obtained for the prototype (or, equivalently, the perfect model) and for the three models. The results are summarized in a table set 6.2 for normal incidence of the solar irradiation and in table set 6.3 for 45° oblique incidence. The prototype temperatures are denoted by T_p and those of the models by T_{MI}, T_{MII}, and T_{MIII}. The errors in the latter temperatures

TABLE 6.2(a) Model temperature before and after correction

Heating Transient: 10 minutes after spacecraft subject to solar irradiation (normal incidence) and internal heating

Surface	Prototype or Perfect Model Temperature T_P	Temperatures of Imperfect Models						$\Delta^{(+)}$	$\Delta^{(-)}$	Δ_t	Model Temperature after Correction	
		Model MI		Model MII		Model MIII						
		T_{MI}	E_{MI}	T_{MII}	E_{MII}	T_{MIII}	E_{MIII}				T_{MC}	E_{MC}
A_1	518.1	518.1	0	518.0	-0.1	518.0	-0.1	-0.01	-0.05	-0.06	518.1	0
A_2	520.5	520.0	-0.5	520.0	-0.5	519.8	-0.7	-0.05	-0.32	-0.37	520.4	-0.1
A_3	429.4	426.2	-3.2	421.9	-7.5	427.5	-1.9	-3.89	1.88	-2.01	428.2	-1.2
A_4	518.1	518.0	-0.1	518.0	-0.1	518.0	-0.1	~0	-0.04	-0.04	518.1	0
A_5	520.2	520.0	-0.2	519.9	-0.3	519.7	-0.5	-0.2	-0.25	-0.27	520.2	0
A_6	412.2	411.4	-0.8	409.2	-3.0	412.0	-0.2	-1.95	0.98	-0.97	412.3	0.1
A_7	401.5	400.9	-0.6	400.6	-0.9	400.9	-0.6	-0.29	-0.11	-0.40	401.3	-0.2
A_8	420.7	419.0	-1.7	415.4	-5.3	420.0	-0.7	-3.23	1.37	-1.86	420.9	0.2
A_9	415.9	412.9	-3.0	410.9	-5.0	413.0	-2.9	-1.76	0.23	-1.53	414.4	-1.5
A_{10}	403.0	401.8	-1.2	401.0	-2.0	401.6	-1.4	-0.66	-0.29	-0.95	402.7	-0.3
A_{11}	476.3	476.3	0	476.3	0	476.3	0	~0	~0	~0	476.3	0
$A_{12}(=A_{10}')$	152.8	153.3	0.5	153.2	0.4	154.1	1.3	-0.07	1.18	1.11	152.2	-0.6

All temperatures in °R

TABLE 6.2(b) Model temperatures before and after correction

Heating Transient: 30 minutes after spacecraft subject to solar irradiation (normal incidence) and internal heating

Surface	Prototype or Perfect Model Temperature T_P	Temperatures of Imperfect Models						$\Delta^{(+)}$	$\Delta^{(-)}$	Δ_t	Model Temperature after Correction	
		Model MI		Model MII		Model MIII						
		T_{MI}	E_{MI}	T_{MII}	E_{MII}	T_{MIII}	E_{MIII}				T_{MC}	E_{MC}
A_1	590.7	590.6	-0.1	590.6	-0.1	590.5	-0.2	-0.04	-0.07	-0.11	590.7	0
A_2	594.9	594.2	-0.7	593.9	-1.0	593.9	-1.0	-0.22	-0.43	-0.65	594.8	-0.1
A_3	474.5	469.0	-5.5	459.4	-15.1	472.0	-2.5	-8.61	4.47	-4.14	473.1	-1.4
A_4	590.5	590.5	0	590.5	0	590.5	0	-0.02	-0.04	-0.06	590.5	0
A_5	593.9	593.5	0	593.4	-0.1	593.4	-0.1	-0.11	-0.20	-0.31	593.9	0
A_6	440.3	436.8	-3.5	430.3	-10.0	438.3	-2.0	-5.83	2.24	-3.59	440.4	0.1
A_7	413.1	409.3	-3.8	406.5	-6.6	409.1	-4.0	-2.52	-0.30	-2.82	412.1	-1.0
A_8	450.6	448.9	-1.7	441.0	-9.6	451.6	1.0	-7.10	4.09	-3.01	451.9	1.3
A_9	445.4	438.7	-6.7	432.8	-12.6	439.6	-5.8	-5.24	1.37	-3.87	442.6	-2.8
A_{10}	424.3	418.3	-6.0	412.9	-11.4	418.3	-6.0	-4.79	-0.01	-4.80	423.1	-1.2
A_{11}	547.6	547.6	0	547.6	0	547.6	0	0.01	~0	0.01	547.6	0
$A_{12}(=A_{10}')$	172.2	172.3	0.1	171.9	-0.3	172.9	0.7	-0.36	0.87	0.51	171.7	-0.5

All temperatures in °R.

TABLE 6.2(c) Model temperatures before and after correction

Heating Transient: 100 minutes after spacecraft subject to solar irradiation (normal incidence) and internal heating

Surface	Prototype or Perfect Model Temperature T_P	Temperatures of Imperfect Models						$\Delta^{(+)}$	$\Delta^{(-)}$	Δ_t	Model Temperature after Correction	
		Model MI		Model MII		Model MIII						
		T_{MI}	E_{MI}	T_{MII}	E_{MII}	T_{MIII}	E_{MIII}				T_{MC}	E_{MC}
A_1	597.8	597.7	-0.1	597.6	-0.2	597.6	-0.2	-0.06	-0.08	-0.14	597.8	0
A_2	603.8	603.1	-0.7	602.6	-1.2	602.7	-1.1	-0.36	-0.47	-0.83	603.9	0.1
A_3	519.1	524.3	5.2	515.0	-4.1	532.5	13.4	-8.35	12.24	3.89	520.4	1.3
A_4	597.6	597.5	-0.1	597.4	-0.2	597.5	-0.1	-0.06	-0.06	-0.12	597.6	0
A_5	602.8	602.1	-0.7	601.7	-1.1	601.9	-0.9	-0.37	-0.33	-0.70	602.8	0
A_6	498.8	499.8	1.0	488.0	-10.8	505.9	7.1	-10.52	9.13	-1.39	501.1	2.3
A_7	479.6	469.4	-10.2	454.1	-25.5	471.1	-8.5	-13.68	2.55	-11.13	480.5	0.9
A_8	499.5	505.0	5.5	494.8	-4.7	512.3	12.8	-9.14	10.81	1.67	503.4	3.9
A_9	511.6	506.9	-4.7	494.2	-17.4	511.9	0.3	-11.36	7.51	-3.85	510.8	-0.8
A_{10}	490.8	486.2	-4.6	472.5	-18.3	490.0	-0.8	-12.25	5.79	-6.46	492.6	1.8
A_{11}	568.0	568.1	0.1	568.1	0.1	568.1	0.1	~0	~0	0	568.0	0
$A_{12}(=A_{10'})$	181.1	181.6	0.5	180.2	-0.9	183.0	1.9	-1.18	2.22	1.04	180.5	-0.6

All temperatures in °R.

TABLE 6.2(d) Model temperatures before and after correction

Heating Transient: 300 minutes after spacecraft subject to solar irradiation (normal incidence) and internal heating

Surface	Prototype or Perfect Model Temperature T_P	Temperatures of Imperfect Models						$\Delta^{(+)}$	$\Delta^{(-)}$	Δ_t	Model Temperature after Correction	
		Model MI		Model MII		Model MIII						
		T_{MI}	E_{MI}	T_{MII}	E_{MII}	T_{MIII}	E_{MIII}				T_{MC}	E_{MC}
A_1	598.0	597.9	-0.1	597.9	-0.1	597.9	-0.1	-0.03	-0.05	-0.08	598.0	0
A_2	604.7	604.4	-0.3	604.2	-0.5	604.2	-0.5	-0.15	-0.30	-0.45	604.9	0.2
A_3	533.9	550.7	16.8	547.6	13.7	563.6	29.7	-2.85	19.22	16.37	534.4	0.5
A_4	597.9	597.8	-0.1	597.8	-0.1	597.8	-0.1	-0.03	-0.03	-0.06	597.9	0
A_5	604.2	604.1	-0.1	603.9	-0.3	603.9	-0.3	-0.17	-0.19	-0.36	604.4	0.2
A_6	524.4	542.1	17.7	538.3	13.9	555.4	31.0	-3.40	19.89	16.49	525.6	1.2
A_7	527.7	540.6	12.9	533.8	6.1	550.5	22.8	-6.14	14.68	8.54	532.1	4.4
A_8	524.0	543.0	19.0	539.2	15.2	555.3	31.3	-3.46	18.32	14.86	528.2	4.2
A_9	546.2	558.3	12.1	551.7	5.5	569.6	23.4	-5.93	16.84	10.91	547.4	1.2
A_{10}	527.7	541.2	13.5	535.5	7.8	551.3	23.6	-5.11	15.04	9.93	531.3	3.6
A_{11}	568.1	568.2	0.1	568.2	0.1	568.2	0.1	0.02	0.02	0.04	568.1	0
$A_{12}(=A_{10}')$	184.9	187.7	2.8	186.9	2.0	190.6	5.7	-0.63	4.42	3.79	183.9	-1.0

All temperatures in °R.

TABLE 6.2(e) Model temperatures before and after correction

Heating Transient: 500 minutes after spacecraft subject to solar irradiation (normal incidence) and internal heating

Surface	Prototype or Perfect Model Temperature T_P	Temperatures of Imperfect Models						$\Delta^{(+)}$	$\Delta^{(-)}$	Δ_t	Model Temperature after Correction	
		Model MI		Model MII		Model MIII						
		T_{MI}	E_{MI}	T_{MII}	E_{MII}	T_{MIII}	E_{MIII}				T_{MC}	E_{MC}
A_1	598.0	597.9	-0.1	597.9	-0.1	597.9	-0.1	-0.01	-0.05	-0.06	598.0	0
A_2	604.8	604.5	-0.3	604.5	-0.3	604.4	-0.4	-0.05	-0.27	-0.32	604.8	0
A_3	534.4	552.8	18.4	551.7	17.3	566.3	31.9	-1.00	20.11	19.11	532.7	-1.7
A_4	597.9	597.9	0	597.9	0	597.8	-0.1	-0.01	-0.03	-0.04	597.9	0
A_5	604.3	604.2	-0.1	604.2	-0.1	604.1	-0.2	-0.04	-0.15	-0.19	604.4	0.1
A_6	525.3	545.3	20.0	544.4	19.1	559.5	34.2	-0.77	21.23	20.46	523.5	1.8
A_7	529.4	545.9	16.5	543.8	14.4	556.9	27.5	-1.89	16.37	14.48	530.1	0.7
A_8	525.0	546.1	21.1	544.9	19.9	559.1	34.1	-1.04	19.40	18.36	526.9	1.9
A_9	547.5	562.3	14.8	559.1	11.6	574.5	27.0	-2.93	18.19	15.26	546.8	-0.7
A_{10}	529.0	545.5	16.5	543.5	14.5	556.4	27.4	-1.78	16.38	14.60	529.7	0.7
A_{11}	568.1	568.2	0.1	568.2	0.1	568.2	0.1	0.02	0.02	0.04	568.1	0
A_{12} (=A_{10}')	185.0	188.2	3.2	187.9	2.9	191.3	6.3	-0.23	4.70	4.47	184.4	-0.6

All temperatures in °R.

TABLE 6.2(f) Model temperatures before and after correction

Steady State

Surface	Prototype or Perfect Model Temperature T_P	Temperatures of Imperfect Models						$\Delta^{(+)}$	$\Delta^{(-)}$	Δ_t	Model Temperature after Correction	
		Model MI		Model MII		Model MIII						
		T_{MI}	E_{MI}	T_{MII}	E_{MII}	T_{MIII}	E_{MIII}				T_{MC}	E_{MC}
A_1	597.9	597.9	0	597.9	0	597.9	0	-0.01	-0.05	-0.06	598.0	0.1
A_2	604.8	604.5	-0.3	604.5	-0.3	604.4	-0.4	-0.03	-0.26	-0.29	604.8	0
A_3	534.4	553.0	18.6	552.2	17.8	566.5	32.1	-0.68	20.20	19.52	533.5	-0.9
A_4	597.9	597.9	0	597.9	0	597.9	0	~0	-0.02	-0.02	597.9	0
A_5	604.3	604.2	-0.1	604.2	-0.1	604.2	-0.1	-0.01	-0.14	-0.15	604.4	0.1
A_6	525.3	545.5	20.2	545.2	19.9	559.8	34.5	-0.31	21.36	21.05	524.4	-0.9
A_7	529.5	546.3	16.8	545.0	15.5	557.4	27.9	-1.15	16.54	15.39	530.9	1.4
A_8	525.0	546.3	21.3	545.6	20.6	559.4	34.4	-0.60	19.51	18.91	527.4	2.4
A_9	547.5	562.6	15.1	560.0	12.5	574.9	27.4	-2.38	18.33	15.95	546.7	-0.8
A_{10}	529.0	545.8	16.8	544.5	15.5	556.8	27.8	-1.19	16.52	15.33	530.4	1.4
A_{11}	568.1	568.2	0.1	568.2	0.1	568.2	0.1	0.02	0.02	0.04	568.1	0
$A_{12}(=A_{10}')$	185.0	188.2	3.2	188.0	3.0	191.4	6.4	-0.16	4.73	4.57	183.6	-1.4

All temperatures in °R.

TABLE 6.2(g) Model temperatures before and after correction

Cooling Transient: 30 minutes after spacecraft moving into shade

Surface	Prototype or Perfect Model Temperature T_P	Temperatures of Imperfect Models						$\Delta^{(+)}$	$\Delta^{(-)}$	Δ_t	Model Temperature after Correction	
		Model MI		Model MII		Model MIII						
		T_{MI}	E_{MI}	T_{MII}	E_{MII}	T_{MIII}	E_{MIII}				T_{MC}	E_{MC}
A_1	376.5	376.5	0	376.5	0	376.4	-0.1	0.01	-0.12	-0.11	376.6	0.1
A_2	390.5	390.1	-0.4	390.2	-0.3	389.7	-0.8	0.03	-0.66	-0.63	390.8	0.3
A_3	516.2	539.6	23.4	540.4	24.2	554.7	38.5	0.78	22.57	23.35	516.2	0
A_4	376.4	376.3	-0.1	376.4	0	376.2	-0.2	0.01	-0.14	-0.13	376.5	0.1
A_5	389.9	389.5	-0.4	389.5	-0.4	388.9	0	0.05	-0.80	-0.75	390.2	0.3
A_6	513.0	536.8	23.8	537.9	24.9	552.3	39.3	0.94	23.14	24.08	512.7	-0.3
A_7	527.0	544.5	17.5	543.6	16.6	555.7	28.7	-0.81	16.73	15.92	528.6	1.6
A_8	522.6	544.5	21.9	544.2	21.6	557.8	35.2	-0.34	19.78	19.44	525.1	2.5
A_9	543.4	559.6	16.2	557.4	14.0	572.2	28.8	-2.02	18.80	16.78	542.8	-0.6
A_{10}	525.5	543.2	17.7	542.4	16.9	554.5	29.0	-0.75	16.86	16.11	527.1	1.6
A_{11}	395.2	395.3	0.1	395.3	0.1	395.3	0.1	0.04	0.04	0.08	395.2	0
$A_{12}(=A_{10}')$	150.4	156.5	6.1	156.3	5.9	162.1	11.7	-0.18	8.37	8.19	148.3	-2.1

All temperatures in °R.

TABLE 6.2(h) Model temperatures before and after correction

Cooling Transient: 200 minutes after spacecraft moving into shade .

Surface	Prototype or Perfect Model Temperature T_P	Temperatures of Imperfect Models						$\Delta^{(+)}$	$\Delta^{(-)}$	Δ_t	Model Temperature after Correction	
		Model MI		Model MII		Model MIII						
		T_{MI}	E_{MI}	T_{MII}	E_{MII}	T_{MIII}	E_{MIII}				T_{MC}	E_{MC}
A_1	229.8	229.7	-0.1	229.8	0	229.5	-0.3	0.07	-0.36	-0.29	230.0	0.2
A_2	275.7	275.4	-0.3	275.7	0	274.5	-0.2	0.25	-1.33	-1.08	276.5	0.8
A_3	500.3	524.6	24.3	525.1	24.7	540.9	40.6	0.45	24.46	24.91	499.7	-0.6
A_4	229.0	228.9	-0.1	229.1	0.1	228.5	-0.5	0.14	-0.58	-0.44	229.4	0.4
A_5	272.7	272.3	-0.4	272.9	0.2	270.9	0	0.50	-2.14	-1.64	274.0	1.3
A_6	491.8	518.4	26.6	519.6	27.8	535.6	43.6	1.11	25.80	26.91	491.4	-0.4
A_7	508.8	528.6	19.8	528.3	19.5	541.3	32.5	-0.24	19.01	18.77	509.8	1.0
A_8	510.4	533.2	22.8	532.8	22.4	547.4	37.0	-0.40	21.23	20.83	512.4	2.0
A_9	525.6	543.6	18.0	541.6	16.0	557.7	32.1	-1.83	21.13	19.30	524.3	-1.3
A_{10}	508.3	527.8	19.5	527.2	18.9	540.6	32.3	-0.54	19.09	18.55	509.3	1.0
A_{11}	235.6	236.0	0.4	236.1	0.5	236.1	0.5	0.16	0.20	0.36	235.6	0
$A_{12}(=A_{10'})$	134.8	142.7	7.9	142.6	7.8	149.8	15.0	-0.15	10.51	10.36	132.4	-2.4

All temperatures in °R.

TABLE 6.3 (a) Model temperatures before and after correction

Heating Transient: 10 minutes after spacecraft subject to solar irradiation (45° incidence) and internal heating

Surface	Prototype or Perfect Model Temperature T_P	Temperatures of Imperfect Models						$\Delta^{(+)}$	$\Delta^{(-)}$	Δ_t	Model Temperature after Correction	
		Model MI		Model MII		Model MIII						
		T_{MI}	E_{MI}	T_{MII}	E_{MII}	T_{MIII}	E_{MIII}				T_{MC}	E_{MC}
A_1	477.4	477.3	-0.1	477.3	-0.1	477.3	-0.1	-0.01	-0.07	-0.08	477.4	0
A_2	370.1	369.5	-0.6	369.5	-0.6	369.3	-0.8	-0.06	-0.44	-0.50	370.1	0
A_3	425.7	423.7	-2.0	419.8	-5.9	425.3	-0.4	-3.53	2.36	-1.17	424.9	-0.8
A_4	481.0	481.0	0	481.0	0	480.9	-0.1	-0.01	-0.06	-0.07	481.0	0
A_5	499.3	498.8	-0.5	498.8	-0.5	498.6	-0.7	-0.06	-0.33	-0.39	499.2	-0.1
A_6	430.4	426.9	-3.5	421.8	-8.6	427.7	-2.7	-4.57	1.19	-3.38	430.3	-0.1
A_7	401.7	401.1	-0.6	400.7	-1.0	401.0	-0.7	-0.34	-0.11	-0.45	401.6	-0.1
A_8	421.3	419.5	-1.8	415.8	-5.5	420.5	-0.8	-3.33	1.40	-1.93	421.5	0.2
A_9	416.9	413.8	-3.1	411.7	-5.2	414.0	-2.9	-1.93	0.27	-1.66	415.5	-1.4
A_{10}	403.6	402.2	-1.4	401.4	-2.2	402.1	-1.5	-0.78	-0.26	-1.04	403.3	-0.3
A_{11}	447.6	447.6	0	447.6	0	447.6	0	0.01	0	0.01	447.6	0
$A_{12}(=A_{10'})$	142.1	142.9	-0.8	142.7	-0.6	143.9	-1.8	-0.10	1.60	1.50	141.4	-0.7

All temperatures in °R.

TABLE 6.3(b) Model temperatures before and after correction

Heating Transient: 30 minutes after spacecraft subject to solar irradiation (45° incidence) and internal heating

Surface	Prototype or Perfect Model Temperature T_P	Temperatures of Imperfect Models						$\Delta^{(+)}$	$\Delta^{(-)}$	Δ_t	Model Temperature after Correction	
		Model MI		Model MII		Model MIII						
		T_{MI}	E_{MI}	T_{MII}	E_{MII}	T_{MIII}	E_{MIII}				T_{MC}	E_{MC}
A_1	535.6	535.4	-0.2	535.4	-0.2	535.4	-0.2	-0.04	-0.12	-0.16	535.6	0
A_2	335.3	333.6	-1.7	333.1	-2.2	332.8	-2.5	-0.37	-1.16	-1.53	335.1	-0.2
A_3	457.7	456.9	-0.8	448.8	-8.9	461.4	3.7	-7.18	-6.79	-0.39	457.2	-0.5
A_4	541.9	541.8	-0.1	541.7	-0.2	541.7	-0.2	-0.06	-0.09	-0.15	541.9	0
A_5	568.3	567.4	-0.9	567.1	-1.2	567.1	-1.2	-0.30	-0.48	-0.78	568.2	-0.1
A_6	480.6	473.2	-7.4	460.8	-19.8	475.7	-4.9	-11.18	3.64	-7.54	480.8	0.2
A_7	414.9	410.7	-4.2	407.5	-7.4	410.6	-4.3	-2.92	-0.23	-3.15	413.9	-1.0
A_8	453.5	451.7	-1.8	443.2	-10.2	454.6	1.1	-7.57	4.38	-3.19	454.9	1.4
A_9	450.5	443.6	-6.9	436.8	-13.7	444.8	5.7	-6.08	1.82	-4.26	447.8	-2.7
A_{10}	427.6	421.3	-6.3	415.1	-12.5	421.4	-6.2	-5.54	0.29	-5.25	426.5	-1.1
A_{11}	498.0	498.0	0	498.0	0	498.0	0	0.01	~0	0.01	498.0	0
A_{12} (=A_{10}')	155.5	155.6	0.1	155.0	-0.5	156.6	1.1	-0.57	1.47	0.90	154.7	-0.8

All temperatures in °R.

TABLE 6.3(c) Model temperatures before and after correction

Heating Transient: 100 minutes after spacecraft subject to solar irradiation (45° incidence) and internal heating

Surface	Prototype or Perfect Model Temperature T_P	Temperatures of Imperfect Models						$\Delta^{(+)}$	$\Delta^{(-)}$	Δ_t	Model Temperature after Correction	
		Model MI		Model MII		Model MIII						
		T_{MI}	E_{MI}	T_{MII}	E_{MII}	T_{MIII}	E_{MIII}				T_{MC}	E_{MC}
A_1	546.3	546.1	-0.2	546.0	-0.3	546.0	-0.3	-0.08	-0.13	-0.21	546.3	0
A_2	296.2	292.3	-3.9	290.3	-5.9	290.6	-5.6	-1.73	-2.51	-4.24	296.5	0.3
A_3	498.1	508.9	10.8	500.2	2.1	520.0	21.9	-7.81	16.67	8.86	500.0	1.9
A_4	553.4	553.1	-0.3	553.0	-0.4	553.0	-0.4	-0.15	-0.13	-0.28	553.4	0
A_5	581.6	580.2	-1.4	579.4	-2.2	579.8	-1.8	-0.78	-0.68	-1.46	581.7	0.1
A_6	552.8	556.0	3.2	540.3	-12.5	565.7	12.9	-14.10	14.45	0.35	555.7	2.9
A_7	490.6	481.1	-9.5	463.2	-27.4	484.2	-6.4	-16.04	4.55	-11.49	492.6	2.0
A_8	507.9	515.1	7.2	504.0	-3.9	523.7	15.8	-9.99	12.83	2.84	512.3	4.4
A_9	524.9	522.7	-2.2	508.3	-16.6	529.7	4.8	-12.84	10.49	-2.35	525.0	0.1
A_{10}	502.6	499.7	-2.9	484.1	-18.5	505.4	2.8	-14.00	8.45	-5.55	505.3	2.7
A_{11}	520.6	520.7	0.1	520.7	0.1	520.7	0.1	~0	0.01	0.01	520.7	0.1
$A_{12}(=A_{10'})$	167.2	168.1	0.9	166.0	-1.2	170.6	3.4	-1.85	3.69	1.84	166.3	-0.9

All temperatures in °R.

TABLE 6.3(d) Model temperatures before and after correction

Heating Transient: 300 minutes after spacecraft subject to solar irradiation (45° incidence) and internal heating

Surface	Prototype or Perfect Model Temperature T_P	Temperatures of Imperfect Models						$\Delta^{(+)}$	$\Delta^{(-)}$	Δ_t	Model Temperature after Correction	
		Model MI		Model MII		Model MIII						
		T_{MI}	E_{MI}	T_{MII}	E_{MII}	T_{MIII}	E_{MIII}				T_{MC}	E_{MC}
A_1	546.5	546.4	-0.1	546.4	-0.1	546.4	-0.1	-0.02	-0.08	-0.10	546.5	0
A_2	290.8	289.8	-1.0	288.6	-2.2	288.7	-2.1	-1.08	-1.61	-2.69	292.5	1.7
A_3	515.2	539.9	24.7	538.7	23.5	556.4	41.2	-1.04	24.72	23.68	516.2	1.0
A_4	553.8	553.7	-0.1	553.6	-0.2	533.6	-0.2	-0.07	-0.08	-0.15	553.8	0
A_5	583.4	582.9	-0.5	582.5	-0.9	582.6	-0.8	-0.33	-0.38	-0.71	583.6	0.2
A_6	573.4	593.6	20.2	588.4	15.0	610.2	36.8	-4.62	24.85	20.23	573.4	0
A_7	540.1	557.6	17.5	551.5	11.4	570.0	29.9	-5.42	18.60	13.18	544.4	4.3
A_8	533.1	555.6	22.5	552.5	19.4	569.9	36.8	-2.77	21.38	18.61	537.0	3.9
A_9	559.6	576.3	16.7	570.3	10.7	590.2	30.6	-5.34	20.76	15.42	560.9	1.3
A_{10}	540.0	558.0	18.0	553.0	13.0	570.6	30.6	-4.46	18.87	14.41	543.6	3.6
A_{11}	520.9	521.0	0.1	521.0	0.1	521.0	0.1	0.02	0.04	0.06	520.9	0
A_{12} (=A_{10})	172.2	176.7	4.5	175.9	3.7	181.2	9.0	-0.73	6.71	5.98	170.7	-1.5

All temperatures in °R.

TABLE 6.3(e) Model temperatures before and after correction

Heating Transient: 500 minutes after spacecraft subject to solar irradiation (45° incidence) and internal heating

Surface	Prototype or Perfect Model Temperature T_P	Temperatures of Imperfect Models						$\Delta^{(+)}$	$\Delta^{(-)}$	Δ_t	Model Temperature after Correction	
		Model MI		Model MII		Model MIII						
		T_{MI}	E_{MI}	T_{MII}	E_{MII}	T_{MIII}	E_{MIII}				T_{MC}	E_{MC}
Λ_1	546.5	546.5	0	546.5	0	546.4	-0.1	0.01	-0.06	-0.05	54.65	0
Λ_2	291.4	291.7	0.3	291.9	0.5	291.0	-0.4	0.19	-1.05	-0.86	29.26	1.2
Λ_3	515.7	541.7	26.0	542.7	27.0	558.7	43.0	0.85	25.41	26.26	515.5	-0.2
Λ_4	553.8	553.7	-0.1	553.7	-0.1	553.7	-0.1	-0.03	-0.07	-0.10	553.8	0
Λ_5	583.4	583.1	-0.3	582.9	-0.5	582.8	-0.6	-0.18	-0.34	-0.52	583.6	0.2
Λ_6	573.9	595.7	21.8	592.9	19.0	612.8	38.9	-2.50	25.66	23.16	572.5	-1.4
Λ_7	541.3	561.8	20.5	560.2	18.9	575.0	33.3	-1.40	19.79	18.39	543.4	2.1
Λ_8	533.7	558.1	24.4	557.5	23.8	572.9	39.2	-0.47	22.16	21.69	536.4	2.7
Λ_9	560.5	579.4	18.9	576.6	16.1	593.9	33.4	-2.53	21.69	19.16	560.3	-0.2
Λ_{10}	541.0	561.3	20.3	559.8	18.8	574.6	33.6	-1.33	19.81	18.48	542.8	1.8
Λ_{11}	520.9	521.0	0.1	521.0	0.1	521.0	0.1	0.03	0.04	0.07	520.9	0
$\Lambda_{12}(=\Lambda_{10}')$	172.3	177.2	4.9	177.0	4.7	181.9	9.6	-0.23	6.96	6.73	170.5	-1.8

All temperatures in °R.

TABLE 6.3(f) Model temperatures before and after correction

Steady State

Surface	Prototype or Perfect Model Temperature T_p	Temperatures of Imperfect Models						$\Delta^{(+)}$	$\Delta^{(-)}$	Δ_c	Model Temperature after Correction	
		Model MI		Model MII		Model MIII						
		T_{MI}	E_{MI}	T_{MII}	E_{MII}	T_{MIII}	E_{MIII}				T_{MC}	E_{MC}
A_1	546.5	546.5	0	546.5	0	546.4	-0.1	0.02	-0.06	-0.04	546.5	0
A_2	291.5	291.9	0.4	292.4	0.9	291.3	-0.2	0.45	-0.98	-0.53	292.5	1.0
A_3	515.8	541.9	26.1	543.1	27.3	558.9	43.1	1.10	25.46	26.56	515.3	-0.5
A_4	553.8	553.7	-0.1	553.7	-0.1	553.7	-0.1	-0.03	-0.07	-0.10	553.8	0
A_5	583.4	583.1	-0.3	582.9	-0.5	582.8	-0.6	-0.15	-0.34	-0.49	583.6	0.2
A_6	573.9	595.8	21.9	593.3	19.4	613.0	39.1	-2.23	25.72	23.49	572.3	-1.6
A_7	541.4	562.0	20.6	561.0	19.6	575.3	33.9	-0.88	19.87	18.99	543.0	1.6
A_8	533.8	558.2	24.4	558.0	24.2	573.1	39.3	-0.17	22.21	22.04	536.2	2.4
A_9	560.6	579.6	19.0	577.2	16.6	594.2	33.6	-2.15	21.75	19.60	560.0	-0.6
A_{10}	541.0	561.5	20.5	560.5	19.5	574.8	33.8	-0.92	19.87	18.95	542.5	1.5
A_{11}	520.9	521.0	0.1	521.0	0.1	521.0	0.1	0.03	0.04	0.07	520.9	0
$A_{12}(=A_{10}')$	172.3	177.3	5.0	177.1	4.8	181.9	9.6	-0.16	6.98	6.82	170.4	-1.9

All temperatures in °R.

TABLE 6.3(g) Model temperatures before and after correction

Cooling Transient: 30 minutes after spacecraft moving into shade

Surface	Prototype or Perfect Model Temperature T_P	Temperatures of Imperfect Models						$\Delta^{(+)}$	$\Delta^{(-)}$	Δ_t	Model Temperature after Correction	
		Model MI		Model MII		Model MIII						
		T_{MI}	E_{MI}	T_{MII}	E_{MII}	T_{MIII}	E_{MIII}				T_{MC}	E_{MC}
A_1	366.5	366.5	0	366.5	0	366.4	-0.1	0.03	-0.10	-0.07	366.5	0
A_2	288.6	289.0	0.4	289.6	1.0	288.3	-0.3	0.48	-1.04	-0.56	289.6	1.0
A_3	512.5	539.1	26.6	540.8	28.3	556.2	43.7	1.46	25.5	27.01	512.1	-0.4
A_4	370.5	370.4	-0.1	370.5	0	370.3	-0.2	0.02	-0.15	-0.13	370.6	0.1
A_5	390.4	390.0	-0.4	390.2	-0.2	389.5	-0.9	0.16	-0.81	-0.65	390.7	0.3
A_6	529.5	557.7	28.2	560.7	31.2	575.4	45.9	2.72	26.51	29.23	528.5	-1.0
A_7	536.7	558.2	21.5	558.1	21.4	571.4	34.7	-0.06	19.75	19.81	538.5	1.8
A_8	529.0	554.0	25.0	554.5	25.5	568.8	39.8	0.49	22.11	22.60	531.4	2.4
A_9	552.6	572.6	20.0	571.3	18.7	587.2	34.6	-1.19	21.75	20.56	552.1	-0.5
A_{10}	534.3	555.7	21.4	555.8	21.5	568.8	34.5	0.13	19.66	19.79	535.9	1.6
A_{11}	383.1	383.3	0.2	383.3	0.2	383.3	0.2	0.05	0.06	0.11	383.1	0
$A_{12}(=A_{10}')$	149.7	157.1	7.4	157.1	7.4	163.5	13.8	0.01	9.64	9.65	147.4	-2.3

All temperatures in °R.

TABLE 6.3(h) Model temperatures before and after correction

Cooling Transient: 200 minutes after spacecraft moving into shade

Surface	Prototype or Perfect Model Temperature T_p	Temperatures of Imperfect Models						$\Delta^{(+)}$	$\Delta^{(-)}$	Δ_t	Model Temperature after Correction	
		Model MI		Model MII		Model MIII						
		T_{MI}	E_{MI}	T_{MII}	E_{MII}	T_{MIII}	E_{MIII}				T_{MC}	E_{MC}
A_1	227.8	227.9	0.1	228.1	0.3	227.7	-0.1	0.16	-0.33	-0.17	228.0	0.2
A_2	269.9	270.0	0.1	270.7	0.8	269.2	-0.7	0.60	-1.31	-0.71	270.7	0.8
A_3	500.5	525.3	24.8	526.4	25.9	541.9	41.4	0.97	24.80	25.77	499.6	-0.9
A_4	228.8	228.8	0	229.1	0.3	228.5	-0.3	0.26	-0.52	-0.26	229.1	0.3
A_5	273.4	273.5	0.1	274.5	0.1	272.2	-0.2	0.90	-1.90	-1.0	274.5	1.1
A_6	492.4	519.7	27.3	521.7	29.3	537.2	44.8	1.85	26.26	28.11	491.6	-0.8
A_7	509.6	530.6	21.0	531.4	21.8	543.7	34.1	0.78	19.58	20.36	510.2	0.6
A_8	510.9	534.4	23.5	534.6	23.7	548.8	37.9	0.23	21.60	21.83	512.5	1.6
A_9	526.2	545.1	18.9	544.0	17.8	559.6	33.4	-1.06	21.60	20.54	524.6	-1.6
A_{10}	509.0	529.4	20.4	529.8	20.8	542.5	33.5	0.30	19.55	19.85	509.6	0.6
A_{11}	234.0	234.4	0.4	234.6	0.6	234.6	0.6	0.19	-0.22	0.41	234.0	0
A_{12} (=A_{10}')	134.8	143.1	8.3	143.2	8.4	150.2	15.4	0.06	10.67	10.73	132.3	-2.5

All temperatures in °R.

are designated by E_{MI}, E_{MII}, and E_{MIII}. Equation (2.3.8) is used to evaluate $\Delta^{(+)}$, which is the correction for all positive errors, and $\Delta^{(-)}$, the correction for all negative errors, is evaluated from (2.3.13). The combined correction Δ_t is simply the algebraic sum of $\Delta^{(+)}$ and $\Delta^{(-)}$. Finally, the corrected model temperatures calculated according to (2.3.14) are denoted by T_{MC} and their errors are E_{MC}. In either set of the foregoing tables, data for the heating transients are listed in tables (a) to (e), the steady state in table (f), and the cooling transients in tables (g) and (h).

An inspection of these tables shows that the proposed correction theory is indeed capable of providing good results when errors in kd and in Cd of the 'original' model MI are up to 25 percent and errors in surface emittance up to 20 percent (corresponding errors in models MII and MIII are much larger). As an example, take the case of heating transient at t = 100 minutes after the sudden change of the thermal condition. Uncorrected model temperatures of errors up to approximately 10°R in MI, 26°R in MII, and 13°R in MIII are brought to within 4°R of the prototype value after correction [see TABLE 6.2(c)]. For the steady state, corresponding errors of up to 21.3, 20.6, and 34.5°R are reduced to less than 2.5°R [see TABLE 6.2(f)]. At a time 30 minutes after cooling begins, uncorrected model temperatures exhibit errors of up to 23.8, 24.9, and 39.3°R, respectively, for the three models. After correction, the maximum error is 2.5°R [see TABLE 6.2(g)]. Data for the 45° solar incidence show similar results.

To test further the performance of the theory, a second set of errors in kd, Cd, ε, and ε' was studied. They are listed in TABLE 6.4. The magnitudes of the various errors are approximately the same as before. However, both positive and negative errors now occur in kd and Cd. Moreover, the modifications for model MIII are carried out in such a manner that the negative errors become *less* negative. The results of this study are summarized in TABLES 6.5(a)-(h) when the spacecraft receives the sun's radiation at normal incidence and in TABLES 6.6(a)-(h) for the 45° oblique incidence. The spacecraft's initial thermal condition, the manner of the initiation of the heating and cooling transients, the relative distribution of internal power dissipation within the bus, etc., are identical to those considered in the earlier study. All data again lend support to the effectiveness of the proposed correction technique. The errors E_{MC} which remain in the corrected model temperatures are, in general, smaller than those shown in TABLES 6.2 and 6.3. Our limited experience seems to indicate that the theory would yield better results when positive and negative errors coexist in each set of the modeling parameters.

6.2 SPACECRAFT SUBJECTED TO CYCLIC HEATING AND COOLING

For an orbiting spacecraft, the temperatures of its various components undergo continuous cyclic changes. Under such condition, there was the concern that the error in the model temperatures might accumulate and it was not certain that the proposed correction technique

TABLE 6.4 Errors in modeling parameters

Surface	Percentage error in modeling parameters											
	Model MI				Model MII				Model MIII			
	δ_{kd} X 100	δ_{Cd} X 100	δ_{ε} X 100	$\delta_{\varepsilon'}$ X 100	δ_{kd} X 100	δ_{Cd} X 100	δ_{ε} X 100	$\delta_{\varepsilon'}$ X 100	δ_{kd} X100	δ_{Cd} X 100	δ_{ε} X 100	$\delta_{\varepsilon'}$ X 100
A_1	0	0	0	0	0	0	0	0	0	0	0	0
A_2	0	0	0	0	0	0	0	0	0	0	0	0
A_3	-20.0	20.0	-28.8	10.0	-20.0	42.0	-28.8	20.0	-11.0	20.0	-18.0	10.0
A_4	0	0	0	0	0	0	0	0	0	0	0	0
A_5	0	0	0	0	0	0	0	0	0	0	0	0
A_6	18.0	-15.0	-32.0	10.0	39.6	-15.0	-32.0	20.0	18.0	-8.2	-20.0	10.0
A_7	20.0	15.0	15.0	-14.7	42.0	33.0	27.0	-14.7	20.0	15.0	15.0	-8.0
A_8	8.0	-15.0	-25.9	-11.5	19.2	-15.0	-25.9	-11.5	8.0	-9.0	-18.0	-8.0
A_9	-10.0	-15.0	25.0	-16.0	-10.0	-15.0	45.0	-16.0	-6.5	-8.2	25.0	-8.0
A_{10}	-18.0	15.0	15.0	-12.8	-18.0	36.0	33.0	-12.8	-10.8	15.0	15.0	-8.0
A_{11}	0	0	0	0	0	0	0	0	0	0	0	0
$A_{12}(=A_{10'})$	0	0	15.0	0	0	0	33.0	0	0	0	15.0	0

δ_{ε} refers to the exterior of the surface in question and $\delta_{\varepsilon'}$ refers to its interior

TABLE 6.5(a) Model temperatures before and after correction

Heating Transient: 10 minutes after spacecraft subject to solar irradiation (normal incidence) and internal heating

Surface	Prototype or Perfect Model Temperature T_P	Temperatures of Imperfect Models						$\Delta^{(+)}$	$\Delta^{(-)}$	Δ_t	Model Temperature after Correction	
		Model MI		Model MII		Model MIII						
		T_{MI}	E_{MI}	T_{MII}	E_{MII}	T_{MIII}	E_{MIII}				T_{MC}	E_{MC}
A_1	518.1	518.0	-0.1	518.0	-0.1	518.1	0	-0.01	-0.09	-0.10	518.1	0
A_2	520.5	519.9	-0.6	519.8	-0.7	520.1	-0.4	-0.04	-0.54	-0.58	520.4	-0.1
A_3	429.4	429.2	-0.2	425.3	-4.1	427.7	-1.7	-3.59	3.78	0.19	429.0	-0.4
A_4	518.1	518.0	-0.1	518.0	-0.1	518.0	-0.1	~0	-0.07	-0.07	518.1	0
A_5	520.2	519.8	-0.4	519.8	-0.4	519.9	-0.3	~0	-0.41	-0.41	520.2	0
A_6	412.2	416.7	4.5	416.7	4.5	414.7	2.5	-0.01	5.17	5.16	411.6	-0.6
A_7	401.5	401.5	0	401.3	-0.2	401.4	-0.1	-0.16	0.15	-0.01	401.5	0
A_8	420.7	427.8	7.1	427.6	6.9	425.0	4.3	-0.19	7.09	6.90	420.9	0.2
A_9	415.9	418.3	2.4	417.8	1.9	416.9	1.0	-0.43	3.55	3.12	415.2	-0.7
A_{10}	403.0	403.0	0	402.5	-0.5	402.9	-0.1	-0.44	0.40	-0.04	403.1	0.1
A_{11}	476.3	476.3	0	476.3	0	476.3	0	~0	~0	0	476.3	0
A_{12} (=A_{10}')	152.8	153.4	0.6	153.4	0.6	153.1	0.3	-0.05	0.90	0.85	152.6	-0.2

All temperatures in °R.

TABLE 6.5(b) Model temperatures before and after correction

Heating Transient: 30 minutes after spacecraft subject to solar irradiation (normal incidence) and internal heating

Surface	Prototype or Perfect Model Temperature T_p	Temperatures of Imperfect Models						$\Delta^{(+)}$	$\Delta^{(-)}$	Δ_t	Model Temperature after Correction	
		Model MI		Model MII		Model MIII						
		T_{MI}	E_{MI}	T_{MII}	E_{MII}	T_{MIII}	E_{MIII}				T_{MC}	E_{MC}
A_1	590.7	590.6	-0.1	590.5	-0.2	590.6	-0.1	-0.03	-0.12	-0.15	590.7	0
A_2	594.9	594.0	-0.9	593.8	-1.1	594.3	-0.6	-0.17	-0.70	-0.87	594.9	0
A_3	474.5	478.0	3.5	470.2	-4.3	473.9	-0.6	-7.19	10.52	3.33	474.7	0.2
A_4	590.5	590.5	0	590.5	0	590.5	0	~0	-0.04	-0.04	590.5	0
A_5	593.9	593.6	-0.3	593.6	-0.3	593.7	-0.2	~0	-0.24	-0.24	593.9	0
A_6	440.3	451.6	11.3	451.4	11.1	446.4	6.1	-0.24	13.27	13.03	438.6	-1.7
A_7	413.1	413.4	0.3	411.8	-1.3	412.8	-0.3	-1.49	1.60	0.11	413.3	0.2
A_8	450.6	466.2	15.6	465.1	14.5	459.9	9.3	-0.99	15.88	14.89	451.3	0.7
A_9	445.4	452.5	7.1	450.6	5.2	448.4	3.0	-1.73	10.25	8.52	443.9	-1.5
A_{10}	424.3	426.1	1.8	422.8	-1.5	424.3	0	-3.00	4.43	1.43	424.6	0.3
A_{11}	547.6	547.6	0	547.6	0	547.6	0	0.01	~0	0.01	547.6	0
$A_{12}(=A_{10}')$	172.2	172.8	0.6	172.6	0.4	172.5	0.3	-0.23	0.98	0.75	172.1	-0.1

All temperatures in °R.

TABLE 6.5(c) Model temperatures before and after correction

Heating Transient: 100 minutes after spacecraft subject to solar irradiation (normal incidence) and internal heating

Surface	Prototype or Perfect Model Temperature T_P	Temperatures of Imperfect Models						$\Delta^{(+)}$	$\Delta^{(-)}$	Δ_t	Model Temperature after Correction	
		Model MI		Model MII		Model MIII						
		T_{MI}	E_{MI}	T_{MII}	E_{MII}	T_{MIII}	E_{MIII}				T_{MC}	F_{MC}
A_1	597.8	597.7	-0.1	597.6	-0.2	597.7	-0.1	-0.03	-0.10	-0.13	597.8	0
A_2	603.8	603.1	-0.7	602.9	-0.9	603.4	-0.4	-0.19	-0.60	-0.79	603.9	0.1
A_3	519.1	542.0	22.9	537.4	18.3	531.3	12.2	-4.26	27.24	22.98	519.0	-0.1
A_4	597.6	597.6	0	597.6	0	597.6	0	-0.01	-0.04	-0.05	597.6	0
A_5	602.8	602.5	-0.3	602.5	-0.3	602.6	-0.2	-0.07	-0.23	-0.30	602.8	0
A_6	498.8	523.7	24.9	521.6	22.8	512.4	13.6	-1.96	28.72	26.76	496.9	-1.9
A_7	479.6	490.1	10.5	482.5	28.9	484.0	4.4	-7.00	15.38	8.38	481.7	2.1
A_8	499.5	526.1	26.6	523.5	24.0	515.4	15.9	-2.45	27.20	24.75	501.4	1.9
A_9	511.6	530.6	20.0	525.8	14.2	520.9	9.3	-4.41	24.56	20.15	510.5	-1.1
A_{10}	490.8	507.6	16.8	501.9	11.1	499.3	8.5	-5.21	20.97	15.76	491.8	1.0
A_{11}	568.0	568.1	0.1	568.1	0.1	568.1	0.1	0.01	0.02	0.03	568.0	0
$A_{12}(=A_{10'})$	181.1	183.7	2.6	183.1	2.0	182.4	1.3	-0.56	3.46	2.90	180.8	-0.3

All temperatures in °R.

TABLE 6.5(d) Model temperatures before and after correction

Heating Transient: 300 minutes after spacecraft subject to solar irradiation (normal incidence) and internal heating

Surface	Prototype or Perfect Model Temperature T_P	Temperatures of Imperfect Models						$\Delta^{(+)}$	$\Delta^{(-)}$	Δ_t	Model Temperature after Correction	
		Model MI		Model MII		Model MIII						
		T_{MI}	E_{MI}	T_{MII}	E_{MII}	T_{MIII}	E_{MIII}				T_{MC}	E_{MC}
A_1	598.0	597.9	-0.1	597.9	-0.1	597.9	-0.1	-0.01	-0.07	-0.08	598.0	0
A_2	604.7	604.3	-0.4	604.3	-0.4	604.5	-0.2	-0.06	-0.43	-0.49	604.8	0.1
A_3	533.9	565.9	32.0	564.6	30.7	552.2	18.3	-1.13	34.62	33.49	532.4	-1.5
A_4	597.9	597.8	-0.1	597.8	-0.1	597.9	0	-0.01	-0.04	-0.04	597.9	0
A_5	604.3	604.0	-0.2	604.0	-0.2	604.2	0	-0.05	-0.21	-0.26	604.3	0.1
A_6	524.4	558.4	34.0	557.3	32.9	543.9	19.5	-1.03	36.66	35.63	522.8	-1.6
A_7	527.7	556.5	28.8	554.2	26.5	544.7	17.0	-2.17	29.87	27.70	528.8	1.1
A_8	524.0	558.5	34.5	557.2	33.2	545.2	21.2	-1.19	33.60	32.41	526.1	2.1
A_9	546.2	574.9	28.7	571.8	25.6	562.2	16.0	-2.86	32.09	29.23	545.7	-0.5
A_{10}	527.7	556.6	28.9	554.4	26.7	544.8	17.1	-1.98	30.00	28.02	528.6	0.9
A_{11}	568.1	568.2	0.1	568.2	0.1	568.2	0.1	0.02	0.04	0.06	568.1	0
$A_{12}(=A_{10}')$	184.9	189.5	4.6	189.3	4.4	187.4	2.5	-0.26	5.53	5.27	184.3	-0.6

All temperatures in °R.

TABLE 6.5(e) Model temperatures before and after correction

Heating Transient: 500 minutes after spacecraft subject to solar irradiation (normal incidence) and internal heating

Surface	Prototype or Perfect Model Temperature T_p	Temperatures of Imperfect Models						$\Delta^{(+)}$	$\Delta^{(-)}$	Δ_t	Model Temperature after Correction	
		Model MI		Model MII		Model MIII						
		T_{MI}	E_{MI}	T_{MII}	E_{MII}	T_{MIII}	E_{MIII}				T_{MC}	E_{MC}
A_1	598.0	597.9	-0.1	597.9	-0.1	597.9	-0.1	-0.01	-0.07	-0.08	598.0	0
A_2	604.8	604.4	-0.4	604.3	-0.5	604.6	-0.2	-0.03	-0.42	-0.45	604.9	0.1
A_3	534.4	566.9	32.5	566.2	31.8	553.2	18.8	-0.72	34.91	34.19	533.7	-0.7
A_4	597.9	597.9	0	597.8	-0.1	597.9	0	~0	-0.04	-0.04	597.9	0
A_5	604.3	604.2	-0.1	604.1	-0.2	604.2	-0.1	-0.03	-0.21	-0.24	604.4	0.1
A_6	525.3	559.9	34.6	559.2	33.9	545.3	20.0	-0.60	36.95	36.35	524.8	-0.5
A_7	529.4	559.2	29.8	557.9	28.5	547.3	17.9	-1.20	30.31	29.11	531.5	2.1
A_8	525.0	560.0	35.0	559.1	34.1	546.6	21.6	-0.75	33.83	33.08	527.7	2.7
A_9	547.5	576.8	29.4	574.4	26.9	564.1	16.6	-2.28	32.34	30.06	547.1	-0.4
A_{10}	529.0	558.7	29.7	557.3	28.3	546.7	17.7	-1.28	30.29	29.01	530.9	1.9
A_{11}	568.1	568.2	0.1	568.2	0.1	568.2	0.1	0.02	0.04	0.06	568.1	0
A_{12} ($=A_{1.0'}$)	185.0	189.8	4.8	189.6	4.6	187.6	2.6	-0.18	5.62	5.44	183.7	-1.3

All temperatures in °R.

TABLE 6.5(f) Model temperatures before and after correction

Steady State

Surface	Prototype or Perfect Model Temperature T_P	Temperatures of Imperfect Models						$\Delta^{(+)}$	$\Delta^{(-)}$	Δ_t	Model Temperature after Correction	
		Model MI		Model MII		Model MIII						
		T_{MI}	E_{MI}	T_{MII}	E_{MII}	T_{MIII}	E_{MIII}				T_{MC}	E_{MC}
A_1	597.9	597.9	0	597.9	0	597.9	0	-0.01	-0.07	-0.08	598.0	0.1
A_2	604.8	604.4	-0.4	604.4	-0.4	604.6	-0.2	-0.03	-0.42	-0.45	604.8	0
A_3	534.4	567.0	32.6	566.2	31.8	553.2	18.8	-0.69	34.91	34.22	532.8	-1.6
A_4	597.9	597.9	0	597.8	-0.1	597.9	0	~0	-0.04	-0.04	597.9	0
A_5	604.3	604.2	-0.1	604.1	-0.2	604.2	-0.1	-0.03	-0.21	-0.25	604.4	0.1
A_6	525.3	559.9	34.6	559.3	34.0	545.3	20.0	-0.57	36.96	36.39	523.5	-1.8
A_7	529.5	559.4	29.9	558.1	28.6	547.4	17.9	-1.13	30.32	29.19	530.2	0.7
A_8	525.0	560.0	35.0	559.2	34.2	546.7	21.7	-0.71	33.83	33.12	526.9	1.9
A_9	547.5	576.9	29.4	574.5	27.0	564.2	16.7	-2.23	32.34	30.11	546.8	-0.7
A_{10}	529.0	558.8	29.8	557.5	28.5	546.8	17.8	-1.22	30.30	29.08	529.7	0.7
A_{11}	568.1	568.2	0.1	568.2	0.1	568.2	0.1	0.02	0.04	0.06	568.1	0
$A_{12}(=A_{10}')$	185.0	189.8	4.8	189.6	4.6	187.6	2.6	-0.17	5.62	5.45	184.4	-0.6

All temperatures in °R.

TABLE 6.5(g) Model temperatures before and after correction

Cooling Transient: 30 minutes after spacecraft moving into shade

Surface	Prototype or Perfect Model Temperature T_P	Temperatures of Imperfect Models						$\Delta^{(+)}$	$\Delta^{(-)}$	Δ_t	Model Temperature after Correction	
		Model MI		Model MII		Model MIII						
		T_{MI}	E_{MI}	T_{MII}	E_{MII}	T_{MIII}	E_{MIII}				T_{MC}	E_{MC}
A_1	376.5	376.4	-0.1	376.4	-0.1	376.5	0	~0	-0.19	-0.19	376.6	0.1
A_2	390.5	389.7	-0.8	389.7	-0.8	390.1	-0.4	~0	-1.04	-1.04	390.7	0.2
A_3	516.2	554.4	38.2	554.7	38.5	539.0	22.8	0.33	38.89	39.21	515.1	-0.9
A_4	376.4	376.2	-0.2	376.2	0	376.3	-0.1	-0.01	-0.23	-0.24	376.5	0.1
A_5	389.9	388.8	-0.1	388.8	-0.1	389.3	-0.6	-0.05	-1.29	-1.34	390.2	0.3
A_6	513.0	550.4	37.4	549.9	36.9	534.8	21.8	-0.43	39.44	39.01	511.4	-1.6
A_7	527.0	557.4	30.4	556.3	29.3	545.3	18.3	-0.95	30.61	29.66	527.7	0.7
A_8	522.6	557.9	35.3	557.2	34.6	544.5	21.9	-0.69	34.11	33.42	524.5	1.9
A_9	543.4	573.6	30.2	571.3	27.9	560.6	17.2	-2.14	32.92	30.78	542.8	-0.6
A_{10}	525.5	556.0	30.5	554.9	29.4	543.8	18.3	-1.02	30.74	29.72	526.3	0.8
A_{11}	395.2	395.3	0.1	395.4	0.2	395.3	0.1	-0.04	-0.07	-0.11	395.2	0
$A_{12}(=A_{10}')$	150.4	159.2	8.8	158.9	8.5	155.3	4.9	-0.24	9.96	9.72	149.5	-0.9

All temperatures in °R.

TABLE 6.5(h) Model temperatures before and after correction

Cooling Transient: 200 minutes after spacecraft moving into shade

Surface	Prototype or Perfect Model Temperature T_p	Temperatures of Imperfect Models						$\Delta^{(+)}$	$\Delta^{(-)}$	Δ_t	Model Temperature after Correction	
		Model MI		Model MII		Model MIII						
		T_{MI}	E_{MI}	T_{MII}	E_{MII}	T_{MIII}	E_{MIII}				T_{MC}	E_{MC}
A_1	229.8	229.4	-0.4	229.4	-0.4	229.6	-0.2	-0.01	-0.57	-0.58	230.0	0.2
A_2	275.7	274.2	-1.5	274.1	-1.6	275.1	-0.6	-0.08	-2.08	-2.16	276.4	0.7
A_3	500.3	540.3	40.0	539.8	39.5	523.7	23.4	-0.39	41.84	41.45	498.8	1.5
A_4	229.0	228.4	-0.6	228.4	-0.6	228.7	-0.3	-0.01	-0.92	-0.93	229.3	0.3
A_5	272.7	270.3	-2.4	270.3	-2.4	271.7	-1.0	-0.05	-3.38	-3.43	273.8	1.1
A_6	491.8	534.5	42.7	534.3	42.5	517.0	25.2	-0.16	44.34	44.18	490.3	-1.5
A_7	508.8	542.6	33.8	541.4	32.6	529.0	20.2	-1.01	34.30	33.29	509.3	0.5
A_8	510.4	547.8	37.4	547.0	36.5	533.4	23.0	-0.81	36.53	35.72	512.1	1.7
A_9	525.6	559.6	34.0	557.2	31.6	545.0	19.4	-2.15	36.92	34.77	524.8	-0.8
A_{10}	508.3	542.0	33.7	540.7	32.4	528.5	20.2	-1.20	34.40	33.20	508.8	0.5
A_{11}	235.6	236.1	0.5	236.3	0.7	236.0	0.4	0.19	0.34	0.53	235.6	0
$A_{12}(=A_{10}')$	134.8	146.3	11.5	145.9	11.1	141.2	6.4	-0.33	12.90	12.57	133.7	-1.1

All temperatures in °R.

TABLE 6.6(a) Model temperatures before and after correction

Heating Transient: 10 minutes after spacecraft subject to solar irradiation (45° incidence) and internal heating

Surface	Prototype or Perfect Model Temperature T_P	Temperatures of Imperfect Models						$\Delta^{(+)}$	$\Delta^{(-)}$	Δ_t	Model Temperature after Correction	
		Model MI		Model MII		Model MIII						
		T_{MI}	E_{MI}	T_{MII}	E_{MII}	T_{MIII}	E_{MIII}				T_{MC}	E_{MC}
A_1	477.4	477.3	-0.1	477.3	-0.1	477.3	-0.1	-0.01	-0.12	-0.13	477.4	0
A_2	370.1	369.3	-0.8	369.2	-0.9	369.6	-0.5	-0.05	-0.74	-0.79	370.0	-0.1
A_3	425.7	427.0	1.3	423.4	-2.3	425.1	-0.6	-3.30	4.63	1.33	425.6	-0.1
A_4	481.0	480.9	-0.1	480.9	-0.1	481.0	0	~0	-0.09	-0.09	481.0	0
A_5	499.3	498.7	-0.6	498.7	-0.6	498.8	-0.5	~0	-0.50	-0.50	499.2	-0.1
A_6	430.4	438.1	7.7	438.0	7.6	434.5	4.1	-0.15	9.22	9.07	429.1	-1.3
A_7	401.7	401.8	0.1	401.6	-0.1	401.7	0	-0.16	0.23	0.07	401.7	0
A_8	421.3	428.7	7.4	428.6	7.3	425.8	4.5	-0.09	7.45	7.36	421.3	0
A_9	416.9	419.8	2.9	419.4	2.5	418.2	1.3	-0.36	4.07	3.71	416.1	-0.8
A_{10}	403.6	403.8	0.2	403.2	-0.4	403.5	-0.1	-0.48	0.61	0.13	403.6	0
A_{11}	447.6	447.6	0	447.6	0	447.6	0	0.01	~0	0.01	447.6	0
$A_{12}(=A_{10'})$	142.1	143.0	0.9	143.0	0.9	142.5	0.4	-0.06	1.25	1.19	141.8	-0.3

All temperatures in °R.

TABLE 6.6(b) Model temperatures before and after correction

Heating Transient: 10 minutes after spacecraft subject to solar irradiation (45° incidence) and internal heating

Surface	Prototype or Perfect Model Temperature T_P	Temperatures of Imperfect Models						$\Delta^{(+)}$	$\Delta^{(-)}$	Δ_t	Model Temperature after Correction	
		Model MI		Model MII		Model MIII						
		T_{MI}	E_{MI}	T_{MII}	E_{MII}	T_{MIII}	E_{MIII}				T_{MC}	E_{MC}
A_1	535.6	535.4	-0.2	535.3	-0.3	535.4	-0.2	-0.03	-0.21	-0.24	535.6	0
A_2	335.3	333.0	-2.3	332.7	-2.6	333.8	-1.5	-0.30	-1.90	-2.20	335.2	-0.1
A_3	457.7	467.0	9.3	460.4	2.7	461.2	3.5	-6.06	14.68	8.62	458.4	0.7
A_4	541.9	541.8	-0.1	541.8	-0.1	541.9	0	~0	-0.10	-0.10	541.9	0
A_5	568.3	567.7	-0.6	567.7	-0.6	567.9	-0.4	-0.02	-0.54	-0.56	568.3	0
A_6	480.6	499.2	18.6	498.1	17.5	490.4	9.8	-0.98	22.26	21.28	477.9	-2.7
A_7	414.9	416.0	1.1	414.4	-0.5	415.1	0.2	-1.55	2.46	0.91	415.1	0.2
A_8	453.5	471.1	17.6	470.5	17.0	464.1	10.6	-0.54	17.94	17.40	453.7	0.2
A_9	450.5	460.4	9.9	458.9	8.4	455.2	4.7	-1.42	13.25	11.83	448.6	-1.9
A_{10}	427.6	431.2	3.6	427.8	0.2	428.7	1.1	-3.11	6.35	3.24	427.9	0.3
A_{11}	498.0	498.0	0	498.0	0	498.0	0	0.01	0.01	0.02	498.0	0
$A_{12}(=A_{10'})$	155.5	156.7	1.2	156.3	0.8	156.0	0.5	-0.33	1.76	1.43	155.2	-0.3

All temperature in °R.

TABLE 6.6(c) Model temperatures before and after correction

Heating Transient: 100 minutes after spacecraft subject to solar irradiation (45° incidence) and internal heating

Surface	Prototype or Perfect Model Temperature T_p	Temperatures of Imperfect Models						$\Delta^{(+)}$	$\Delta^{(-)}$	Δ_t	Model Temperature after Correction	
		Model MI		Model MII		Model MIII						
		T_{MI}	E_{MI}	T_{MII}	E_{MII}	T_{MIII}	E_{MIII}				T_{MC}	E_{MC}
A_1	546.3	546.1	-0.2	546.1	-0.2	546.2	-0.1	-0.04	-0.17	-0.21	546.3	0
A_2	296.2	292.4	-3.8	291.3	-4.9	293.7	-2.5	-1.05	-3.19	-4.24	296.7	0.5
A_3	498.1	529.3	31.2	525.0	26.9	515.3	17.2	-3.88	35.30	31.42	497.9	-0.2
A_4	553.4	553.3	-0.1	553.2	-0.2	553.3	-0.1	-0.03	-0.11	-0.14	553.4	0
A_5	581.6	580.9	-0.7	580.7	-0.9	581.1	-0.5	-0.18	-0.55	-0.73	581.7	0.1
A_6	552.8	586.1	33.3	582.5	29.7	570.8	18.0	-3.31	38.88	35.57	550.6	-2.2
A_7	490.6	507.5	16.9	499.6	9.0	498.7	8.1	-7.29	22.17	14.88	492.6	2.0
A_8	507.9	539.8	31.9	537.6	29.7	527.0	19.1	-2.04	32.56	30.52	509.3	1.4
A_9	524.9	550.8	25.9	546.1	21.2	538.3	13.4	-4.27	31.66	27.39	523.4	-1.5
A_{10}	502.6	526.1	23.5	520.6	18.0	515.0	12.4	-5.05	28.01	22.96	503.1	0.5
A_{11}	520.6	520.7	0.1	520.7	0.1	520.7	0.1	0.02	0.04	0.06	520.6	0
$A_{12}(=A_{10'})$	167.2	171.8	4.6	171.0	3.8	169.4	2.2	-0.74	5.95	5.21	166.6	-0.6

All temperatures in °R.

TABLE 6.6(d) Model temperatures before and after correction

Heating Transient: 300 minutes after spacecraft subject to solar irradiation (45° incidence) and internal heating

Surface	Prototype or Perfect Model Temperature T_P	Temperatures of Imperfect Models						$\Delta^{(+)}$	$\Delta^{(-)}$	Δ_t	Model Temperature after Correction	
		Model MI		Model MII		Model MIII						
		T_{MI}	E_{MI}	T_{MII}	E_{MII}	T_{MIII}	E_{MIII}				T_{MC}	E_{MC}
A_1	546.5	546.4	-0.1	546.4	-0.1	546.4	-0.1	-0.01	-0.11	-0.12	546.5	0
A_2	290.8	289.4	-1.4	289.0	-1.8	290.2	-0.6	-0.37	-1.79	-2.16	291.6	0.8
A_3	515.2	556.4	41.2	556.1	40.9	539.4	24.2	-0.31	43.10	42.79	513.7	-1.5
A_4	553.8	553.7	-0.1	553.6	-0.2	553.7	-0.1	-0.03	-0.10	-0.13	553.8	0
A_5	583.4	582.9	-0.5	582.8	-0.6	583.1	-0.3	-0.13	-0.50	-0.63	583.5	0.1
A_6	573.4	614.0	40.6	611.8	38.4	596.4	23.0	-2.04	44.73	42.69	571.3	-2.1
A_7	540.1	575.3	35.2	573.5	33.4	561.0	20.9	-1.66	36.08	34.42	540.9	0.8
A_8	533.1	572.6	39.5	571.9	38.8	557.4	24.3	-0.69	38.55	37.86	534.8	1.7
A_9	559.6	594.5	34.9	591.8	32.2	579.4	19.8	-2.50	38.20	35.70	558.8	-0.8
A_{10}	540.0	575.2	35.2	573.5	33.5	560.9	20.9	-1.54	36.12	34.58	540.6	0.6
A_{11}	520.9	521.0	0.1	521.1	0.2	521.0	0.1	0.03	0.07	0.10	520.9	0
$A_{12}(=A_{10}')$	172.2	179.4	7.2	179.1	6.9	176.1	3.9	-0.28	8.44	8.16	171.3	-0.9

All temperatures in °R.

TABLE 6.6(e) Model temperatures before and after correction

Heating Transient: 500 minutes after spacecraft subject to solar irradiation (45° incidence) and internal heating

Surface	Prototype or Perfect Model Temperature T_P	Temperatures of Imperfect Models						$\Delta^{(+)}$	$\Delta^{(-)}$	Δ_t	Model Temperature after Correction	
		Model MI		Model MII		Model MIII						
		T_{MI}	E_{MI}	T_{MII}	E_{MII}	T_{MIII}	E_{MIII}				T_{MC}	E_{MC}
A_1	546.5	546.4	-0.1	546.4	-0.1	546.4	-0.1	~0	-0.10	-0.10	546.5	0
A_2	291.4	290.6	-0.8	290.6	-0.8	291.2	-0.2	~0	-1.57	-1.57	292.1	0.7
A_3	515.7	557.3	41.6	557.4	41.7	540.2	24.5	0.09	43.23	43.32	514.0	-1.7
A_4	553.8	553.7	-0.1	553.7	-0.1	553.7	-0.1	-0.02	-0.10	-0.12	553.8	0
A_5	583.4	583.0	-0.4	582.8	-0.6	583.2	-0.2	-0.11	-0.51	-0.62	583.6	0.2
A_6	573.9	614.8	40.9	613.0	39.1	597.1	23.2	-1.73	44.82	43.09	571.7	-2.2
A_7	541.3	577.2	35.9	576.2	34.9	562.9	21.6	-0.87	36.18	35.31	541.9	0.6
A_8	533.7	573.7	40.0	573.3	39.6	558.4	24.7	-0.32	38.60	38.28	535.4	1.7
A_9	560.5	595.9	35.4	593.7	33.2	580.8	20.3	-2.02	38.23	36.21	559.7	-0.8
A_{10}	541.0	576.6	35.6	575.6	34.6	562.4	21.4	-0.97	36.16	35.19	541.4	0.4
A_{11}	520.9	521.0	0.1	521.1	0.2	521.0	0.1	0.04	0.07	0.11	520.9	0
$A_{12}(=A_{10}')$	172.3	179.7	7.4	179.5	7.2	176.3	4.0	-0.18	8.48	8.30	171.4	-0.9

All temperatures in °R.

TABLE 6.6(f) Model temperatures before and after correction

Steady State

Surface	Prototype or Perfect Model Temperature T_P	Temperatures of Imperfect Models						$\Delta^{(+)}$	$\Delta^{(-)}$	Δ_t	Model Temperature after Correction	
		Model MI		Model MII		Model MIII						
		T_{MI}	E_{MI}	T_{MII}	E_{MII}	T_{MIII}	E_{MIII}				T_{MC}	E_{MC}
A_1	546.5	546.4	-0.1	546.4	-0.1	546.4	-0.1	0.01	-0.10	-0.09	546.5	0
A_2	291.5	290.7	-0.8	290.7	-0.8	291.3	-0.2	0.04	-1.56	-1.52	292.2	0.7
A_3	515.8	557.3	41.5	557.5	41.7	540.3	24.5	0.11	43.23	43.34	514.0	-1.8
A_4	553.8	553.7	-0.1	553.7	-0.1	553.7	-0.1	-0.02	-0.10	-0.12	553.8	0
A_5	583.4	583.0	-0.4	582.8	-0.6	583.2	-0.2	-0.11	-0.51	-0.62	583.6	0.2
A_6	573.9	614.9	41.0	613.0	39.1	597.2	23.3	-1.71	44.82	43.11	571.8	-2.1
A_7	541.4	577.2	35.8	576.3	34.9	562.9	21.5	-0.83	36.18	35.35	541.9	0.5
A_8	533.8	573.7	39.9	573.4	39.6	558.5	24.7	-0.30	38.60	38.30	535.4	1.6
A_9	560.6	595.9	35.3	593.7	33.1	580.8	20.2	-1.99	38.22	36.23	559.7	-0.9
A_{10}	541.0	576.7	35.7	575.7	34.7	562.4	21.4	-0.93	36.16	35.23	541.5	0.5
A_{11}	520.9	521.0	0.1	521.1	0.2	521.0	0.1	0.04	0.07	0.11	520.9	0
$A_{12}(=A_{10'})$	172.3	179.7	7.4	179.5	7.2	176.4	4.1	-0.17	8.48	8.31	171.4	-0.9

All temperatures in °R.

TABLE 6.6(g) Model temperatures before and after correction

Cooling Transient: 30 minutes after spacecraft moving into shade

Surface	Prototype or Perfect Model Temperature T_p	Temperatures of Imperfect Models						$\Delta^{(+)}$	$\Delta^{(-)}$	Δ_t	Model Temperature after Correction	
		Model MI		Model MII		Model MIII						
		T_{MI}	E_{MI}	T_{MII}	E_{MII}	T_{MIII}	E_{MIII}				T_{MC}	E_{MC}
A_1	366.5	366.4	-0.1	366.4	-0.1	366.4	-0.1	~0	-0.16	-0.16	366.5	0
A_2	288.6	287.7	-0.9	287.7	-0.9	288.3	-0.3	0.05	-1.68	-1.63	289.3	0.7
A_3	512.5	554.2	41.7	554.4	41.9	537.2	24.7	0.25	43.03	43.28	510.9	-1.6
A_4	370.5	370.2	-0.3	370.2	-0.3	370.3	-0.2	-0.03	-0.30	-0.33	370.6	0.1
A_5	390.4	389.0	-1.4	388.8	-1.6	389.6	-0.8	-0.16	-1.56	1.72	390.7	0.3
A_6	529.5	568.7	39.2	567.6	38.1	552.3	22.8	-1.02	41.62	40.60	528.1	-1.4
A_7	536.7	571.8	35.1	571.2	34.5	558.0	21.3	-0.57	35.16	34.59	537.2	0.5
A_8	529.0	567.4	38.4	566.8	37.8	552.8	23.8	-0.56	37.09	36.53	530.9	1.9
A_9	552.6	586.4	33.8	584.1	31.5	572.0	19.4	-2.12	36.51	34.39	552.1	-0.5
A_{10}	534.4	568.7	34.4	567.9	33.5	555.1	20.7	-0.75	34.54	33.79	534.9	0.5
A_{11}	383.1	383.3	0.2	383.4	0.3	383.3	0.2	0.06	0.11	0.17	383.1	0
$A_{12}(=A_{10'})$	149.7	160.0	10.3	159.8	10.1	155.4	5.7	-0.19	11.48	11.29	148.7	-1.0

All temperatures in °R.

TABLE 6.6(h) Model temperatures before and after correction

Cooling Transient: 200 minutes after spacecraft moving into shade

Surface	Prototype or Perfect Model Temperature T_p	Temperatures of Imperfect Models						$\Delta^{(+)}$	$\Delta^{(-)}$	Δ_t	Model Temperature after Correction	
		Model MI		Model MII		Model MIII						
		T_{MI}	E_{MI}	T_{MII}	E_{MII}	T_{MIII}	E_{MIII}				T_{MC}	E_{MC}
A_1	227.8	227.4	-0.4	227.4	-0.4	227.7	-0.1	~0	-0.57	-0.57	22.80	0.2
A_2	269.9	268.4	-1.5	268.3	-1.6	269.3	-0.6	-0.03	-2.27	-2.30	270.7	0.8
A_3	500.5	540.7	40.2	540.3	39.8	524.1	23.6	-0.29	42.00	41.71	498.9	-1.6
A_4	228.8	228.1	-0.7	228.1	-0.7	228.5	-0.3	-0.01	-0.94	-0.95	229.1	0.3
A_5	273.4	271.0	-2.4	271.0	-2.4	272.4	-1.0	-0.03	-3.36	-3.39	274.4	1.0
A_6	492.4	535.2	42.8	535.1	42.7	517.6	25.2	-0.08	44.46	44.38	490.8	-1.6
A_7	509.6	543.7	34.1	542.8	33.2	530.1	20.5	-0.82	34.50	33.68	510.0	0.4
A_8	510.9	548.5	37.6	547.7	36.8	534.0	23.1	-0.73	36.65	35.92	512.5	1.6
A_9	526.2	560.4	34.2	558.2	32.0	545.8	19.6	-2.04	37.04	35.00	525.4	-0.8
A_{10}	509.0	542.9	33.9	541.8	32.8	529.3	20.3	-1.06	34.54	33.48	509.5	0.5
A_{11}	234.0	234.6	0.6	234.8	0.8	234.4	0.4	0.20	0.36	0.56	234.0	0
$A_{12}(=A_{10'})$	134.8	146.5	11.7	146.1	11.3	141.3	6.5	-0.30	12.97	12.67	133.8	-1.0

All temperatures in °R.

would still be capable of providing satisfactory results. To obtain some answers to these questions, additional computer experimentation was carried out in which the hypothetical spacecraft was subjected to direct sun's irradiation at normal incidence for 200 minutes, followed by its entry into the shade for 100 minutes and the cycle repeated itself thereafter. The internal power dissipation was left unaltered at all times. At the very beginning, the spacecraft had a uniform temperature of 400°R throughout and the errors in the modeling parameters were taken as those listed in TABLE 6.4. Other conditions were the same as those used in the earlier studies. The computation was continued for five complete cycles. Because of the massive data generated, only temperatures at 30 and 200 minutes from the start of each cycle and those at the end of each cycle are presented herein. In addition, data for the third and fourth cycle are omitted in the interest of conserving space. This is illustrated in Fig. 6.1. Details of the temperature data are given in TABLES 6.7(a)-(i). It goes without saying that the results are very encouraging indeed. A second experiment of the same kind was also conducted in which the heating and cooling time were doubled; so was the period of the cycle. The results were equally good. Details may be supplied upon request.

The foregoing studies have established, beyond doubt, the usefulness of the proposed concept of imperfect modeling when the errors in the modeling parameters are restricted such that the linear theory is applicable and when they are properly controlled, as pointed out in

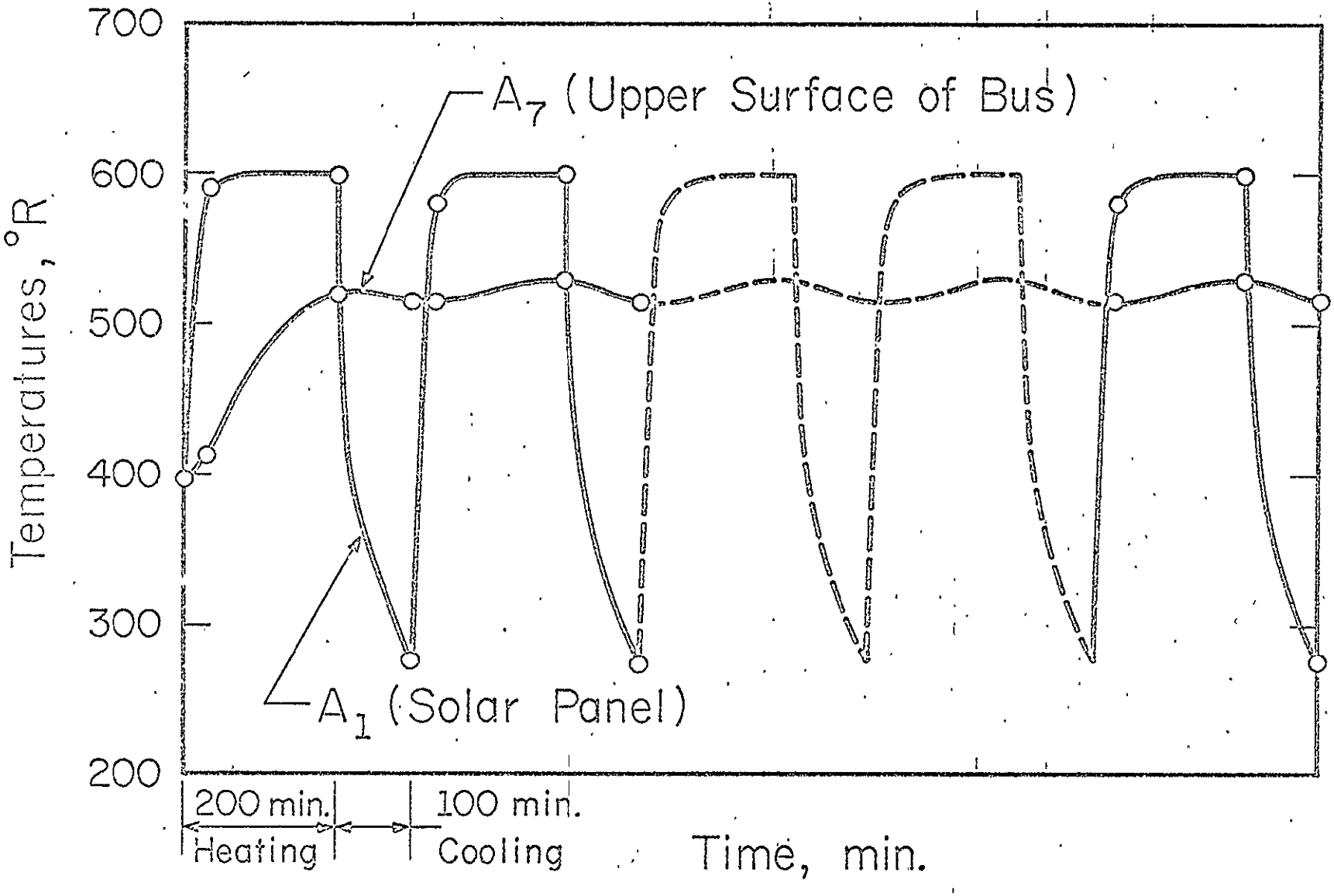

Figure 6.1 Cyclic heating and cooling of the hypothetical spacecraft (open circle o denotes instant for which data are presented in TABLE 6.7)

TABLE 6.7(a) Model temperatures before and after correction
(Spacecraft subject to cyclic heating and cooling)

30 minutes from start of the first cycle

Surface	Prototype or Perfect Model Temperature T_p	Temperatures of Imperfect Models						$\Delta^{(+)}$	$\Delta^{(-)}$	Δ_t	Model Temperature after Correction	
		Model MI		Model MII		Model MIII						
		T_{MI}	E_{MI}	T_{MII}	E_{MII}	T_{MIII}	E_{MIII}				T_{MC}	E_{MC}
A_1	590.7	590.6	-0.1	590.5	-0.2	590.6	-0.1	-0.03	-0.12	-0.15	590.7	0
A_2	594.9	594.0	-0.9	593.8	-1.1	594.3	-0.6	-0.17	-0.70	-0.87	594.9	0
A_3	474.5	478.0	3.5	470.2	-4.3	473.9	-0.6	-7.19	10.52	3.33	474.7	0.2
A_4	590.5	590.5	0	590.5	0	590.5	0	~0	-0.04	-0.04	590.5	0
A_5	593.9	593.6	-0.3	593.6	-0.3	593.7	-0.2	~0	-0.24	-0.24	593.9	0
A_6	440.3	451.6	11.3	451.4	11.1	446.4	6.1	-0.24	13.27	13.03	438.6	-1.7
A_7	413.1	413.4	0.3	411.8	-1.3	412.8	-0.3	-1.49	1.60	0.11	413.3	0.2
A_8	450.6	466.2	15.6	465.1	14.5	459.9	9.3	-0.99	15.88	14.89	451.3	0.7
A_9	445.4	452.5	7.1	450.6	5.2	448.4	3.0	-1.73	10.25	8.53	443.9	-1.5
A_{10}	424.3	426.1	1.8	422.8	-1.5	424.3	0	-3.00	4.43	1.43	424.6	0.3
A_{11}	547.6	547.6	0	547.6	0	547.6	0	0.01	~0	0.01	547.6	0
$A_{12}(=A_{10'})$	172.2	172.8	0.6	172.6	0.4	172.5	0.3	-0.24	0.98	0.74	172.1	-0.1

All temperatures in °R.

TABLE 6.7(b) Model temperatures before and after correction

200 minutes from start of the first cycle

Surface	Prototype or Perfect Model Temperature T_P	Temperatures of Imperfect Models						$\Delta^{(+)}$	$\Delta^{(-)}$	Δ_t	Model Temperature after Correction	
		Model MI		Model MII		Model MIII						
		T_{MI}	E_{MI}	T_{MII}	E_{MII}	T_{MIII}	E_{MIII}				T_{MC}	E_{MC}
A_1	597.9	597.8	-0.1	597.8	-0.1	597.9	0	-0.01	-0.08	-0.09	597.9	0
A_2	604.6	604.1	-0.5	604.0	-0.6	604.3	-0.3	-0.10	-0.46	-0.56	604.7	0.1
A_3	531.3	561.5	30.2	559.2	27.9	548.3	17.0	-2.07	33.31	31.24	530.2	-1.1
A_4	597.8	597.8	0	597.8	0	597.8	0	-0.01	-0.04	-0.05	597.8	0
A_5	604.0	603.8	-0.2	603.7	-0.3	603.9	-0.1	-0.08	-0.22	-0.30	604.1	0.1
A_6	520.3	552.3	31.9	550.3	30.0	538.3	18.0	-1.78	35.22	33.44	518.8	-1.5
A_7	519.9	544.8	24.9	540.0	20.1	534.0	14.1	-4.42	27.53	23.11	521.7	1.8
A_8	519.8	552.4	32.6	550.2	30.4	539.6	19.8	-2.01	32.43	30.42	522.0	2.2
A_9	540.4	566.8	26.4	562.5	22.1	554.6	14.2	-3.94	30.77	26.83	539.9	-0.5
A_{10}	521.5	547.7	26.2	544.0	22.5	536.5	15.0	-3.46	28.47	25.01	522.7	1.2
A_{11}	568.1	568.2	0.1	568.2	0.1	568.2	0.1	0.02	0.03	0.05	568.1	0
$A_{12}(=A_{10'})$	184.2	188.4	4.2	187.9	3.7	186.4	2.2	-0.44	5.14	4.70	183.7	-0.5

All temperatures in °R.

TABLE 6.7(c) Model temperatures before and after correction

End of first cycle

Surface	Prototype or Perfect Model Temperature T_P	Temperatures of Imperfect Models						$\Delta^{(+)}$	$\Delta^{(-)}$	Δ_t	Model Temperature after Correction	
		Model MI		Model MII		Model MIII						
		T_{MI}	E_{MI}	T_{MII}	E_{MII}	T_{MIII}	E_{MIII}				T_{MC}	E_{MC}
A_1	274.7	274.4	-0.3	274.4	-0.3	274.5	-0.2	-0.03	-0.38	-0.41	274.8	0.1
A_2	304.2	302.8	-1.4	302.6	-1.6	303.5	-0.7	-0.14	-1.75	-1.89	304.7	0.5
A_3	503.3	542.3	39.0	541.7	38.4	526.2	22.9	-0.56	40.85	40.29	502.0	-1.3
A_4	274.4	273.9	-0.5	273.8	-0.6	274.1	-0.3	-0.04	-0.58	-0.62	274.5	0.1
A_5	302.6	300.4	-2.2	300.2	-2.4	301.5	-1.1	-0.20	-2.68	-2.88	303.3	0.7
A_6	496.4	537.1	40.7	536.4	40.0	520.2	23.8	-0.61	42.67	42.06	495.0	-1.4
A_7	514.1	545.5	31.4	543.6	29.5	532.8	18.7	-1.75	32.13	30.38	515.1	1.0
A_8	513.6	549.7	36.1	548.4	34.8	535.8	22.2	-1.18	35.29	34.11	515.6	2.0
A_9	530.2	562.1	31.9	559.2	29.0	548.3	18.1	-2.66	35.09	32.43	529.7	-0.5
A_{10}	513.0	544.6	31.6	542.7	29.7	531.8	18.8	-1.73	32.54	30.81	513.8	0.8
A_{11}	289.7	290.0	0.3	290.1	0.4	289.9	0.2	0.09	0.18	0.27	289.7	0
$A_{12}(=A_{10}')$	138.3	148.8	10.5	148.4	10.1	144.1	5.8	-0.45	11.95	11.50	137.3	-1.0

All temperatures in °R.

TABLE 6.7(d) Model temperatures before and after correction

30 minutes from start of the second cycle

Surface	Prototype or Perfect Model Temperature T_p	Temperatures of Imperfect Models						$\Delta^{(+)}$	$\Delta^{(-)}$	Δ_t	Model Temperature after Correction	
		Model MI		Model MII		Model MIII						
		T_{MI}	E_{MI}	T_{MII}	E_{MII}	T_{MIII}	E_{MIII}				T_{MC}	E_{MC}
A_1	580.6	580.5	-0.1	580.5	-0.1	580.5	-0.1	-0.01	-0.09	-0.10	580.6	0
A_2	590.5	590.1	-0.4	590.0	-0.5	590.3	-0.2	-0.08	-0.40	-0.48	590.6	0.1
A_3	518.3	552.3	33.9	550.5	32.2	537.4	19.1	-1.54	37.56	36.02	516.2	-2.1
A_4	580.4	580.4	0	580.3	-0.1	580.4	0	-0.01	-0.09	-0.10	580.4	0
A_5	589.6	589.5	-0.1	589.5	-0.1	589.6	0	-0.05	-0.30	-0.35	589.9	0.3
A_6	504.5	543.7	39.2	543.1	38.6	527.4	22.9	-0.56	41.28	40.72	503.0	-1.5
A_7	513.5	545.4	32.0	543.6	30.2	532.5	19.0	-1.66	32.84	31.18	514.3	0.8
A_8	513.9	550.2	36.3	549.0	35.1	536.2	22.3	-1.08	35.61	34.53	515.7	1.8
A_9	531.1	563.3	32.2	560.5	29.4	549.3	18.2	-2.58	35.44	32.86	530.4	-0.7
A_{10}	513.4	545.3	31.9	543.4	30.0	532.3	18.9	-1.75	33.01	31.26	514.0	0.6
A_{11}	521.2	521.4	0.2	521.4	0.2	521.3	0.1	0.05	0.11	0.16	521.2	0
$A_{12}(=A_{10},.)$	176.4	181.8	5.4	181.5	5.1	179.3	2.9	-0.25	6.27	6.02	175.8	-0.6

All temperature in °R.

TABLE 6.7(e) Model temperatures before and after correction

200 minutes from start of the second cycle

Surface	Prototype or Perfect Model Temperature T_P	Temperatures of Imperfect Models						$\Delta^{(+)}$	$\Delta^{(-)}$	Δ_t	Model Temperature after Correction	
		Model MI		Model MII		Model MIII						
		T_{MI}	E_{MI}	T_{MII}	E_{MII}	T_{MIII}	E_{MIII}				T_{MC}	E_{MC}
Λ_1	598.0	597.9	-0.1	597.9	-0.1	597.9	-0.1	-0.01	-0.07	-0.08	598.0	0
Λ_2	604.7	604.4	-0.3	604.3	-0.4	604.5	-0.2	-0.04	-0.41	-0.45	604.8	0.1
Λ_3	534.0	566.5	32.5	565.6	31.6	552.7	18.7	-0.83	35.00	34.17	532.3	-1.7
Λ_4	597.9	597.8	-0.1	597.8	-0.1	597.9	0	-0.01	-0.03	-0.04	597.9	0
Λ_5	604.2	604.1	-0.1	604.1	-0.1	604.2	0	-0.03	-0.19	-0.22	604.3	0.1
Λ_6	524.6	559.2	34.6	558.5	33.9	544.6	20.0	-0.70	37.14	36.44	522.8	-1.8
Λ_7	528.1	558.1	30.0	556.5	28.4	545.9	17.8	-1.44	30.71	29.27	528.8	0.7
Λ_8	524.2	559.3	35.1	558.4	34.2	545.9	21.7	-0.85	34.05	33.20	526.1	1.9
Λ_9	546.5	576.0	29.5	573.4	26.9	563.1	16.6	-2.41	32.66	30.25	545.7	-0.8
Λ_{10}	527.9	557.8	29.9	556.2	28.3	545.7	17.8	-1.44	30.63	29.19	528.6	0.7
Λ_{11}	568.1	568.2	0.1	568.2	0.1	568.2	0.1	0.02	0.04	0.06	568.1	0
$\Lambda_{12}(=\Lambda_{10}')$	184.9	189.7	4.8	189.5	4.6	187.5	2.6	-0.20	5.63	5.43	184.3	-0.6

All temperatures in °R.

TABLE 6.7(f) Model temperatures before and after correction

End of second cycle

Surface	Prototype or Perfect Model Temperature T_p	Temperatures of Imperfect Models						$\Delta^{(+)}$	$\Delta^{(-)}$	Δ_t	Model Temperature after Correction	
		Model MI		Model MII		Model MIII						
		T_{MI}	E_{MI}	T_{MII}	E_{MII}	T_{MIII}	E_{MIII}				T_{MC}	E_{MC}
A_1	274.8	274.5	-0.3	274.5	-0.3	274.6	-0.2	~0	-0.36	-0.36	274.9	0.1
A_2	304.4	303.2	-1.2	303.3	-1.1	303.9	-0.5	0.01	-1.66	-1.65	304.9	0.5
A_3	503.9	543.5	39.6	543.3	39.4	527.2	23.3	-0.11	41.16	41.05	502.4	-1.5
A_4	274.5	274.0	-0.5	274.0	-0.5	274.2	-0.3	-0.01	-0.57	-0.58	274.6	0.1
A_5	303.0	301.0	-2.0	300.9	-2.1	302.0	-1.0	-0.06	-2.62	-2.68	303.7	0.7
A_6	497.3	538.6	41.3	538.4	41.1	521.6	24.3	-0.16	43.00	42.84	495.8	-1.5
A_7	515.7	548.2	32.5	547.3	31.6	535.3	19.6	-0.78	32.66	31.88	516.3	0.6
A_8	514.5	551.1	36.6	550.3	35.8	537.1	22.6	-0.78	35.57	34.84	516.3	1.8
A_9	531.4	564.1	32.7	561.8	30.4	550.1	18.7	-2.07	35.41	33.34	530.7	-0.7
A_{10}	514.2	546.7	32.5	545.6	31.4	533.7	19.5	-1.02	32.90	31.88	514.8	0.6
A_{11}	289.8	290.0	0.2	290.1	0.3	290.0	0.2	0.10	0.18	0.28	289.8	0
$A_{12}(=A_{10}')$	138.6	149.4	10.8	149.1	10.5	144.6	6.0	-0.28	12.07	11.79	137.6	-1.0

All temperatures in °R.

TABLE 6.7(g) Model temperatures before and after correction

30 minutes from start of the fifth cycle

Surface	Prototype or Perfect Temperature T_P	Temperatures of Imperfect Models						$\Delta^{(*)}$	$\Delta^{(-)}$	Δ_t	Model Temperature after Correction	
		Model MI		Model MII		Model MIII						
		T_{MI}	E_{MI}	T_{MII}	E_{MII}	T_{MIII}	E_{MIII}				T_{MC}	E_{MC}
A_1	580.6	580.5	-0.1	580.5	-0.1	580.5	-0.1	-0.01	-0.08	-0.09	580.6	0
A_2	590.5	590.2	-0.3	590.1	-0.4	590.3	-0.2	-0.04	-0.38	-0.42	590.6	0.1
A_3	518.6	553.0	34.4	551.6	33.0	538.1	19.5	-1.22	37.74	36.52	516.4	-2.2
A_4	580.4	580.4	0	580.4	0	580.4	0	~0	-0.08	-0.08	580.5	0.1
A_5	589.7	589.6	-0.1	589.6	-0.1	589.8	0.1	-0.01	-0.30	-0.31	589.9	0.2
A_6	505.1	544.7	39.6	544.4	39.3	528.3	23.2	-0.23	41.48	41.25	503.4	-1.7
A_7	514.5	547.2	32.7	546.1	31.6	534.1	19.6	-0.96	33.15	32.19	515.0	0.5
A_8	514.4	551.2	36.8	550.3	35.9	537.0	22.6	-0.76	35.77	35.01	516.1	1.7
A_9	531.8	564.5	32.7	562.2	30.4	550.5	18.7	-2.14	35.61	33.47	531.1	-0.7
A_{10}	514.2	546.7	32.5	545.3	31.1	533.5	19.3	-1.23	33.22	31.99	514.7	0.5
A_{11}	521.2	521.4	0.2	521.4	0.2	521.3	0.1	0.06	0.11	0.17	521.2	0
$A_{12}(=A_{10}')$	176.5	182.0	5.5	181.8	5.3	179.5	3.0	-0.18	6.33	6.15	175.8	-0.7

All temperatures in °R.

TABLE 6.7(h) Model temperatures before and after correction

200 minutes from start of the fifth cycle

Surface	Prototype or Perfect Model Temperature T_p	Temperatures of Imperfect Models						$\Delta^{(+)}$	$\Delta^{(-)}$	Δ_t	Model Temperature after Correction	
		Model MI		Model MII		Model MIII						
		T_{MI}	E_{MI}	T_{MII}	E_{MII}	T_{MIII}	E_{MIII}				T_{MC}	E_{MC}
Λ_1	598.0	597.9	-0.1	597.9	-0.1	597.9	-0.1	-0.01	-0.07	-0.08	598.0	0
Λ_2	604.7	604.4	-0.3	604.3	-0.4	604.5	-0.2	-0.04	-0.41	-0.45	604.8	0.1
Λ_3	534.0	566.5	32.5	565.7	31.7	552.7	18.7	-0.79	35.01	34.22	532.3	-1.7
Λ_4	597.9	597.8	-0.1	597.8	-0.1	557.9	0	~0	-0.03	-0.03	597.9	0
Λ_5	604.2	604.1	-0.1	604.1	-0.1	604.2	0	-0.03	-0.19	-0.22	604.3	0.1
Λ_6	524.6	559.3	34.7	558.6	34.0	544.6	20.0	-0.66	37.15	36.49	522.8	-1.8
Λ_7	528.1	558.2	30.1	556.7	28.6	546.1	18.0	-1.36	30.71	29.35	528.8	0.7
Λ_8	524.3	559.4	35.1	558.5	34.2	545.9	21.6	-0.91	34.05	33.24	526.1	1.8
Λ_9	546.5	576.1	29.6	573.5	27.0	563.2	16.7	-2.35	32.66	30.31	545.8	-0.7
Λ_{10}	528.0	557.9	29.9	556.4	28.4	545.8	17.8	-1.38	30.63	29.25	528.6	0.6
Λ_{11}	568.1	568.2	0.1	568.2	0.1	568.2	0.1	0.02	0.04	0.06	568.1	0
Λ_{12} $(=\Lambda_{10}')$	184.9	189.7	4.8	189.5	4.6	187.5	2.6	-0.66	37.15	36.49	184.3	-0.6

All temperatures in °R.

TABLE 6.7(i) Model temperatures before and after correction

End of the fifth cycle

Surface	Prototype or Perfect Model Temperature T_P	Temperatures of Imperfect Models						$\Delta^{(+)}$	$\Delta^{(-)}$	Δ_t	Model Temperature after Correction	
		Model MI		Model MII		Model MIII						
		T_{MI}	E_{MI}	T_{MII}	E_{MII}	T_{MIII}	E_{MIII}				T_{MC}	E_{MC}
A_1	274.8	274.5	-0.3	274.5	-0.3	274.6	-0.2	~0	-0.36	-0.36	274.9	0.1
A_2	304.4	303.2	-1.2	303.3	-1.1	303.9	-0.5	0.01	-0.17	-0.16	304.9	0.5
A_3	503.9	543.5	39.6	543.4	39.5	527.2	23.3	-0.10	41.17	41.07	502.4	-1.5
A_4	274.5	274.0	-0.5	274.0	-0.5	274.2	-0.3	-0.01	-0.57	-0.58	274.6	0.1
A_5	303.0	301.0	-2.0	300.9	-2.1	302.0	-1.0	-0.06	-2.62	-2.68	303.7	0.7
A_6	497.3	538.6	41.3	538.5	41.2	521.6	24.3	-0.15	43.00	42.85	495.8	-1.5
A_7	515.7	548.2	32.5	547.4	31.7	535.3	19.6	-0.77	32.66	31.89	516.3	0.6
A_8	514.5	551.1	36.6	550.4	35.9	537.1	22.6	-0.72	35.57	34.85	516.3	1.8
A_9	531.4	564.1	32.7	561.8	30.4	550.1	18.7	-2.06	35.40	33.34	530.7	-0.7
A_{10}	514.2	546.7	32.5	545.6	31.4	533.7	19.5	-1.01	32.90	31.89	514.8	0.6
A_{11}	289.8	290.0	0.2	290.1	0.3	290.0	0.2	0.10	0.18	0.28	289.8	0
$A_{12}(=A_{10}')$	138.6	149.4	10.8	149.1	10.5	144.6	6.0	-0.27	12.07	11.80	137.6	-1.0

All temperatures in °R.

Chapter 2. During the course of the present investigation, additional observations, some of which are quite essential for the successful application of the theory, have been made. They are discussed briefly in the section which follows.

6.3 SOME RELEVANT OBSERVATIONS

6.3.1 Influence of Decreasing and Increasing Model Errors on Prediction Reliability

The errors in the various modeling parameters as listed in TABLES 6.1 and 6.4 are of the order of 20 to 25 percent in kd and Cd and of 10 to 20 percent in ε and ε' for the 'original' model MI. It would be of interest to know how the reliability of the final corrected temperature data be altered by increasing and by decreasing such errors. To this end, the computations described in Section 6.1 were repeated, first with all errors reduced to one-half of their respective values as shown in the tables. It was found that the improvement in the accuracy of the corrected model temperatures of T_{MC} was totally insignificant. In no case did it exceed 1°R. Thus, if the present theory is used for the correction of data gathered with imperfect models, there is no real need of striving for the undue reduction of modeling errors, provided that they are kept within limits. This welcoming fact allows additional flexibility in model fabrication. On the other hand, when errors in the modeling parameters are doubled, the reliability of the correction procedure deteriorates rapidly. Errors in T_{MC} as large as 20°R have been noted.

This points to the need of a development of a more general theory which could accommodate greater errors in the modeling parameters.

6.3.2 Proper Control of Model Errors and Selection of Experimental Conditions

It has been demonstrated in Chapter 2 that the best results obtainable from the present theory arise when the ratios $\xi_p^{(+)}/\xi_{p*}^{(+)}$ and $\xi_p^{(-)}/\xi_{p*}^{(-)}$ are close to 1/2 [see Fig. 2.3(a.1) and (b.2)] or 2 [see Fig. 2.3(a.2) and (b.1)], depending on whether, in the modification experiments, the *magnitude* of the δ's increases or decreases. These ratios, evaluated for the simple error space, are, respectively, 0.474 and 0.532 for models prescribed in TABLE 6.1 and are 0.474 and 1.64 for models prescribed in TABLE 6.4. The ranges of errors shown in these tables are, in fact, selected with the guidance of the said theoretical requirements. The question which naturally arises is: In the modification experiments with models MII and MIII, would it not be desirable to strive for smaller errors? That is, to make the positive errors become less positive and negative errors less negative.† To see if this were the case, the computations described under Section 6.1 and pertaining to models prescribed in TABLE 6.4 were repeated, but with both positive errors in model MII and negative errors in MIII kept less than 5 percent. The change gave rise to rather unfavorable ratios in ξ; namely, $\xi_p^{(+)}/\xi_{p*}^{(+)} = 0.31$ and $\xi_p^{(-)}/\xi_{p*}^{(-)} = 0.22$. It was found that the computed data for T_{MC} showed

†Such modification scheme may be unrealistic in practice. However, this is NOT the point in question here.

little or no improvement over those given in TABLES 6.5 and 6.6.

In the discussion of error paths in the multi-dimensional error space, four possibilities are considered as illustrated in Fig. 2.3. In the first modification experiment, all positive errors remain positive after modification, whether they become smaller or larger. Likewise, in the second modification experiment, all negative errors remain negative. Clearly, such are not the only possibilities; it is physically feasible to have *mixed* errors (positive and negative) after modification, although they should always be avoided for reasons to be seen shortly. Consider, for instance, the experimentation with MIII. Some of the originally negative errors may become positive after modification while others remain negative. Under such circumstance, the parabola joining the error states P, $P^{*(-)}$ and $O^{(-)}$ in subspace $S^{(-)}$ would have a relatively sharp curvature, thus creating a condition that is in direct conflict with the fundamental assumption upon which the theory is built.

To provide a pictorial illustration, we consider a three-dimensional simple error space shown in Fig. 6.2. The coordinates of the point P which is associated with the original model MI are all negative. Suppose that, after modification, δ_1^* and δ_2^* remain negative, but δ_3^* become positive. Thus, the point $P^{*(-)}$ would be as shown in Fig. 6.2(a). The error path joining P, $P^{*(-)}$ and $O^{(-)}$ makes a sharp bend as illustrated and it would totally invalidate the linear theory developed in [1] and in this report. On the other hand, if δ_3^* remains negative as shown in Fig. 6.2(b), the error path would have a gentle curvature

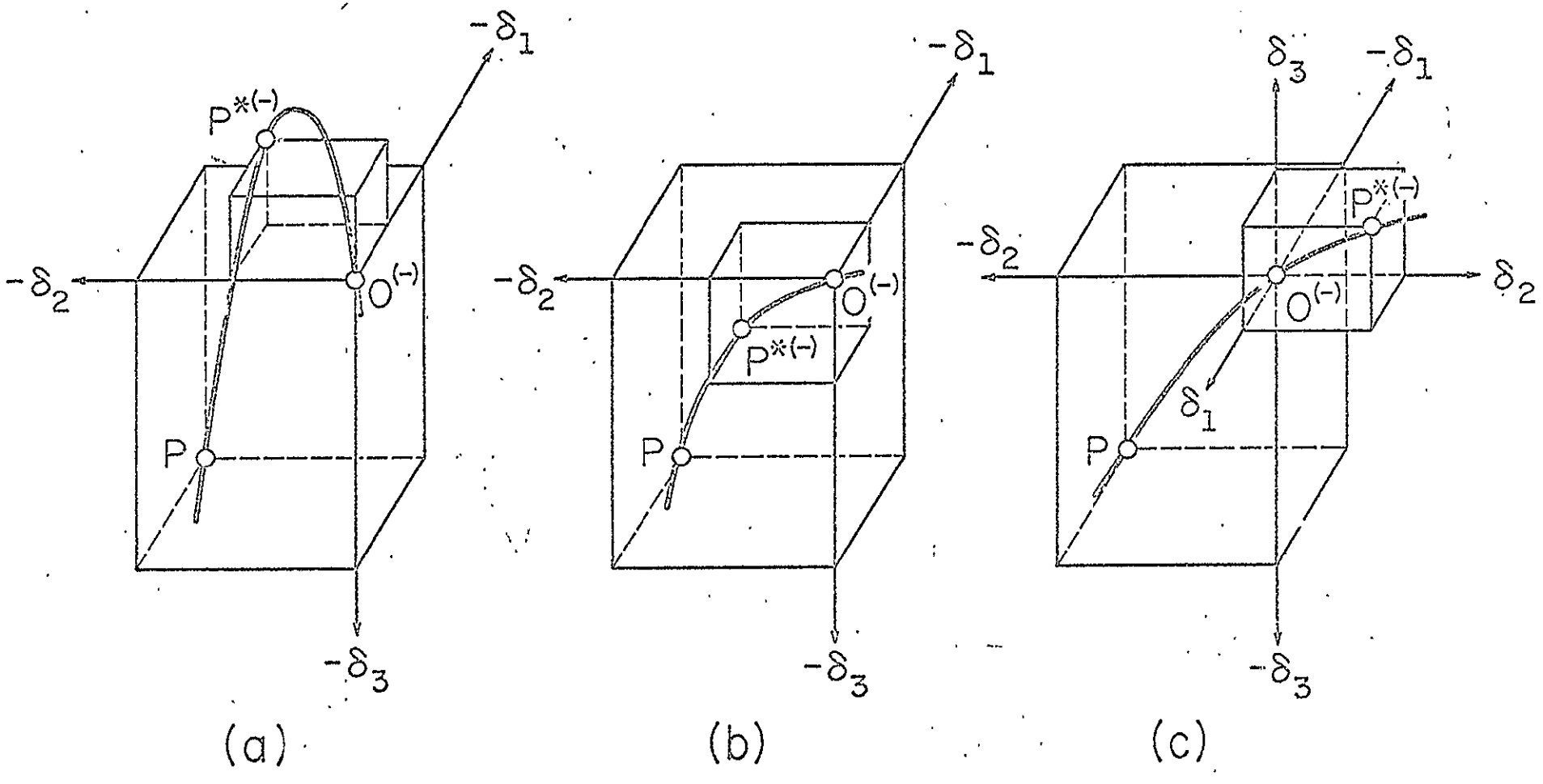

Figure 6.2 Schematic representation of error path as affected by model design

which is small everywhere along the path. If all δ^*'s are made positive, it is again possible to have an error path which has a uniformly small curvature. This is illustrated in Fig. 6.2(c). The three points through which the parabola passes must now be of the sequence P, $O^{(-)}$, and $P^{*(-)}$. The extension of the foregoing consideration to the design of model MII experimentation is obvious.

Extensive numerical calculations have been carried out, not only for the hypothetical spacecraft considered in the present report, but also for a totally different problem, namely, the correlation of boiling heat transfer data, and the results conclusively demonstrate the validity of the arguments just given. The nature of the error paths has a controlling influence on the reliability of the theory. Error paths exhibiting small and sharply changing radius of curvature, such as that of Fig. 6.2(a), should not be considered in any circumstance.

6.4 CONCLUSIONS AND RECOMMENDATION

Based on the evidence provided by a computer experimentation of the application of the proposed new theory of imperfect modeling to the study of the thermal performance of a hypothetical spacecraft, the following conclusions may be drawn. The hypothetical spacecraft has major radiative and conductive heat flow paths that crudely simulate those of the '64 Mariner family of space vehicles.

(1) When errors in kd and Cd of up to 25 percent and in surface emittance of up to 20 percent exist in the model and when the spacecraft is subject to either a simple heating and

cooling transient with an intervening steady condition or when it experiences a continuous cyclic transient, the indicated model temperatures would entail errors of 10, 20, and 30°R.and higher. These errors were reduced to less than 3°R after a correction according to the theory. There is no evidence of error accumulation under the cyclic condition investigated.

(2) While the theory is deduced under the basic assumption that the errors in the modeling parameters are small and that they have independent effects on the dependent variable or variables, there is no need to strive for the undue, costly reduction of these errors. Rather, in the modification experiments, the model design and/or the test conditions should be properly controlled in order that the ratios $\xi_p^{(+)}/\xi_{p*}^{(+)}$ and $\xi_p^{(-)}/\xi_{p*}^{(-)}$ do not deviate excessively from 1/2 when the *magnitudes* of the δ's generally increase or 2 when they generally decrease.

(3) The reliability of the theory deteriorates rapidly when errors in the modeling parameters become large. At the present time, it is not feasible to describe *quantitatively* what is meant by 'large' or 'small' error.

In view of the success, as well as the limitations found in connection with the performance of the theory, it is recommended that further investigation be launched with emphasis on developing a means of treating large errors.

REFERENCES

[1] Chao, B. T., "A Study of Thermal Scale Modeling with Imperfect Models," Proposal Gr-2-2404 submitted to Jet Propulsion Laboratory, Pasadena, California, May 28, 1969.

[2] Bobco, R. P., "Radiation Heat Transfer in Semigray Enclosures with Specularly and Diffusely Reflecting Surfaces," J. Heat Transfer, Trans. ASME, Series C, 86, 123-130 (1964).

[3] Plamondon, J. A. and Landram, C. S., "Radiation Heat Transfer from Nongray Surfaces with External Radiation," in Thermophysics and Temperature Control of Spacecraft and Entry Vehicles, edited by G. B. Heller, Progress in Astronautics and Aeronautics, v. 18, 173-197 (1966).

[4] Hering, R. G., "Radiative Heat Exchange and Equilibrium Surface Temperature in a Space Environment," J. Spacecraft and Rockets, 5, 47-54 (1968).

[5] Chao, B. T. and Wedekind, G. L., "Similarity Criteria for Thermal Modeling of Spacecraft," J. Spacecraft and Rockets, 2, 146-152 (1965).

[6a] Chao, B. T., DePaiva, J. S. and Huang, M. N., "Transient Thermal Behavior of Simple Structures in a Simulated Space Environment by Model Testing," ME-TR-NGR-048, University of Illinois, Urbana, July, 1967, 78 pp.

[6b] Chao, B. T., DePaiva, J. S. and Huang, M. N., "Results of Transient Thermal Modeling of Simple Structures in a Simulated Space Environment," ME-TR-JPL-951660-1, University of Illinois, Urbana, November, 1967, 51 pp.

[6c] Chao, B. T. and Huang, M. N., "Transient Thermal Modeling with Simulated Solar Radiation," ME-TR-JPL-951660-2, University of Illinois at Urbana-Champaign, March, 1969, 55 pp.

[7] Hamilton, D. C. and Morgan, W. R., "Radiant-Interchange Configuration Factors," NACA TN 2836, 1952.

[8] Strong, P. F. and Emslie, A. G., "The Method of Zones for the Calculation of Temperature Distribution," report prepared by Arthur D. Little, Inc., to Jet Propulsion Laboratory, Pasadena, California, No. 1, July, 1963.

APPENDIX A

THERMAL RESISTANCE OF MULTI-LAYER INSULATION

The superinsulation used in today's spacecraft is a multi-layer aggregate of aluminized mylar or teflon. In the ideal condition, the layers form parallel planes and have no physical contact with each other. For the purpose of our present analysis, such condition is assumed. Here again, we adopt a semi-gray, two-region spectral subdivision of properties; namely, the solar and the infrared region. The directional properties of the surface are taken into account by the simple diffuse-specular model; i.e., $\rho = \rho_d + \rho_s$. All emitted radiant energies are assumed diffuse.

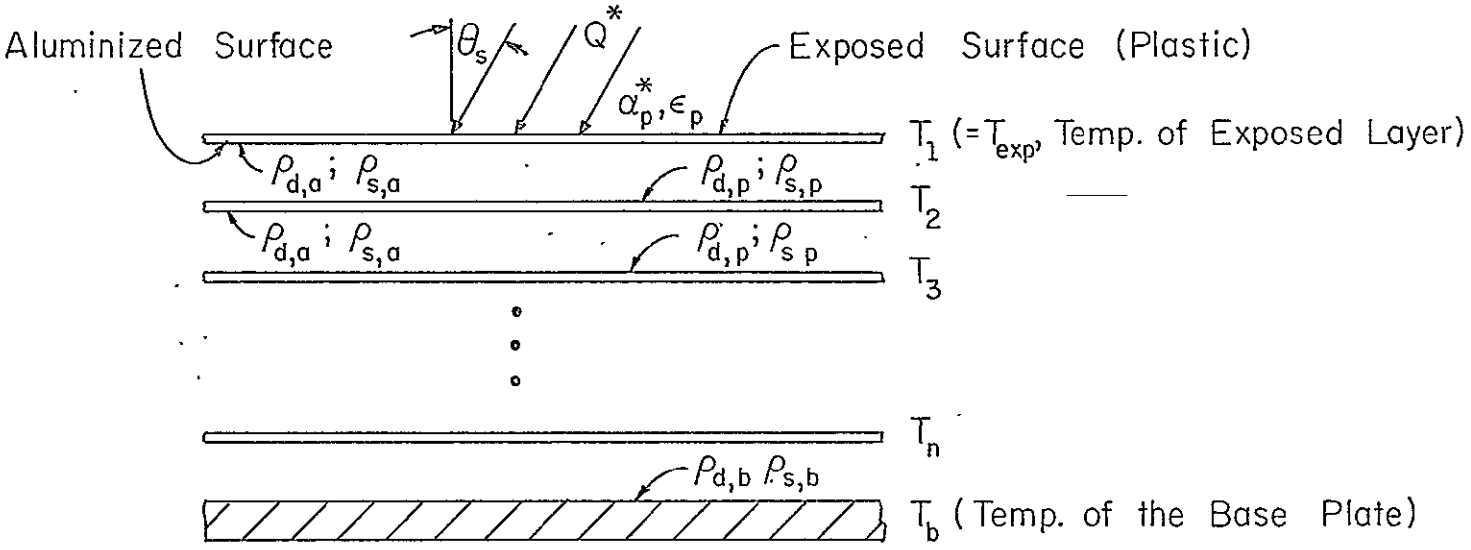

Fig. A.1 A Base Plate Covered with Superinsulation

Figure A.1 depicts a base plate at temperature T_b covered with a superinsulation of n-layers. The exposed surface is plastic and

is absorbing sun's radiation at a rate:

$$\frac{Q^*}{A} = \alpha_p^* S \cos \theta_s \tag{A.1}$$

where α_p^* is the solar absorptance of the plastic layer and S is the *local* solar constant (at the outer fringes of earth's atmosphere, S = 442 Btu/hr-ft^2). All properties shown in Fig. A.1 without an asterisk are for the infrared range and the subscript 'a' refers to aluminum and 'p' refers to plastic. Appropriate values of reflectances and absorptances of aluminized mylar or teflon currently used in spacecraft applications are listed in Table A.1.

TABLE A.1

REFLECTANCES AND ABSORPTANCES OF ALUMINIZED MYLAR†

	Solar Range (0.25μ-2.5μ)			Infrared Range (> 5μ)		
	ρ_s^*	ρ_d^*	α^*	ρ_s	ρ_d	$\alpha(=\varepsilon)$
Aluminized side	0.85	0	0.15	0.95	0.00	0.05
Plastic side	0.85	0	0.15	0.00	0.50	0.50

Consider a typical section of two adjacent layers of the super-insulation; e.g., A_2 and A_3 of Fig. A.1. We assume that the temperature of each layer is uniform and that the edge effects are negligible. Figure A.2 shows the equivalent resistance network when steady condition prevails. In the figure, E_b is the black body emissive power, B denotes the diffuse radiosity and E_{23} is the exchange factor.

†Data transmitted to the author by Mr. W. A. Hagemeyer of JPL.

The subscripts 2 and 3 have the usual meaning.

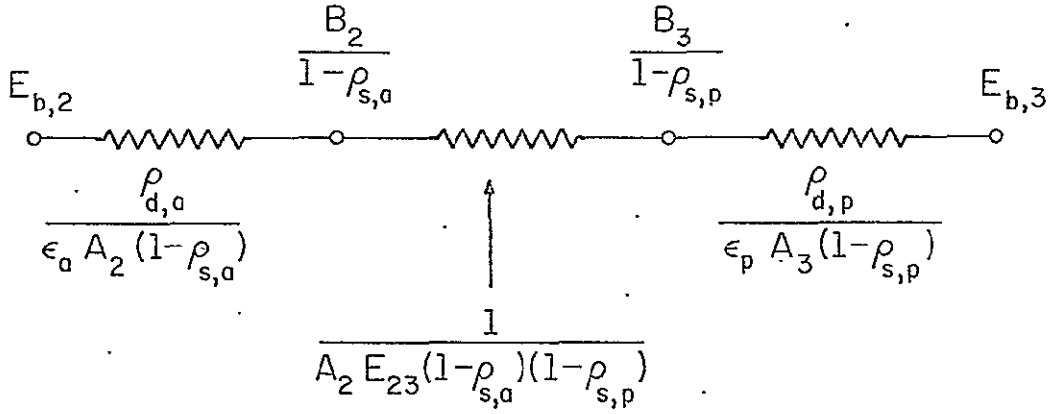

Fig. A.2 Radiation Network for Infinite Parallel Planes

Since $A_2 = A_3 = A$, the thermal 'resistance' per unit area is

$$R = \frac{E_{b,3} - E_{b,2}}{Q/A} = \frac{\rho_{d,a}}{\epsilon_a (1 - \rho_{s,a})} + \frac{\rho_{d,p}}{\epsilon_p (1 - \rho_{s,p})} + \frac{1}{E_{23}(1 - \rho_{s,a})(1 - \rho_{s,p})} \tag{A.2}$$

The exchange factor E_{23} can be easily evaluated using the image technique. Recognizing that the separation distance between layers is very small as compared with the lateral extent of the superinsulation, one finds

$$E_{23} = 1 + \rho_{s,a}\rho_{s,p} + \rho_{s,a}^2\rho_{s,p}^2 + \cdots = \frac{1}{1 - \rho_{s,a}\rho_{s,p}} \tag{A.3}$$

Hence,

$$R = \frac{\rho_{d,a}}{\epsilon_a (1 - \rho_{s,a})} + \frac{\rho_{d,p}}{\epsilon_p (1 - \rho_{s,p})} + \frac{1 - \rho_{s,a}\rho_{s,p}}{(1 - \rho_{s,a})(1 - \rho_{s,p})} \tag{A.4}$$

If the surfaces are diffuse, $\rho_{s,a} = \rho_{s,p} = 0$, and Eq. (A.4) simplifies to

$$R = \frac{1}{\varepsilon_a} + \frac{1}{\varepsilon_p} - 1$$

which is a well-known result.

The resistance per unit area R' between the aluminum surface of the last layer of the superinsulation and the protected surface of the base plate can also be evaluated from Eq. (A.4), provided that the three properties associated with the plastic, namely, ε_p, $\rho_{d,p}$ and $\rho_{s,p}$, and replaced by the corresponding properties of the base plate, ε_b, $\rho_{d,b}$ and $\rho_{s,b}$.

The inward 'leakage' heat flux through the superinsulation $\frac{Q}{A}$ can be determined from a consideration of the heat balance at its outermost exposed surface. It is

$$\frac{Q}{A} = \alpha_p^* S \cos\theta - \varepsilon_p \sigma T_{exp}^4 = \frac{\sigma T_{exp}^4 - \sigma T_b^4}{\sum R} \qquad \text{(A.5a)}$$

with

$$\sum R = (n - 1)R + R' \qquad \text{(A.5b)}$$

n being the total number of layers in the superinsulation. In practice, for the sunlit surfaces of the spacecraft,

$$\frac{Q}{A} \ll \begin{cases} \alpha_p^* S \cos \theta_s \\ \text{or} \\ \varepsilon_p \sigma T_{exp}^4 \end{cases} \tag{A.6}$$

and, hence, a valid approximation for Eq. (A.5a) is

$$\frac{Q}{A} \simeq \frac{1}{\sum R}\left(\frac{\alpha_p^*}{\varepsilon_p} S \cos \theta_s - \sigma T_b^4\right) \tag{A.7}$$

which may be either positive or negative. When the superinsulation sees *only* the empty space, any possible heat leak is away from the surface. A straightforward calculation leads to

$$-\frac{Q}{A} = \frac{\sigma T_b^4}{\frac{1}{\varepsilon_p} + \sum R} \tag{A.8}$$

where $\sum R$ is again given by Eq. (A.5b).

While the foregoing results were obtained under the assumption of steady heat flow, they may be used for transient analysis without entailing significant errors since the heat capacity of multilayer insulation is usually quite small and, in spacecraft application, the transients are seldom very rapid.

To ascertain the effectiveness of of superinsulation in reducing surface heat flux, we consider an aluminum base plate, with and without the superinsulation, when it is exposed to

a. sun's irradiation of a local intensity of 300 Btu/hr-ft^2 and

b. the black empty space.

The plate has a temperature of 528°R and is either highly polished or is sprayed with PV-100 white paint. Bv using Eq. (A.4) and the relevant data in TABLE A.1, one finds

$$R = 21 \text{ for aluminized mylar or teflon, plastic side out}$$

$$R' = \begin{cases} 38.8 \text{ when the aluminum base plate is highly polished} \\ 20.2 \text{ when the base plate is covered with PV-100 white paint} \end{cases}$$

Then, it follows from Eq. (A.5b) that, for a five-layer superinsulation, $\sum R = 122.8$ and 104.2, respectively, for the highly polished and painted base plate. The corresponding values for a ten-layer insulation are 227.8 and 209.2; and for a twenty-layer insulation, 437.8 and 419.2.

With the foregoing information, the leakage surface flux can be readily calculated from Eq. (A.7) and Eq. (A.8). The results are shown in Table A.2. In practice, the effectiveness of insulation is somewhat less due to the unavoidable conduction leaks.

TABLE A.2

Effect of Multi-Layer Insulation on Surface Heat Flux, Btu/hr-ft^2, of an Aluminum Base Plate at 528°R

	Based Plate Highly Polished				Base Plate Covered with PV-100 White Paint			
	Without Superinsulation	With Superinsulation (number of layers)			Without Superinsulation	With Superinsulation (number of layers)		
		5	10	20		5	10	20
Surface Exposed to Sun's Irradiation	53.3	-0.35	-0.19	-0.10	- 50.6	-0.41	-0.21	-0.10
Surface Exposed to Empty Space at 0°R	- 6.7	-1.07	-0.58	-0.30	-111	-1.25	-0.63	-0.32

The positive value is for heat flow into the base plate; all negative values are for heat flow away from the base plate.

APPENDIX B

A NUMERICAL EXAMPLE

As an example, we consider the case in which errors in the modeling parameters are as shown in TABLE 6.1 and the sun's rays strike the solar panels at normal incidence. Specifically, we refer to data listed in TABLE 6.2(d) which is for a heating transient, 300 minutes after the spacecraft is subjected to solar radiation and internal heating. The choice of TABLE 6.2(d) for illustration is totally arbitrary, any other tabulated data given in the report may serve the purpose equally well.

First, we note that the perfect model temperatures listed under T_p are calculated from the equation set (3.3.6) using the theoretically correct values of the modeling parameters. This is achieved by the combined Newton-Raphson and Gauss-Seidel procedure as explained in Chapter 5. The various temperatures of the three imperfect models T_{MI}, T_{MII}, and T_{MIII} are computed from the same equation set using the same procedure, but with modeling parameters entailing errors as listed in TABLE 6.1.

To illustrate how the various corrections are computed, it is sufficient to work out the details for one of the surfaces, say A_6. At t = 300 minutes after the start of the heating transient, T_{MI} = 542.1°R, T_{MII} = 538.3°R, and T_{MIII} = 555.4°R. These may be compared with the theoretically correct temperature of 524.4°R and, hence, their respective errors are 17.7, 13.9, and 31.0°R. All

temperatures cited here may be read from TABLE 6.2(d) in entries following A_6. In passing, we note that the three temperatures associated with the three imperfect models correspond to the function ϕ of Chapter 2 as follows:

$$T_{MI} \rightarrow \tilde{\phi}_i$$
$$T_{MII} \rightarrow \tilde{\phi}_i^{*(+)}$$
$$T_{MIII} \rightarrow \tilde{\phi}_i^{*(-)}$$

DETERMINATION OF CORRECTION FOR POSITIVE ERRORS, $\Delta^{(+)}$

From TABLE 6.1, it is seen that the various *positive* errors are:

(a) for Model MI

	A_1	A_2	A_3	A_4	A_5	A_6	A_7	A_8	A_9	A_{10}	A_{11}	A_{12}
δ_{kd}	--	--	0.25	--	--	0.25	0.20	0.25	0.25	0.20	--	--
δ_{Cd}	--	--	0.25	--	--	0.20	0.25	0.25	0.25	0.25	--	--
δ_{ε}	--	--	--	--	--	--	0.15	--	0.25	0.15	--	0.15
$\delta_{\varepsilon'}$	--	--	0.10	--	--	0.10	--	--	--	--	--	--

(b) for Model MII

	A_1	A_2	A_3	A_4	A_5	A_6	A_7	A_8	A_9	A_{10}	A_{11}	A_{12}
δ^*_{kd}	--	--	0.55	--	--	0.45	0.40	0.575	0.45	0.44	--	--
δ^*_{Cd}	--	--	0.525	--	--	0.50	0.55	0.575	0.45	0.60	--	--
δ^*_{ε}	--	--	--	--	--	--	0.27	--	0.45	0.33	--	0.33
$\delta^*_{\varepsilon'}$	--	--	0.20	--	--	0.20	--	--	--	--	--	--

The asterisk designates errors after modification. In the present instance, all errors become *more* positive after modification. Hence, the error path is as illustrated in Fig. 2.3(a.1) and (2.3.8) is the appropriate formula for determining $\Delta^{(+)}$.

From the foregoing data, we may readily calculate

$$\sum \delta_j^2 = 0.25^2 + 0.25^2 + 0.10^2 + 0.25^2 + 0.20^2 + 0.10^2 + 0.20^2 + 0.25^2 + 0.15^2 + 0.25^2 + 0.25^2 + 0.25^2 + 0.25^2 + 0.25^2 + 0.20^2 + 0.25^2 + 0.15^2 + 0.15^2 = 0.833$$

$$\sum (\delta_j^*)^2 = 0.55^2 + 0.525^2 + 0.20^2 + 0.45^2 + 0.50^2 + 0.20^2 + 0.40^2 + 0.55^2 + 0.27^2 + 0.575^2 + 0.575^2 + 0.45^2 + 0.45^2 + 0.45^2 + 0.44^2 + 0.60^2 + 0.33^2 + 0.33^2 = 3.687$$

$$\sum \delta_j \delta_j^* = 0.25 \times 0.55 + 0.25 \times 0.525 + 0.10 \times 0.20 + 0.25 \times 0.45 + 0.20 \times 0.50 + 0.10 \times 0.20 + 0.20 \times 0.40 + 0.25 \times 0.55 + 0.15 \times 0.27 + 0.25 \times 0.575 + 0.25 \times 0.575 + 0.25 \times 0.45 + 0.25 \times 0.45 + 0.25 \times 0.45 + 0.20 \times 0.44 + 0.25 \times 0.60 + 0.15 \times 0.33 + 0.15 \times 0.33 = 1.740$$

Using (2.3.9a), we find

$$\frac{\eta_p^{(+)}}{\xi_p^{(+)}} = \left[\frac{0.833 \text{ X } 3.687}{1.740^2} - 1\right]^{1/2} = 0.112$$

$$\frac{\xi_p^{(+)}}{\xi_{p^*}^{(+)}} = \frac{1.740}{3.687} = 0.472$$

Also, $\xi_{p^*}^{(+)} = \sqrt{3.687} = 1.92$. Hence, from (2.3.4a,b), we determine

$$a = 0.112 \text{ X } \frac{1}{1 - 0.472} = 0.212$$

$$b = -\frac{0.212}{1.92} = -0.110$$

and, from (2.3.5c),

$$\lambda = 1 - 2 \text{ X } 0.472 = 0.056$$

Substituting the foregoing values of a and λ in (2.3.6b) gives,

$$f(a,\lambda) = 0.0549$$

and, hence, the ratio of arc lengths is

$$\frac{s^{*(+)}}{s^{(+)}} = \frac{2}{1 - 0.0549} = 2.116$$

as according to (2.3.6a). Finally, the required correction for all positive errors is given by (2.3.8)

$$\Delta^{(+)} = \frac{538.3 - 542.1}{2.116 - 1} = -3.40^{\circ}R$$

which is listed in TABLE 6.2(d).

DETERMINATION OF CORRECTION FOR NEGATIVE ERRORS, $\Delta^{(-)}$

From TABLE 6.1, it is seen that the various *negative* errors are:

(a) for Model MI

	A_1	A_2	A_3	A_4	A_5	A_6	A_7	A_8	A_9	A_{10}	A_{11}	A_{12}
δ_{kd}	--	--	--	--	--	--	--	--	--	--	--	--
δ_{Cd}	--	--	--	--	--	--	--	--	--	--	--	--
δ_{ε}	--	--	-0.18	--	--	-0.20	--	-0.18	--	--	--	--
$\delta_{\varepsilon'}$	--	--	--	--	--	--	-0.08	-0.08	-0.08	-0.08	--	--

and $\delta_{\Sigma R} = -0.102$ for superinsulation covering A_7 and A_{10}.

(b) for Model MIII

	A_1	A_2	A_3	A_4	A_5	A_6	A_7	A_8	A_9	A_{10}	A_{11}	A_{12}
δ^*_{kd}	--	--	--	--	--	--	--	--	--	--	--	--
δ^*_{Cd}	--	--	--	--	--	--	--	--	--	--	--	--
δ^*_{ε}	--	--	-0.288	--	--	-0.32	--	-0.259	--	--	--	--
$\delta^*_{\varepsilon'}$	--	--	--	--	--	--	-0.147	-0.115	-0.16	-0.128	--	--

and $\delta^*_{\Sigma R} = -0.205$ for superinsulation covering A_7 and A_{10}. Again, the asterisk denotes errors after modification. Since all errors become *more* negative after modification, the error path is as illustrated in Fig. 2.3(b.2). From the data, we find

$$\sum \delta_j^2 = (-0.18)^2 + (-0.20)^2 + (-0.08)^2 + (-0.18)^2 + (-0.08)^2 + (-0.08)^2 + (-0.08)^2 + 2x(-0.102)^2 = 0.1512$$

$$\sum (\delta_j^*)^2 = (-0.288)^2 + (-0.32)^2 + (-0.147)^2 + (-0.259)^2$$
$$+ (-0.115)^2 + (-0.16)^2 + (-0.128)^2$$
$$+ 2x(-0.205)^2 = 0.412$$

$$\sum \delta_j \delta_j^* = (-0.18)(-0.288) + (-0.20)(-0.32)$$
$$+ (-0.08)(-0.147) + (-0.18)(-0.259)$$
$$+ (-0.08)(-0.115) + (-0.08)(-0.16)$$
$$+ (-0.08)(-0.128) + 2(-0.102)(-0.205) = 0.247$$

Hence,

$$\frac{\eta_p^{(-)}}{\xi_p^{(-)}} = \left[\frac{0.1512 \times 0.412}{0.247^2} - 1\right]^{1/2} = 0.158$$

$$\frac{\xi_p^{(-)}}{\xi_{p^*}^{(-)}} = \frac{0.247}{0.412} = 0.601$$

$$\xi_{p^*}^{(-)} = \sqrt{0.412} = 0.642$$

and

$$a = 0.158 \frac{1}{1 - 0.601} = 0.395$$

$$b = -\frac{0.395}{0.642} = -0.615$$

$$\lambda = 1 - 2 \times 0.601 = -0.202$$

$$f(a,\lambda) = -0.198 \quad \text{(from 2.3.6b)}$$

$$s^{*(-)}/s^{(-)} = \frac{2}{1 + 0.198} = 1.669 \quad \text{(from 2.3.13b)}$$

and

$$\Delta^{(-)} = \frac{555.4 - 542.1}{1.669 - 1} = 19.89^{\circ}R \quad \text{(from 2.3.13a)}$$

which is given in TABLE 6.2(d). The total required correction is

$$\Delta_t = \Delta^{(+)} + \Delta^{(-)} = -3.40 + 19.89 = 16.49^{\circ}R$$

and, hence, the corrected model temperature is

$$T_{Mc} = 542.1 - 16.49 = 525.6^{\circ}R$$

Upon comparing with the theoretically correct value of 524.4°R, one sees that the error in T_{Mc} is 1.2°R.